CYNDIA MARA BEZERRA DOS SANTOS

# ANÁLISE DA MODULAÇÃO DA EXPRESSÃO GÊNICA DE *Trypanosoma cruzi* AO LONGO DA CURVA DE CRESCIMENTO E EM DIFERENTES CONDIÇÕES DE ESTRESSE

Tese apresentada como requisito parcial à obtenção do grau de Doutor em Biologia Celular e Molecular, no Curso de Pós-Graduação em Biologia Celular e Molecular, Setor de Ciências Biológicas, da Universidade Federal do Paraná.

Orientador: Christian Macagnam Probst
Co-orientadora: Daniela Parada Pavoni

CURITIBA

2016

Universidade Federal do Paraná
Sistema de Bibliotecas

Santos, Cyndia Mara Bezerra dos
Análise da modulação da expressão gênica de *Trypanosoma cruzi* ao longo da curva de crescimento em diferentes condições de estresse. / Cyndia Mara Bezerra dos Santos. – Curitiba, 2016.
148 f.: il. ; 30cm.

Orientador: Christian Macagnam Probst
Coorientador: Daniela Parada Pavoni

Tese (doutorado) - Universidade Federal do Paraná, Setor de Ciências Biológicas. Programa de Pós-Graduação em Biologia Celular e Molecular.

1. Tripanossoma cruzi 2. Chagas, Doença de 3. Proteômica 4. Expressão gênica I. Título II. Probst, Christian Macagnam III. Pavoni, Daniela Parada IV. Universidade Federal do Paraná. Setor de Ciências Biológicas. Programa de Pós-Graduação em Biologia Celular e Molecular.

CDD (20. ed.) 616.9363

## PARECER

A banca examinadora, instituída pelo colegiado do Programa de Pós-Graduação em Biologia Celular e Molecular, do Setor de Ciências Biológicas, da Universidade Federal do Paraná, composta por:

***Prof. Dr. Christian Macagnan Probst***
*Orientador e presidente da banca*
*Instituto Carlos Chagas – ICC*

Aprovada

***Profa. Dra. Angélica Beate Winter Boldt***
*Universidade Federal do Paraná – UFPR*

Aprovada

***Profa. Dra. Erika Izumi***
*Universidade Federal Tecnológica do Paraná´- UTFPR*

Aprovada

***Profa. Dra. Lyris Martins Franco de Godoy***
*Instituto Carlos Chagas - ICC*

Aprovada

***Profa. Dra. Magda Clara Vieira da Costa Ribeiro***
*Universidade Federal do Paraná - UFPR*

***Suplentes:***

***Prof. Dr. Stênio Perdigão Fragoso***
*Instituto Carlos Chagas – ICC*

***Profa. Dra. Carolina Camargo de Oliveira***
*Universidade Federal do Paraná – UFPR*

Após arguir a candidata ***Cyndia Mara Bezerra dos Santos***, em relação ao seu trabalho intitulado: "Análise da modulação da expressão gênica de *Trypanosoma cruzi* ao longo da curva de crescimento e em diferentes condições de estresse", são de parecer favorável à aprovação da acadêmica, habilitando-a ao título de Doutor em Biologia Celular e Molecular.
A obtenção do título está condicionada à implementação das correções sugeridas pelos membros da banca examinadora, bem como ao cumprimento integral das exigências estabelecidas no Regimento Interno deste Programa de Pós-Graduação.

Curitiba, 29 de Agosto de 2016.

À minha mãe Nilza minha maior fonte
de inspiração e aos meus avós
Lourenço (*in memorian*) e Davilina por
sempre incentivarem meus estudos.

## AGRADECIMENTOS

A Deus.

Aos meus orientadores, Dr. Christian Macagnan Probst e Dra. Daniela Parada Pavoni, pela oportunidade de ingressar na biologia molecular, área que sempre desejei trabalhar.

Ao Dr. Marco Aurélio Krieger pelo apoio e confiança.

À Dra. Rita de Cássia P. Rampazzo pela amizade e ajuda, sempre disposta.

À Dra. Adriana Ludwig pela amizade e ajuda imensurável na escrita e correções da tese. Pelo incentivo e paciência, me ajudando no momento em que eu estava quase desistindo. Grande exemplo de pesquisadora e grande amiga!! Muuuuuuuuito obrigado.

À Msc. Juliana C. Amorim por toda colaboração no preparo das amostras até as análises de proteômica, discussão, paciência e amizade, sempre muito querida.

Ao Dr. Rafael L. Kessler pelas discussões, incentivo e grande ajuda nas análises. Ao Dr. Alexandre H. Inoue pelo auxílio em técnicas laboriosas.

Ao Msc. Maykol Noll pela ajuda bioinformática e amizade.

À Msc. Priscila M. Hiraiwa pela ajuda nas análises de citometria e por ser uma grande amiga. Aos tecnologistas Paulo Arauco pelo preparo das lâminas de RNA-Seq e Dr. Michel Batista pelo processamento das amostras de proteômica.

Ao Dr. Fabrício K. Marchini pela colaboração nesse trabalho.

Dra. Elizabeth Cunha pela discussão, ajuda na temida bioquímica e pela amizade.

A todos os amigos do Laboratório de Genômica que compartilharam momentos de tensão e também de risadas.

A todos profissionais que auxiliaram de forma direta ou indireta para que esta tese fosse finalizada.

Ao Conselho Nacional de Desenvolvimento Científico e Tecnológico (CNPq) e Coordenação de Aperfeiçoamento de Pessoal de Nível Superior (CAPEs) pelo auxílio financeiro.

À minha amada mãe por sua incrível capacidade de acreditar em mim e não medir esforços para que eu chegasse até esta etapa de minha vida. Seu cuidado e dedicação foram o que deram a esperança para seguir.

A toda minha família que de alguma forma significou segurança e certeza de que não estou sozinha nessa caminhada.

“Aprender é a única coisa de que a mente nunca se cansa, nunca tem medo e nunca se arrepende”.

Leonardo da Vinci

## RESUMO

O *Trypanosoma cruzi* é o agente da doença de Chagas, sendo um protozoário flagelado pertencente à ordem Kinetoplastida. Este parasita está distribuído em 21 países. Possui um ciclo de vida bastante complexo com diferenças morfológicas ultra-estruturais, funcionais e bioquímicas, apresentando sob diferentes formas nos hospedeiros invertebrados e vertebrados. A forma epimastigota é não infectiva e proliferativa, encontrada naturalmente no trato digestivo do inseto vetor, podendo ser cultivada in vitro. Um importante passo para melhor entendimento desse parasita é estudo das suas características celulares e moleculares apresentadas durante a sua curva de crescimento. Nesse trabalho foi apresentada uma visão global do perfil de expressão gênica a partir das frações de mRNA total e polissomal ao longo de 10 dias da curva de crescimento de epimastigotas de *T. cruzi*. Usando a metodologia de RNA-seq, 2491 genes diferencialmente expressos (DEGs) foram identificados, dos quais 768 foram modulados em ambas as frações. De acordo com os padrões de modulação encontrados, os DEGs foram agrupados em 13 clusters e alguns destes apresentaram enriquecimento de termos de ontologia gênica (GO) indicando os processos biológicos e moleculares envolvidos. Análises do perfil polissomal podem revelar quais genes estão sendo traduzidos em uma determinada condição, assim o padrão de expressão desses mRNAs pode ser diferente nas frações de total e polissomal. No entanto, foi encontrada uma extensa sobreposição dos padrões de modulação para a maioria dos clusters. Claramente durante a fase estacionária o conteúdo de polissomos apresentou uma forte diminuição associado ao surgimento de grânulos de mRNA. Isto sugere que durante esta fase a maioria dos transcritos isolados a partir do colchão de sacarose está provavelmente associada a complexos de mRNA invés de polirribossomos. Isto pode indicar que os mRNAs da fase estacionária podem estar sendo protegidos por esses grânulos para posterior tradução quando o ambiente se tornar novamente favorável. Vários aspectos da curva de crescimento deste parasita foram destacados, principalmente em relação as alterações pelas quais o parasita transita ao longo da fase estacionária. Além disso, foi investigada uma possível via de controle através da concentração de glicose a qual foi proposta a partir de comparações com estudos de Saccharomyces cerevisiae. Para um estudo complementar da curva de crescimento foi realizada uma abordagem de proteômica. Os dados preliminares mostraram uma boa identificação de grupos de proteínas (3.249), a maioria representando uma proteína por grupo. Algumas proteínas diferencialmente expressadas (DEPs) foram detectadas, apesar do baixo poder estatístico das análises. Dentre 68 DEPs identificadas, 21 mostraram correlação no padrão de modulação com os dados de transcritômica. Também foi apresentada uma análise de transcritômica preliminar de epimastigotas em fase estacionária inicial submetidos a diferentes condições nutricionais (PBS, TAU e TAU3AAG) por 1, 2, 4, 6 e 24 horas. Foram identificados 612, 804 e 941 supra-genes diferencialmente expressos nos meios PBS, TAU e TAU3AAG, respectivamente. A maioria dos supra-genes modulados foram comuns nas três condições. Juntos, esses estudos representam uma etapa importante na obtenção de dados em larga escala que geração de conhecimento sobre o comportamento e resposta do parasita em diferentes condições ambientais.



Palavras-chave: *Trypanosoma cruzi*, doença de Chagas, curva de crescimento, RNA-seq, polissomos, proteômica e estresse.

## ABSTRACT

The *Trypanosoma cruzi* is a flagellated protozoa that belongs to the Kinetoplastida order and is the etiologic agent of Chagas disease, an endemic illness distributed in 21 countries. The *T. cruzi* life cycle is complex including morphological, functional and biochemical changes. The epimastigote form is proliferative and non-infective, founded naturally in the insect vector gut and can be cultivated *in vitro*. An important step to comprehend the *T. cruzi* biology is the study of cellular and molecular features presented during its growth curve. Here, we show a global view of gene expression profile for total and polysomal RNA fractions along 10 days of the *T. cruzi* epimastigote growth curve in vitro. A total of 2491 differential expressed genes (DEGs) were established using RNA-Seq approach, of which 768 were modulated in both fractions. According to the modulation pattern, these DEGs were grouped into 13 clusters and some of them show enrichment to important GO terms, indicating molecular and cellular biological processes involved. The polysomal profile might reveal mRNAs that are being translated and their expression pattern could be different from the total RNA fraction, nevertheless, in most clusters we see remarkable overlapped modulation. Moreover, at the stationary phase the polysomal content greatly decline while the RNA granules seems to increase. This suggests that most of mRNAs isolated from sucrose cushion at this growth stage should be associated with granules instead with polyribosomes. This possible indicates that stationary phase mRNAs are being protected by granules for further translation when the environment becomes favorable. We highlight some views on the *T. cruzi* growth curve, mainly related to the alteration that the parasite pass along the stationary phase. Moreover, a possible sensing pathway for glucose depletion was suggested for *T. cruzi* based on *Saccharomyces cerevisiae* studies comparison. Growth curve complementary study was performed using proteomic approach. Preliminary data shows the identification of 3,249 protein groups, mostly representing one protein per group. Some differential expressed proteins (DEPs) were identified, besides the limited statistical power. Among the 68 DEPs identified, 21 showed correlation in their proteomic and transcriptomic modulation pattern. Preliminary transcriptomic analysis of epimastigote in early stationary phase under three nutritional different conditions (PBS, TAU, TAU3AAG) during 1, 2, 4, 6 and 24 hours were also present here. Total of 612, 804 and 941 differential expressed supra-genes were identified in PBS, TAU and TAU3AAG conditions, respectively. Most of supra-genes were common to all treatments. Together, these works represent an important step for large scale data generation that will provide insights into the parasite behavior and response to different environmental conditions.



Key-words: *Trypanosoma cruzi*, Chagas disease, growth curve, RNA-seq, polysomes, proteome and stress.

## LISTA DE ABREVIATURAS E SIGLAS

Acetil-CoA - Acetil Coenzima A

AMPc - 3´5´-adenosina-monofosfato-cíclico ATP - Adenina trifosfato

BLAST - Basic Local Alignment Search Tool

BSA - Albumina de Soro Bovino (Bovine Serum Albumin)

CDC - Centros de Controle e Prevenção de Doenças (Centers for Disease Control and Prevention)

CHIP-seq - Imunoprecipitação da cromatina (ChIP, chromatin immunoprecipitation) seguido de sequenciamento

DAPI - 4', 6-Diamidino-2-fenilindol

DIC - Contraste por Interferência Diferencial Dm - Delphis marsupialis

DNA - Ácido Desoxirribonucleico

dNTP - Desoxirribonucleotídeo trifosfatados

DO - Densidade Ótica no comprimento de onda (λ)

DTU - Unidade discreta (Discrete Typing Unit) Gel 2D - Gel Bidimensional

HEPES - (N-[2-hidroxietil]-1-piperazino N´-[2-ácido etanosulfônico]) IBMP - Instituto de Biologia Molecular do Paraná

ICC - Instituto Carlos Chagas

IF - Ensaio de Imunofluorescência

IOC - Instituto Oswaldo Cruz

kDNA - DNA do cinetoplasto (kinetoplast DNA) LIT - Liver Infusion Tryptose

ME - Mini-exon

mRNA - RNA mensageiro (messenger RNA) mRNP - Ribonucleoproteína mensageira

NP-40 - Nonil fenoxi polietoxietanol O2 - Oxigênio

PBS - Solução Salina tamponada com Fosfato (Phosphate Buffered Saline)

PCR - Reação em cadeia da polimerase pH - Potencial Hidrogeniônico

Pi - Fosfato inorgânico

PMSF - Fluoreto de fenil metil sulfonil RNA - Ácido Ribonucleico

RNAP - Polimerase do Ácido Ribonucleico RNase – Ribonuclease

RNA-seq - Sequenciamento massivo de RNA rRNA - RNA ribossomal

SDS - Dodecil sulfato de sódio (Sodium dodecyl sulfate)

SDS-PAGE - Eletroforese em gel de poliacrilamida contendo SDS (Sodiumdodecyl sulfate- polyacrilamide gel eletrophoresis)

SFB - Soro fetal bovino

SSC - Tampão NaCl-Citrato de Sódio (Standard Saline-Citrate)

SL-RNA - Spliced

TAU - Urina artificial de Triatomíneo (Triatomine Artificial Urine)

TAU3AAG - Urina artificial de Triatomíneo (Triatomine Artificial Urine) adicionado de prolina, ácido glutâmico e ácido aspártico.

TBE - Tampão Tris-Boro-EDTA

Tris - Tris (hidroximetil) aminometano tRNA - RNA transportador

UTR - Regiões não traduzidas (Untranslated region) UV - Ultravioleta

WHO - Organização Mundial da Saúde (World Health Organization)

**SUMARIO**

# 1 INTRODUÇÃO

## 1.1 A DOENÇA DE CHAGAS

Em 1909, o médico sanitarista e pesquisador do Instituto Oswaldo Cruz (IOC) Carlos J. Ribeiro das Chagas (1878-1934) foi o primeiro e único a descrever uma doença infecciosa por completo. Em seus estudos ele relatou ao mundo científico o patógeno que afetava humanos, o vetor de transmissão, assim como ciclo de vida do parasita e a epidemiologia da doença (CHAGAS, 1909), a qual foi denominada de doença de Chagas, em sua homenagem.

A doença de Chagas é causada pelo protozoário *Trypanosoma cruzi* que pode ser transmitido de diferentes maneiras, destacando-se a transmissão através do inseto vetor, mas também podendo ocorrer através da transfusão sanguínea, transmissão congênita, acidente laboratorial, transmissão oral e transplante de órgãos (DIAS, 2000). O período de incubação depende da forma que a infecção ocorreu, sendo de aproximadamente uma a duas semanas em casos de transmissão vetorial e de três meses quando a transmissão é transfusional (COURA; DIAS, 2009). Após infecção diferentes fatores como cepa, virulência, sexo, idade e ambiente irão marcar a evolução da doença. A fase aguda é microscopicamente detectável devido à alta parasitemia, porém os sinais clínicos são geralmente rápidos e inespecíficos, incluindo febre, mal-estar, hepatoesplenomegalia e linfocitose atípica. Em casos raros, um nódulo de pele (chagoma) ou edema palpebral prolongado indolor (sinal de Romaña) pode indicar o local da inoculação. A grande maioria das infecções agudas não é detectada, sendo considerada uma fase silenciosa revisto por (BERN, 2015). Entretanto em casos mais graves, meningoencefalite e miocardite pode levar o paciente à morte. Esta fase dura entre 4 a 12 semanas, não parecendo haver cura espontânea em humanos (RASSI; RASSI; MARIN-NETO, 2010).

Em pessoas que sobrevivem à fase aguda, a resposta imune mediada por células controla a replicação parasitária, com a parasitemia desaparecendo com 4 a 8 semanas e os sintomas desaparecendo (RASSI; RASSI; MARCONDES DE REZENDE, 2012). A fase crônica possui uma evolução lenta e pode durar toda a vida do paciente, sendo que grande parte dos pacientes permanecem assintomáticos. Entretanto estima-se que 20 a 30% das pessoas infectadas irão progredir a cardiomiopatias ou problemas do trato digestivo como megaesôfago e megacólon associado a quadros de disfagia e constipação intestinal ao longo de anos e décadas (revisto por DIAS, 2000).

O tratamento para a doença de Chagas é baseado em duas drogas: benzonidazol e o nifurtimox. O benzonidazol é considerado a primeira linha de tratamento por apresentar melhor

eficácia e efeitos colaterais mais brandos que o nifurtimox (BERN et al., 2007). Essas drogas apresentam eficácia acima de 80% na fase aguda e de 8% a 30% na fase crônica. O tratamento é atrapalhado devido ao esquema terapêutico prolongado, variabilidade genética dos parasitas, cepas naturalmente resistentes aos fármacos e às reações adversas indesejáveis que em certos casos levam o paciente a interromper o uso do medicamento, sem a obtenção do sucesso terapêutico (OLIVEIRA et al., 2008).

A doença de Chagas é uma das principais patologias parasitárias de mais larga distribuição da América Latina e Caribe, onde 40% do total de indivíduos vivem abaixo da linha de pobreza. Apresenta um grande impacto social e econômico quando comparados aos efeitos combinados de outras doenças parasitárias como malária, leishmaniose e esquistossomose. Segundo a Organização Mundial de Saúde (WHO, 2016), essa doença é endêmica em 21 países das Américas, afetando cerca de 7 a 8 milhões de pessoas (RASSI; RASSI; MARIN-NETO, 2010). Estima-se que nas Américas 28.000 novos casos são registrados a cada ano, e 8.000 recém-nascidos tornam-se infectados durante a gestação. Além disso, cerca de 65 milhões de pessoas nas Américas vivem em áreas de exposição para Chagas e correm o risco de contrair a doença (WHO, 2016). No Brasil, os dados mais recentes de prevalência e incidência associados à doença de Chagas em casos crônicos, decorrentes de infecções adquiridas no passado, estimam aproximadamente três milhões de indivíduos afetados, enquanto casos de doença aguda, entre o período de 2000 a 2013, foram registrados 1.570 pessoas (MINISTÉRIO DA SAÚDE, 2015). Contudo, o perfil epidemiológico global da doença de Chagas é o resultado da transmissão do vetor ao longo da vida da população atual da América Latina e da migração em grande escala da população rural ao longo dos últimos 50 anos (BERN, 2015) (Figura 1).

Figura 1 – Prevalência da infecção por *Trypanosoma cruzi* no continente Americano. São mostradas as prevalências baseados em dados publicados.

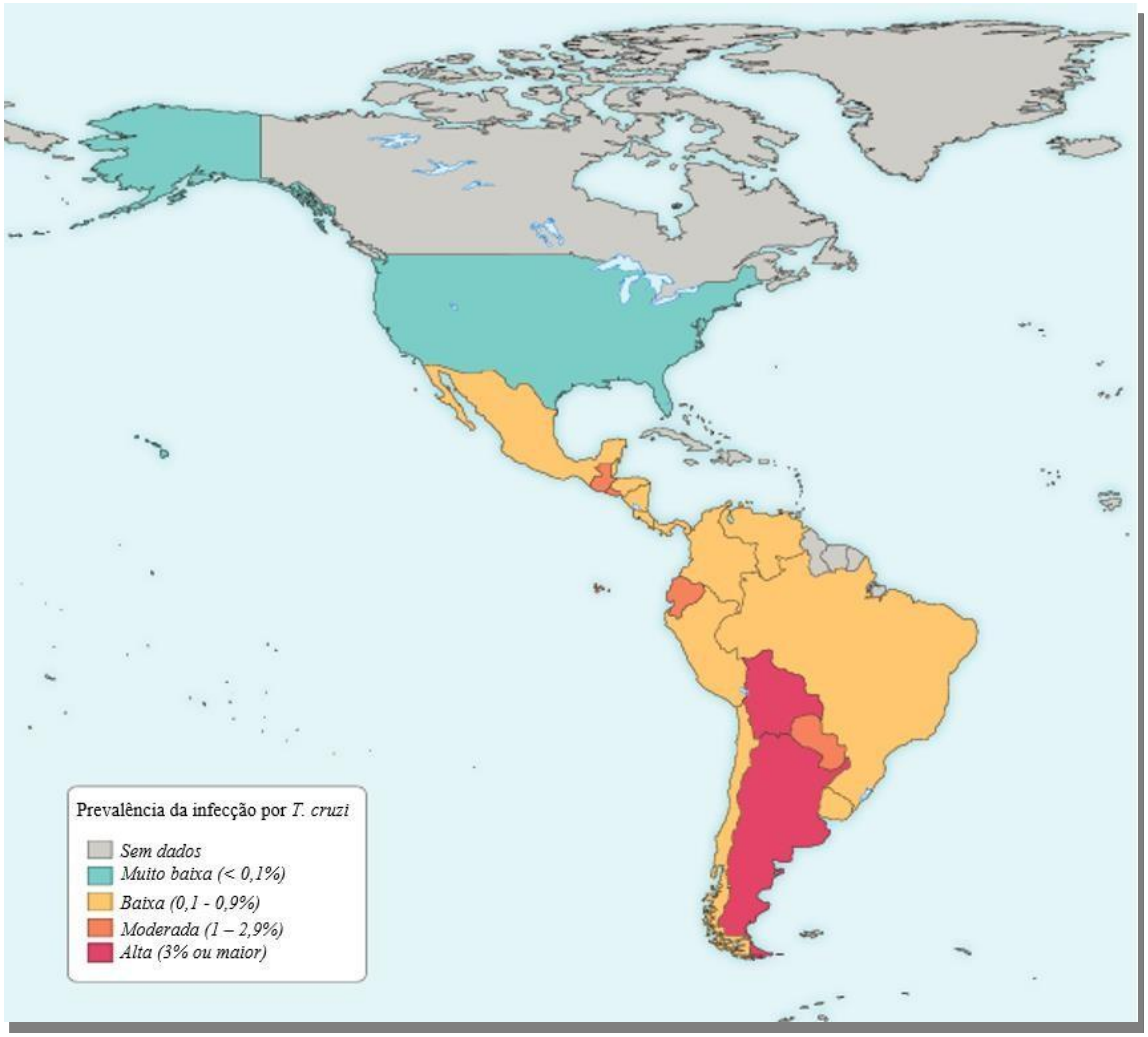


Modificado de Bern (2015).

## 1.2 O TRYPANOSOMA CRUZI

O agente causador da doença de Chagas é o protozoário unicelular flagelado *Trypanosoma cruzi* que pertence à Ordem Kinetoplastida, classe Trypanosomatida, família Trypanosomatidae e gênero *Trypanosoma*. Uma característica específica dos organismos da ordem Kinetoplastida é a existência de pelo menos uma região especializada de sua mitocôndria única, chamada cinetoplasto, que aloja uma rede organizada de DNA, denominada DNA do cinetoplasto ou kDNA, o qual chega a representar aproximadamente 30% do DNA total da célula (DE SOUZA, 1984). Dependendo da fisiologia do protozoário o kDNA pode ter sua forma e organização interna alterada, assim a ultraestrutura do kDNA das formas amastigota e epimastigota apresentam-se em formato de bastão medindo cerca de 1 µm de comprimento e

0,1 µm de espessura, enquanto nas formas tripomastigotas o kDNA torna-se menos compactado adquirindo forma arredondada. Outra característica marcante do kDNA é que ele está dividido em uma rede de maxicírculos, que apresentam dimensões semelhantes ao DNA mitocondrial encontrado na maioria das células eucarióticas, e uma rede de minicírculos, envolvidos no processo de edição do RNA mensageiro formado a partir dos maxicírculos. Os tripanossomatídeos também possuem outras estruturas celulares peculiares, como os peroxissomos, reservossomos, microtúbulos subpeliculares, glicossomos e a presença de um flagelo único (DE SOUZA, 1984; SOARES et al., 1989).

O *T. cruzi* possui uma grande diversidade intraespecífica, originada por divisão clonal e subsequente evolução paralela das diferentes linhagens e cepas (ZINGALES et al., 1999). Ao longo dos anos, houve uma alternância de tendências "taxonômicas" de classificação da diversidade genética do *T. cruzi*, mas os estudos mais recentes de filogenia mostraram que sua população pode ser dividida em dois grupos, denominados DTU I e DTU II (do inglês, *Discrete Typing Unit*). Além disso, as cepas foram classificadas em seis subpopulações DTUs I, IIb, IIc, IIa, IId e IIe (TIBAYRENC, 2003). Em 2009 um encontro com pesquisadores da área (*Second Satellite Meeting)* aconteceu para unificar a nomenclatura do *T. cruzi*, renomeando essas cepas de TcI a TcVI (ZINGALES et al., 2009). A vasta diversidade genética encontrada nesses parasitas, associado a fatores como genética do hospedeiro, infecções mistas, além de fatores culturais e geográficos, possui implicações para as formas clínicas da doença, como o desenvolvimento de cardiopatia, megaesôfago e megacólon, isoladamente ou em combinação, apesar da patogenia da infecção pelo *T. cruzi* ainda não ter sido totalmente elucidada (CAMPBELL; WESTENBERGER; STURM, 2004; MANOEL-CAETANO; SILVA, 2007; ZINGALES, 2011).

## 1.3 MECANISMO DE TRANSCRIÇÃO POLICISTRÔNICA

Os tripanossomatídeos possuem os três tipos de RNA polimerases, RNAP I, RNAP II e RNAP III (CORNELISSEN et al., 1989, 1990). RNAP I é responsável pela transcrição de genes de rRNA, e assim como outros eucariotos, possui um promotor bem caracterizado. A RNAP III tem como função a transcrição de genes de rRNA 5S, tRNAs e snRNAs e a RNAP II, por sua vez, é a responsável pela transcrição dos RNAs mensageiros (mRNA) (revisto por CAMPBELL; THOMAS; STURM, 2003).

O processo de transcrição na maioria dos organismos procariotos e eucariotos é regulado

no seu início por uma região promotora a montante da região codificadora do gene. Assim, a regulação transcricional tem importante contribuição para o controle da expressão gênica em procariotos e eucariotos. Porém, o *T. cruzi* possui um único promotor para RNA polimerase (RNAP) II caracterizado até o momento, para o gene que codifica a sequência líder (SL, do inglês *spliced leader*) indicando que o início da transcrição de mRNAs nesses parasitas, em geral, independe da existência de promotores (LUO; BELLOFATTO, 1997). Os tripanosomatídeos raramente usam esse tipo de regulação, provavelmente também devido ao seu tipo de organização genômica (explicada a seguir), além da frequente ausência de promotores (revisto por KRAMER, 2012).

Nos tripanossomatídeos, os genes estão organizados em grandes grupos poliscistrônicos, formados por dezenas a centenas de genes codificadores de proteínas arranjados na mesma fita de DNA. Os genes de um policistron estão separados uns dos outros por pequenas regiões intergênicas. Além disso, as regiões codificadoras de proteínas não estão interrompidas por íntrons, com exceção de poucos genes, como o codificador da poli-A polimerase (MAIR et al., 2000). Cada arranjo policistrônico possui uma região a montante não transcrita que pode chegar a 13 kb, chamada de região de troca de fita (SSR do inglês, *Strand Switch Region*). Na fita oposta do DNA, um segundo conjunto gênico é iniciado pela outra extremidade da SSR (revisto por PALENCHAR; BELLOFATTO, 2006).

Os genes contidos no mesmo policistron geralmente não codificam para proteínas de função relacionadas e são transcritos em uma única molécula de RNA policistrônica precursora. (TEIXEIRA, 1998; VANHAMME; PAYS, 1995). Essa transcrição policistrônica pela RNAP II em tripanossomatídeos parece ser regulada por fatores epigenéticos. Resultados recentes mostram que estruturas específicas da cromatina nas SSRs podem compensar a aparente falta de promotores definidos. Foi demonstrado que prováveis sítios de início de transcrição por RNAP II são marcados por uma cromatina mais solta, com nucleossomos distintos e menos estáveis devido à presença de formas variantes das histonas H2A e H2B, H2AZ e H2BV, respectivamente (SIEGEL et al., 2009).

Apesar da síntese em uma mesma molécula precursora, os genes de uma mesma unidade policistrônica podem apresentar grandes diferenças nos níveis de expressão, evidenciando que em tripanossomatídeos a regulação da expressão gênica ocorra em nível pós-transcricional (VANHAMME; PAYS, 1995). Algumas exceções são os transcritos de prociclinas, VSGs (do inglês, *Variant Surface Glycoprotein*) que são genes codificadores de proteínas de superfície celular de *T. brucei* e alguns genes associados a VSGs, que são transcritos pela polimerase I de RNA possuindo promotores específicos (GÜNZL et al., 2003).

O processamento de mRNA individuais a partir do precursor policistrônico ocorre através de reação de *trans-splicing* que adiciona uma sequência conservada de aproximadamente 39 nucleotídeos, denominada SL ou mini-éxon (ME), na porção 5' do transcrito. Além desta modificação, ocorre a adição de uma cauda poli-A na extremidade 3'. Os mecanismos de *trans-splicing* e poliadenilação são acoplados (LEBOWITZ et al., 1993).

A reação de *trans-splicing* ocorre com a participação de duas moléculas de RNA, uma doadora e outra aceptora. A molécula de RNA doadora é um precursor do ME que possui 110 nucleotídeos em *T. cruzi* (ZWIERZYNSKI; BUCK, 1991), apresentando na sua extremidade 5' um cap com modificações químicas nos quatro primeiros nucleotídeos após a 7-metilguanosina, denominado cap 4 (PERRY; WATKINS; AGABIAN, 1987). A molécula de RNA aceptora é o transcrito da unidade policistrônica que receberá a sequência do ME. A separação dos genes contíguos no pré-mRNA policistrônico ocorre com a adição da cauda poli-A na extremidade 3' do primeiro e ligação simultânea do ME na extremidade 5' do segundo (revisto por PALENCHAR; BELLOFATTO, 2006), dessa forma todos os mRNAs irão possuir um SL na extremidade 5' (DE LANGE et al., 1984; MARTÍNEZ-CALVILLO et al., 2010).

Para a reação de poliadenilação parece não haver sinal específico, porém ocorre a uma distância relativamente fixa de aproximadamente 100 a 400 nucleotídeos a montante do sítio de *splicing* (MATTHEWS; TSCHUDI; ULLU, 1994). A adição do ME e da cauda poli-A são reguladas por sequências ricas em resíduos de pirimidinas em específicos sítios de poliadenilação e *trans-splicing* (CAMPOS et al., 2008). Além disso, a presença de uma sequência consenso AG no sítio de trans-*splicing* é fundamental. Deleções nestas regiões resultam no impedimento do correto processamento destes transcritos (CAMPOS et al., 2008; MATTHEWS; TSCHUDI; ULLU, 1994).

## 1.4 REGULAÇÃO DA EXPRESSÃO GÊNICA

Todos os organismos são capazes de modular a expressão de genes em resposta a estímulos externos e internos. Em geral, organismos unicelulares são capazes de alterar a expressão gênica mediante duas situações principais: primeiro, para otimizar a sobrevivência da célula em resposta a mudanças no meio ambiente e segundo, para gerar vias que conduzam ao desenvolvimento de diferentes formas em resposta a outros sinais (SCHWEDE; KRAMER; CARRINGTON, 2012). Como visto anteriormente, alterações na expressão gênica são alcançadas principalmente pelo controle do início da transcrição e tripanosomatídeos parecem não ter esse controle (revisto por VANHAMME; PAYS, 1995). Assim, a modulação da

expressão gênica nesses parasitas deve acontecer por outros mecanismos após o término da transcrição, através da regulação pós-transcricional. A regulação pós-transcricional irá ocorrer em diferentes pontos, detalhados como**:** processamento do mRNA e exportação do núcleo; degradação citoplasmática dos mRNAs; associação à maquinaria de tradução e estabilidade proteica.

O processamento do mRNA é dado pelo acoplamento dos processos de *trans-splicing* e da poliadenilação, e o tamanho dos tratos de polipirimidina e a sua distância em relação aos sítios de poliadenilação e *trans-splicing* têm sido relacionados com a eficiência no *trans-splicing* de vários genes. Além disso, *trans-splicing* alternativo de genes específicos das diferentes formas do parasita parecem estar associados a fatores proteicos específicos que interagem com a maquinaria de *splicing* e poliadenilação (MANNING-CELA; GONZÁLEZ; SWINDLE, 2002). A exportação de mRNAs maduros do núcleo ocorre através dos poros nucleares por um controle seletivo pouco compreendido (revisto por CLAYTON; SHAPIRA, 2007).

Em tripanossomatídeos o modelo de degradação citoplasmática dos mRNAs é dado por duas vias, uma regulada e outra constitutiva (não regulada). A via regulada é rápida e parece ser independente de deadenilação. Estudos sugerem que ela pode ser limitante para mRNAs instáveis estágio-específico, como ocorre em células de mamíferos. A via constitutiva é dependente de deadenilação e opera de forma mais lenta durante a degradação de mRNA estável e provavelmente uma subpopulação de mRNAs instáveis (revisto por HAILE; PAPADOPOULOU, 2007).

A associação à maquinaria de tradução irá ocorrer com mRNAs disponíveis no citoplasma e que não estão vinculados aos mecanismos de degradação. Fatores que regulam o acesso desses mRNAs à maquinaria de tradução poderiam atuar como um mecanismo de controle pós-transcricional, bem como repressores da síntese proteica podem impedir a circularização do mRNA e a formação do complexo necessário para iniciação da tradução (RICHTER; SONENBERG, 2005). A regulação da tradução é alcançada através de sinais específicos na região 3'-UTR dos mRNAs (revisto por CLAYTON; SHAPIRA, 2007).

Em *T. cruzi*, foi demonstrado que moléculas de RNA mensageiro podem ser mantidas estáveis e não associadas a polissomos, desmobilizadas no citoplasma, sendo passíveis de tradução *in vitro* (GOLDENBERG et al., 1985). Há evidências de que o controle da associação à maquinaria de tradução seja o mecanismo principal na expressão diferencial de alguns genes regulados durante a metaciclogênese de *T. cruzi* (ÁVILA et al., 2003; DALLAGIOVANNA et al., 2001). Além disso, o número expandido de potenciais fatores de tradução nos *Tritryps*

(*T. cruzi*, *T. brucei* e *L. major*) sugere um alto nível de especialização e controle da tradução nesses organismos (IVENS et al., 2005a)

A estabilidade da proteína representa uma importante estratégia para manutenção de sua atividade biológica e sua degradação é um processo seletivo, já que grande heterogeneidade entre as taxas de degradação das diferentes proteínas são observadas na célula. Assim, o tempo entre a síntese de uma proteína e seu momento de degradação pode representar uma forma de controle da expressão gênica pós-traducional com importante papel em tripanossomatídeos. Além disso, foi demonstrado em *T. brucei* que a degradação proteica foi parcialmente responsável pela diminuição estágio-específica de proteínas ligadoras de RNA (revisto por HAILE; PAPADOPOULOU, 2007).

## 1.5 CICLO BIOLÓGICO

O *T. cruzi* é um parasita cujo ciclo de vida é heteróxeno, envolvendo a passagem obrigatória por dois hospedeiros, sendo um invertebrado (inseto) e um vertebrado (mamífero). Os hospedeiros invertebrados são insetos hematófagos da família Reduviidae, subfamília Triatominae, popularmente conhecidos como barbeiros. Dentre as espécies de maior importância epidemiológica podemos citar *Triatoma infestans, Panstrongylus megistus, Triatoma brasiliensis, Triatoma pseudomaculata e Triatoma sordida*, porém outras 47 espécies já foram relatadas e apresentam importância na manutenção do ciclo natural em mamíferos silvestres (COURA; DIAS, 2009). Como hospedeiros vertebrados, foram descritas mais de 100 espécies de mamíferos, como marsupiais, roedores, morcegos, primatas e alguns carnívoros, além do homem (DIAS, 2000).

O ciclo biológico do *T. cruzi* tem sido amplamente revisto desde a sua primeira divulgação por Carlos Chagas em 1909 (ANDRADE; ANDREWS, 2005; BRENER, 1973; CHAGAS, 1909; TANOWITZ et al., 1992; TYLER; ENGMAN, 2001) e está representado na Figura 2. Este ciclo é bastante complexo, sendo que o parasita se apresenta sob diferentes formas nos diferentes hospedeiros. Nos invertebrados as formas envolvidas são epimastigotas e tripomastigotas metacíclicas, enquanto nos mamíferos são as formas tripomastigotas sanguíneas e amastigotas. Assim, ao longo do ciclo de vida observam-se diferenças morfológicas ultraestruturais, funcionais e bioquímicas, que diferenciam uma forma da outra.

Além disso, as formas tripomastigotas sanguíneas e metacíclicas apresentam-se como formas infectivas e não proliferativas, e os epimastigotas e amastigotas como formas não infectivas e proliferativas (TANOWITZ et al., 1992; TYLER; ENGMAN, 2001; ZELEDÓN, 1999). No hospedeiro mamífero, onde a doença pode realmente se estabelecer, uma série de alterações fisiológicas foi evidenciada, enquanto no inseto vetor nenhum tipo de dano tem sido observado (RASSI; RASSI; MARIN-NETO, 2010).

Figura 2 – Ciclo Biológico do *Trypanosoma cruzi* . Descrição detalhada no texto.

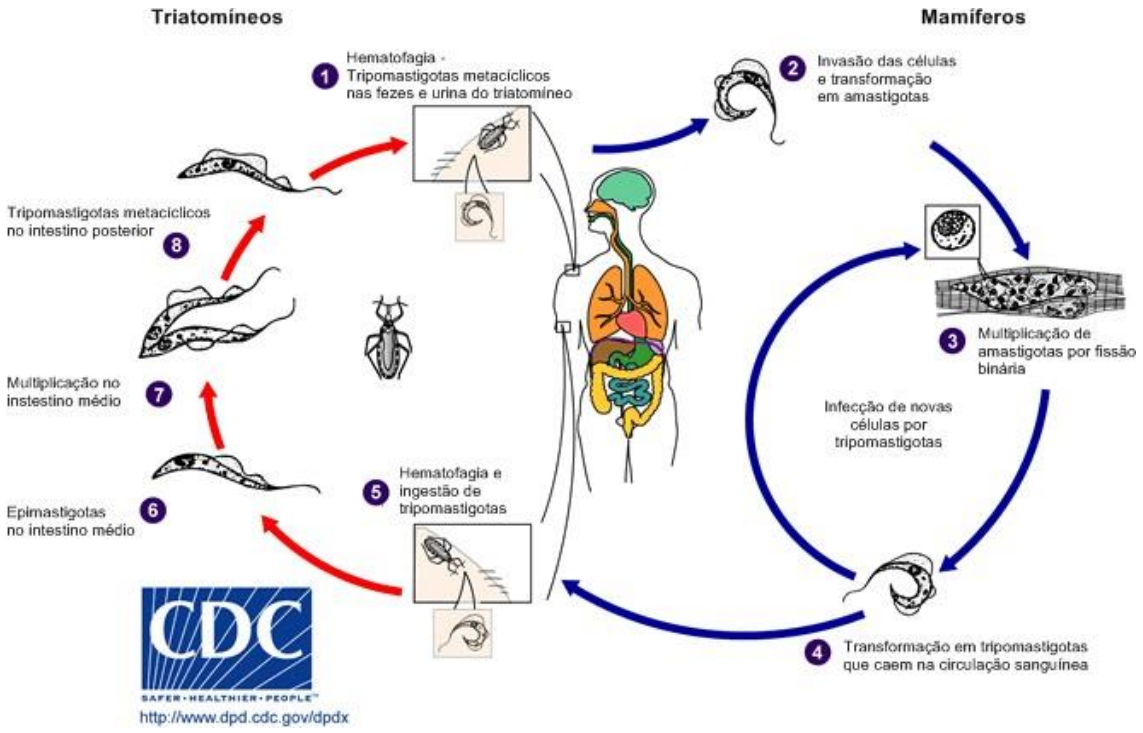


Fonte: Modificado de http://www.dpd.cdc.gov/dpdx/HTML/TrypanosomiasisAmerican.htm

Conforme a ilustração acima, a infecção natural pelo *T. cruzi* ocorre através da liberação de formas tripomastigotas metacíclicas nas excretas do triatomíneo infectado durante o repasto sanguíneo. A invasão do parasita ao hospedeiro mamífero ocorre através de lesões na pele, normalmente no próprio local da picada, ou através das mucosas. Ao atingir a corrente sanguínea essas formas são altamente infectantes, podendo invadir os primeiros tipos celulares que encontram, como macrófagos, fibroblastos e células epiteliais (BURLEIGH; ANDREWS, 1995). Ao invadir estas células, o tripomastigota metacíclico sofre diferenciação para a forma amastigota, a qual se divide no citoplasma celular formando um pseudocisto (ANDREWS,

1993). Altas densidades de amastigotas intracelulares dão origem a tripomastigotas sanguíneos. O alto número de protozoários dentro da célula mamífera leva ao seu rompimento, liberando novos tripomastigotas sanguíneos na corrente circulatória, dessa forma estes parasitas recém-liberados podem invadir novas células localizadas próximas ao sítio de infecção e alcançar diferentes tecidos do hospedeiro (revisto por TYLER; ENGMAN, 2001).

A continuidade do ciclo biológico do *T. cruzi* se dá no inseto triatomíneo ao fazer o repasto sanguíneo no hospedeiro mamífero infectado, onde ocorre a ingestão das formas tripomastigotas sanguíneas, que após alguns dias se transformam em epimastigotas. Uma vez a infecção estabelecida no estômago do inseto vetor, as formas epimastigotas do parasito se dividem repetidamente por divisão binária, posteriormente podendo aderir às membranas perimicrovilares das células intestinais. Em grande número, os epimastigotas migram para a porção posterior do intestino e se ligam à cutícula retal, sofrem o processo de metaciclogênese, diferenciando-se em tripomastigotas metacíclicos, podendo assim ambas as formas, diferenciadas ou não, serem eliminadas juntamente com as excretas do inseto. Assim, após em média 3 a 4 semanas, a fase do ciclo no inseto é finalizada, permitindo que as formas infectivas sejam transmitidas para o hospedeiro vertebrado durante o repasto sanguíneo, dando continuidade ao ciclo biológico (revisto por TYLER; ENGMAN, 2001).

## 1.6 METACICLOGÊNESE *IN VITRO*

A compreensão dos diferentes processos de diferenciação celular que ocorrem durante o ciclo de vida do *T. cruzi* sempre foi alvo de muitos estudos e especulações por parte dos pesquisadores. O estudo dos aspectos celulares, bem como dos mecanismos de regulação da expressão gênica envolvidos nesses processos, foi auxiliado pela possibilidade de obtenção *in vitro* de uma maior quantidade de parasitas em diferentes formas evolutivas e em vários estágios de diferenciação. O principal exemplo é a mimetização das condições químicas do processo de metaciclogênese, o qual ocorre na porção posterior do intestino do inseto vetor levando à diferenciação celular das formas epimastigotas em formas tripomastigotas metacíclicas (BONALDO et al., 1988; CONTRERAS et al., 1985). A metaciclogênese *in vitro* tornou-se um modelo apropriado para o estudo dos mecanismos envolvidos na regulação da diferenciação e da expressão gênica no parasita (CONTRERAS et al., 1985).

A manutenção da forma epimastigota pode ser feita em um meio de cultura rico em nutrientes, o meio LIT (do inglês, *Liver Infusion Tryptose*). A metaciclogênese *in vitro* inicia-se após um estresse nutricional, que é efetuado pela transferência dos epimastigotas cultivados

em meio LIT para o meio TAU (do inglês, *Triatomine Artificial Urine*), que mimetiza as condições iônicas encontradas na urina do inseto vetor. Após duas horas de incubação nesse meio, os parasitas são transferidos para o meio de diferenciação (TAU3AAG) que consiste no meio TAU suplementado com glicose e três aminoácidos (L-prolina, ácido L-glutâmico, ácido L-aspártico), onde permanecem por 96 horas. Nestas condições, cerca de 80% dos parasitas se diferenciam em tripomastigotas metacíclicos (BONALDO et al., 1988; CONTRERAS et al., 1985). A metaciclogênese *in vitro* permite a obtenção de tripomastigotas metacíclicos com as mesmas propriedades biológicas descritas para o parasita que se diferencia no inseto vetor (CONTRERAS et al., 1988b), além disso, estudos *in vitro* mostram que o estresse nutricional é um fator importante para a indução do processo de metaciclogênese. A transformação *in vitro* das formas epimastigotas em tripomastigotas metacíclicas requer primeiramente a adesão dos parasitas a um substrato (BONALDO et al., 1988), semelhante ao que foi descrito para o processo de metaciclogênese no interior do triatomíneo (KOLLIEN; SCHMIDT; SCHAUB, 1998; ZELEDÓN, 1999). Os fenômenos de adesão e de diferenciação celular são interrompidos se após um período de estresse nutricional, as condições nutricionais ideais forem restauradas. Deste modo, é possível que o estresse nutricional esteja associado à expressão de proteínas de adesão (FIGUEIREDO; ROSA; SOARES, 2000).

No início da metaciclogênese, especialmente durante o estresse nutricional e o princípio do processo de adesão, ocorre uma vasta reprogramação da expressão gênica e foi possível observar que as alterações na expressão gênica precedem as alterações morfológicas ocorridas na metaciclogênese (CONTRERAS; MOREL; GOLDENBERG, 1985). Durante a metaciclogênese podem ser observados genes de expressão transiente e regulação pós-transcricional (ÁVILA et al., 2001; DALLAGIOVANNA et al., 2001). Do mesmo modo, alterações bioquímicas e na composição da superfície celular podem ser observadas logo após o estresse nutricional (CONTRERAS; MOREL; GOLDENBERG, 1985; DE ANDRADE et al., 1991; ESTEVES et al., 1989). Vinte e quatro horas depois do início do processo de diferenciação, as formas epimastigotas em diferenciação apresentam-se resistentes à lise pelo sistema complemento do hospedeiro (CONTRERAS et al., 1988b), uma propriedade das formas tripomastigotas metacíclicas (NOGUEIRA; BIANCO; COHN, 1975).

O processo de metaciclogênese também pode ser influenciado por outros fatores. O aminoácido L-prolina utilizado como fonte de carbono e energia pode estimular a diferenciação (CONTRERAS; MOREL; GOLDENBERG, 1985). O AMPc também é capaz de estimular a metaciclogênese (GONZALES-PERDOMO; ROMERO; GOLDENBERG, 1988) e foi

encontrado na urina do inseto vetor *Rhodinius prolixus* (KOLLIEN; SCHAUB, 2000). Além disso, a presença e a concentração dos íons $Ca^{2+}$, $K^{+}$, $PO_4^{-}$ e $HCO_3$ facilitam a metaciclogênese, enquanto o ânion $Cl^{-}$ a impede (KRASSNER et al., 1991).

## 1.7 CURVA DE CRESCIMENTO

Em microbiologia, a curva de crescimento é a representação da relação da mudança no número de células (densidade) dentro de uma cultura experimental, em diferentes momentos de uma escala de tempo, sendo representada em forma de gráfico. Além disso, a curva de crescimento também é uma ferramenta muito comum em estudos de ecologia, em que são usadas para controlar aumento e diminuição das populações de plantas, animais e outros organismos multicelulares ao longo do tempo (GOTELLI; COLWELL, 2001; PECKOVÁ; LOM, 1990; VIVES; SALICRÚ, 2005).

A curva de crescimento é classicamente dividida em quatro fases, na ordem em que aparecem: fase de adaptação; fase exponencial; fase estacionária; e a fase de declínio. A fase de adaptação é o período da ausência de divisão celular, em que as células se encontram em intensa atividade metabólica, sendo uma fase que pode inexistir. A fase exponencial ocorre quando as células iniciam seu processo de divisão máxima entrando no período de crescimento. Durante esse período, a reprodução celular encontra-se extremamente ativa, e o tempo de geração atinge um valor constante, sendo o período de maior atividade metabólica da célula. A fase estacionária é alcançada no determinado momento que a velocidade de crescimento diminui. O número de células mortas é equivalente ao número de células novas, a população se torna estável e a atividade metabólica dessa fase é diminuída. E a fase de declínio se dá quando a população parasitária que entra em morte celular excede o de células novas; essa fase continua até que a população tenha diminuído para uma pequena fração do número de células da fase anterior, ou até que tenha desaparecido totalmente (TORTORA; FUNKE; CASE, 2012).

O cultivo das formas epimastigotas do *T. cruzi* permite avaliar todas as fases da curva de crescimento, entretanto as fases exponencial e estacionária apresentam maior importância biológica, pois a primeira está envolvida na proliferação e manutenção do parasita no meio em que ele se encontra (*in vivo* ou *in vitro*) e a segunda está associada a transição do parasita na preparação para a sua diferenciação pela metaciclogênese, o que tem sido observado desde o início do trabalho de CAMARGO (1964) em que o surgimento de formas tripomastigotas metacíclicas eram relatadas ao longo da fase estacionária. Portanto, o entendimento do que

ocorre com o parasita durante a transição da fase exponencial para fase estacionária tem importante relevância no entendimento da biologia desse protozoário.

### 1.7.1 Fase estacionária

O momento de entrada na fase estacionária ainda não foi claramente definido em epimastigotas de *T. cruzi*. Como definição geral, a fase estacionária se refere a uma característica comum observada no crescimento de diversos microrganismos em cultura em que a taxa de crescimento para devido à depleção de nutrientes. Além disso, as células em fase estacionária tornam-se diferenciadas de maneira que permitem que sua viabilidade seja prolongada por longos períodos sem a adição de nutriente, mas mantendo sua habilidade de voltar a proliferar imediatamente após que a disponibilidade de nutrientes seja reestabelecida (WERNER-WASHBURNE et al., 1993). Assim, culturas de epimastigotas de fase estacionária quando diluídas em um novo meio de cultivo com nutrientes frescos retomam o crescimento. Em ambientes naturais, a equivalência da fase estacionária em culturas pode ser encontrada no intestino do vetor na presença de pouca quantidade de nutrientes (HERNÁNDEZ et al., 2012). Células de *T. cruzi* que colonizam o intestino do vetor podem sobreviver por pelo menos 60 dias entre as refeições de sangue do inseto (KOLLIEN; SCHMIDT; SCHAUB, 1998). Esta fase tem um aspecto crítico na biologia de células de diferentes microrganismos, porém em tripanossomatídeos existem poucos estudos genéticos sobre este período (HERNÁNDEZ et al., 2012).

Como mencionado acima, a falta de nutrientes é um dos fatores mais importantes para que o organismo entre em fase estacionária, sendo o mais comum dos estresses encontrados por diferentes organismos, estimando que grande parte da biomassa de microrganismos no mundo exista sob baixa condição nutricional. Dessa forma, a transição da fase exponencial para fase estacionária em epimastigotas de *T. cruzi* é marcada pelo esgotamento da glicose em meio de cultura e na adaptação da célula em catabolizar aminoácidos, indicada pela grande quantidade de excreção de amônia no meio (CAZZULO et al., 1985). Este cenário está ligado a uma complexa interação do catabolismo da glicose preferencial por fermentação, a modificação do metabolismo e a regulação da expressão gênica ativada pelos baixos níveis de glicose, e subsequentemente a resposta a essa depleção de fontes de carbono fazem da entrada na fase estacionária um processo bem mais complicado do que a simples resposta a jejum de um nutriente (HERNÁNDEZ et al., 2012).

Na fase estacionária também tem sido relatada uma maior taxa de degradação de proteínas intracelulares (HENRIQUEZ et al., 1993), possivelmente como um meio para fornecer aminoácidos. Curiosamente, a degradação de proteínas durante a fase exponencial é diminuída se os meios das culturas testadas são suplementados com glicose ou soro (HENRIQUEZ et al., 1993). Além disso, os padrões proteolíticos de epimastigotas de *T. cruzi* observados em géis sustentam o aumento da atividade proteolítica durante a fase estacionária. Interessantemente, foi descrito que durante a metaciclogênese, o *T. cruzi* usa proteínas e lipídios previamente armazenados em reservossomos, o que é consistente com a sua utilização como fonte de energia primária (SOARES et al., 1989). Compatível com esses dados, um trabalho de análises proteômicas com gel 2D de células *T. cruzi* submetidos a metaciclogênese, identificou dois *spots* de proteínas de glutamato desidrogenase que apareciam acumuladas durante o estresse nutricional (PARODI-TALICE et al., 2007). Estas enzimas estão ligadas ao metabolismo do carbono e do nitrogênio que catalisam a desaminação reversível da L-glutamato a 2-oxoglutarato. A caracterização destas proteínas e os mecanismos envolvidos no seu aumento durante o começo da metaciclogênese poderiam ser informativos para compreender melhor a resposta ao estresse nutricional. Quanto ao catabolismo de tripomastigotas metacíclicos, tem sido relatado que estas células têm um catabolismo não glicolítico e derivam a sua energia exclusivamente a partir de proteínas e aminoácidos (URBINA; OSORNO; ROJAS, 1990). Todas estas observações sugerem que o metabolismo de células em fase estacionária alterna para um estágio de pré-adaptação para os processos celulares que ocorrem durante metaciclogênese.

Outro importante fator que parece estar associado à transição das fases exponencial para estacionária é a densidade celular, que ao aumentar ao longo da curva de crescimento associada à depleção de nutrientes leva a variações na morfologia e complexidade mitocondrial do parasita (TYLER; ENGMAN, 2000). Formas epimastigotas apresentam morfologicamente definidas como o estágio em que o cinetoplasto e a base do flagelo estão posicionados anteriores ao núcleo. Se as células nesse estágio forem mantidas em fase de crescimento exponencial, a morfologia celular parece se manter homogênea, entretanto durante a fase estacionária foi demonstrado o alongamento do corpo celular e do flagelo (TYLER; ENGMAN, 2000). Este fenômeno tem sido associado ao consumo de glicose a partir do meio, onde o flagelo mais longo se liga ao substrato, processo que é requerido para o desenvolvimento de formas metacíclicas (BONALDO et al., 1988), assim a extensão desta estrutura pode representar uma adaptação para esse processo de desenvolvimento. Outra hipótese que pode ser somada é que, em um

cenário de privação de nutrientes, a extensão do flagelo pode fornecer uma maior área de membrana para a absorção de nutrientes. A ocorrência de transportadores de glicose no flagelo de células de *Leishmania* pode ser paradigmático para esta proposta (SNAPP; LANDFEAR, 1997).

Estudos da morfologia do núcleo de epimastigotas de *T. cruzi* de células estacionárias revelaram características intermediárias em comparação aos núcleos das células de fase exponencial e tripomastigotas metacíclicos. Em tripomastigotas metacíclicos, o núcleo tem sido caracterizado como uma organela alongada, com elevado quantidade de heterocromatina dispersa e ausência de nucléolos, condizente com o reduzido volume de proteínas ribossomais já relatado nesta fase do desenvolvimento (ATWOOD et al., 2005; CAROLINA et al., 2001). Os epimastigotas de fase exponencial apresentam um nucléolo granular bastante sólido que é acentuadamente reduzido durante a fase estacionária. Em imagens de microscopia eletrônica, os núcleos das células estacionárias aparecem com uma distribuição de heterocromatina dispersa e aumentada. Entretanto se essas culturas são diluídas em meio novo, o crescimento celular recomeça, e a arquitetura nuclear novamente apresenta um nucléolo robusto e a heterocromatina aparece focalizada na periferia (NEPOMUCENO-MEJÍA et al., 2010).

De um ponto de vista energético, todo o processo de transcrição e síntese proteica das células em crescimento é um processo bastante oneroso, sendo geralmente regulada. Assim, quando a atividade transcricional foi comparada entre culturas de epimastigotas de fase exponencial e de fase estacionária, verificou-se que durante a fase exponencial existe um aumento de seis a dez vezes no processo de transcrição em relação às células estacionárias (NEPOMUCENO-MEJÍA et al., 2010). Nesse cenário, a abundância individual de quatro mRNAs "*housekeeping*", como actina, triosefosfato-isomerase, tripanotiona redutase e a proteína ribossomal S4, foram reduzidas para menos de metade ao longo da fase estacionária (CEVALLOS et al., 2005). Além disso, a meia-vida desses transcritos (e de espécies precursoras de rRNA) é expandido por três a sete vezes nestas culturas estacionárias. A ocorrência de um mecanismo para poupar energia, o qual poderia permitir que as células sobrevivessem durante prolongadas condições de estresses poderia ser hipotetizado. Um mecanismo que poderia ter um papel na estabilização de transcritos em resposta a um estresse nutricional em epimastigotas seria o recrutamento de mRNAs para grânulos citoplasmáticos de ribonucleoproteína microscopicamente visíveis (CASSOLA; GAUDENZI; FRASCH, 2007). Aparentemente estes grânulos armazenam transcritos impedindo a sua degradação em condições de inanição. Curiosamente, os grânulos de mRNA nunca foram observados durante metaciclogênese *in vitro* (CASSOLA; GAUDENZI; FRASCH, 2007). Tendo em conta que a

resposta ao estresse nutricional e a metaciclogênese são eventos que podem estar relacionados, mas ainda processos distintos, o aparecimento de tais grânulos pode refletir um fenômeno relacionado as células em condição de estresse e não em um estado de comprometimento para sua diferenciação em tripomastigota metacíclico. Esta hipótese pode ser apoiada pelo fato que após a adição de nutrientes para as células em jejum, grânulos de mRNA são desmontados (CASSOLA; GAUDENZI; FRASCH, 2007).

Com relação à síntese de proteínas, estudos mostraram a ocorrência da fosforilação no fator de iniciação da tradução 2 (eIF2α), a qual provoca a inibição da síntese proteica de maneira geral, fato necessário para ocorrer a metaciclogênese (SONENBERG; HINNEBUSCH, 2009). Dessa forma, a hipótese de que exista um mecanismo para economia da energia, acionado quando a taxa de crescimento das células é reduzida neste organismo é apoiada pela diminuição da expressão gênica e da síntese de proteína total que ocorre durante a desaceleração do crescimento ou do processo de metaciclogênese (HERNÁNDEZ et al., 2012).

## 1.8 METABOLISMO DO TRYPANOSOMA CRUZI

A maioria dos tripanossomatídeos dependem de fontes de carbono disponíveis em seus hospedeiros para o seu metabolismo energético (BRINGAUD; RIVIÈRE; COUSTOU, 2006). O inseto hematófago obtém sua energia predominantemente de L-prolina e L-glutamina, sendo os maiores constituintes da sua hemolinfa e fluidos tissulares (BURSELL, 1981), dessa maneira as formas epimastigotas, presentes no inseto, dependem do catabolismo de aminoácidos, preferencialmente de L-prolina (CANNATA; CAZZULO, 1984). Além disso, em *T. cruzi* a utilização de D-prolina é possível devido ao fato do parasita expressar uma prolina racemase, enzima que catalisa a reação de interconversão entre L-prolina e D-prolina (ATWOOD et al., 2005).

Embora todos os estágios do *T. cruzi* possam ser obtidos em diferentes tipos de culturas ou meios de diferenciação, a maioria dos trabalhos de metabolismo são realizados nas formas epimastigotas, mas estudos com os outros estágios celulares já mostraram características metabólicas similares. Ainda que epimastigotas normalmente vivam num ambiente em que a glicose é supostamente escassa (intestino do inseto), eles preferem glicose aos aminoácidos, mesmo que a L-prolina e outros aminoácidos sejam facilmente transportados e consumidos (CAZZULO, 1994). O mesmo é verificado em tripomastigotas, onde a expressão de transportadores de glicose é ainda maior do que em epimastigotas (SILBER et al., 2009). Já a forma intracelular amastigota, onde a glicose livre não é abundante e não há expressão de

transportadores de glicose, acredita-se que essa forma obtém sua energia principalmente a partir de aminoácidos, apesar de não se descartar a oxidação de ácidos graxos (SILBER et al., 2009).

### 1.8.1 Fermentação aeróbica da glicose

Em geral, tripanossomatídeos possuem uma alta taxa de consumo de carboidratos quando cultivados em meio axênico (CAZZULO, 1992), assim o crescimento de epimastigotas de *T. cruzi* em meio complexo é inicialmente suportado por um rápido consumo de glicose, quando sua biomassa é aumentada após a completa depleção da fonte de carboidrato disponível (URBINA, 1994a). De forma incomum eles degradam os carboidratos incompletamente, mesmo na presença de $O_2$. Dessa forma, em vez de oxidar a glicose completamente a $CO_2$ e $H_2O$ (CAZZULO, 1992), eles excretam para o meio fermentativo compostos ainda reduzidos deste catabolismo, como ácidos monocarboxílicos e dicarboxílicos, sendo principalmente succinato e em menores quantidades L-alanina e acetato (URBINA, 1994a).

Outra particularidade em tripanossomatídeos é a ausência completa do “efeito Pasteur” durante a glicólise. Esse efeito ocorre entre a troca de um ambiente anaeróbico para aeróbico, acompanhado pela rápida diminuição do consumo de glicose, regulado pela concentração de enzimas específicas da via glicolítica e do ciclo do ácido cítrico. Entretanto esses parasitas mostram um "efeito Pasteur reverso", o que significa que o consumo de glicose pode ser ainda menor em condições anaeróbias. Este comportamento estranho está relacionado com a falta dos principais controles na via glicolítica (revisto por MAUGERI; CANNATA; CAZZULO, 2011).

Tanto a via glicolítica como a via pentose fosfato são operativas em epimastigotas de *T. cruzi* (CANNATA; CAZZULO, 1984). A via glicolítica em tripanossomatídeos possui uma característica peculiar, pois ocorre de forma compartimentalizada, pois esses parasitas apresentam uma organela especial, o glicossomo, que possui as seis primeiras enzimas envolvidas nessa via. Em adição, este sub-compartimento celular também possui enzimas de outras vias metabólicas, como a via da pentose fosfato, β-oxidação de ácidos graxos, salvamento da purina, via biossintética para pirimidinas, outros lipídeos e esqualeno (MICHELS et al., 2006).

### 1.8.2 Via glicolítica

A glicose é consumida por transporte facilitado, sendo que o gene codificador para proteína transportadora de glicose está presente no genoma em um cluster com 12 cópias em tandem (TETAUD et al., 1994). Após entrar na célula, a glicose é direcionada ao glicossomo, onde as enzimas presentes através de sete reações sequenciais a convertem em 3-fosfoglicerato. A primeira reação é a fosforilação da glicose em glicose-6-fosfato e é catalisada por duas enzimas diferentes, a hexocinase (HK) e a glicocinase (GK). A HK de *T. cruzi* não apresenta inibição regulatória pela concentração de glicose-6-fosfato como em outros eucariotos. A glicose-6-fosfato é convertida em frutose-6-fosfato pela enzima fosfoglicose isomerase; essa enzima está presente em epimastigotas de *T. cruzi* sob duas isoformas, uma glicossomal e outra citosólica. A terceira reação é catalisada pela enzima fosfofrutocinase (PFK), a qual em muitos organismos é a principal enzima regulatória da via glicolítica, entretanto em alguns tripanossomatídeos parece ser nula ou pouco afetada por efetores como adenosina trifosfato (ATP), citrato e fósforo inorgânico (Pi). Na última reação de fosforilação que é realizada pela enzima fosfogliceratocinase (PGK), o *T. cruzi* possui três isoformas para essa enzima, as PGKA e PGKC que são glicossomais e a PGKC que é citosólica, todas expressas em epimastigotas. O 3-fosfoglicerato no citosol sofre mais duas reações em que é convertido em fosfoenolpiruvato (PEP), que é oxidado a piruvato, que por sua vez produzirá L-alanina. O PEP que está no citosol pode retornar ao glicossomo, onde pode ser convertido a L-alanina ou a succinato. O piruvato que alcança a mitocôndria será oxidado em Acetil-CoA, que por sua vez entra no ciclo do ácido cítrico.

### 1.8.3 Vias das pentoses fosfato

Assim como na maioria dos eucariotos, o principal destino catabólico da glicose-6-fosfato é a degradação glicolítica até piruvato. Entretanto a glicose-6-fosfato pode ser também direcionada à via das pentoses fosfato (PPP, do inglês *pentose phosphate pathway*), na qual ocorrerá a oxidação da glicose-6-fosfato até pentoses-fosfatos. As principais funções dessa via são a redução de $NADP^+$ em NADPH, necessárias para reações biossintéticas e também para a proteção das células contra o estresse oxidativo acometido pelas espécies reativas de oxigênio (ROS, do inglês *Reactive Oxygen Species*), bem como para a produção de ribose-5-fosfato, usado na síntese de ácido nucleico. As sete enzimas dessa via estão presentes nos quatro principais estágios do ciclo de vida do parasita, sendo de localização citosólica, com exceção

da epimerase ribose-5-fosfato (Ru5PE). Experimentos com epimastigotas em condições normais demonstraram que 10% da glicose é metabolizada pela PPP e quando submetido a presença de 0,2 mM de azul de metileno, um mimetizador de estresse oxidativo, o dobro de glicose passa a ser metabolizada por essa via (MAUGERI; CAZZULO, 2004).

A via das pentoses fosfato é dividida em duas fases, uma oxidativa e uma não oxidativa. A fase oxidativa começa com a oxidação da glicose-6-fosfato, pela enzima glicose-6-fosfato desidrogenase, a qual controla o fluxo da via e é responsiva pela proporção de $NADP^+$/NADPH na célula. Essa enzima está codificada em genes multicópias em três diferentes cromossomos em CL Brener (IGOILLO-ESTEVE; CAZZULO, 2006). Dessa reação é formado o éster intramolecular 6-fosfoglicona-lactona, formando o primeiro NADPH. Em seguida a lactona é hidrolisada ao ácido livre 6-fosfogliconato por uma lactonase específica, que sofre oxidação e descarboxilação pela 6-fosfogliconato-desidrogenase para formar a cetopentose ribulose-5-fosfato, formando o segundo NADPH.

### 1.8.4 Metabolismo de aminoácidos

Após a exaustão da glicose do meio de cultivo de epimastigotas de *T. cruzi*, acontece o catabolismo de proteínas e aminoácidos com a formação de $-NH_2$ que pode ser convertido em $NH_3$ (CANNATA; CAZZULO, 1984; CAZZULO, 1992). Existem três formas de obtenção de aminoácidos pelos parasitas, através do transporte, biossíntese a partir de precursores metabólicos e através da degradação de proteínas (CANNATA; CAZZULO, 1984). Classicamente tem sido reportado que o *T. cruzi* pode metabolizar os aminoácidos asparagina, aspartato, glutamina, glutamato, leucina, isoleucina e prolina (CAZZULO, 1992; ZELEDON, 1960), os quais podem ser convertidos em glutamato ou aspartato no citoplasma e ser encaminhados à mitocôndria para entrar no ciclo do ácido cítrico (SILBER et al., 2005). O acúmulo de $NH_3$ devido ao catabolismo dos aminoácidos é detoxificado por um conjunto de enzimas desidrogenases e transaminases. As desidrogenases fazem a transferência de $NH_3$ para acetoácidos, como o α-cetoglutarato, o qual é convertido em glutamato (BARDERI et al., 1998). As transaminases são responsáveis pela transferência do grupo $-NH_2$ de grande parte dos aminoácidos para o piruvato, e assim produzindo alanina e liberando os acetoácidos para serem oxidados ou reciclados como intermediários no ciclo do ácido cítrico, dessa forma o parasita evita o acumulo de $NH_3$ que pode ser tóxico para si e acumula L-alanina (SILBER et al., 2005, 2006).

## 1.9 CONDIÇÕES DE ESTRESSE

O *T. cruzi* passa por diversas modificações durante seu ciclo de vida, o que impõe a esse parasita uma grande habilidade de adaptação a diversas situações ambientais, que podem ser alteradas rapidamente para que eles possam sobreviver e dar continuidade ao ciclo. Dentre as diferentes condições ambientais a que este parasita está exposto nos hospedeiros, podem se destacar as diferenças de temperatura, a disponibilidade de nutrientes e as alterações de pH. Como visto anteriormente, a exposição de formas epimastigotas de *T. cruzi* a um ambiente pobre em nutrientes in vivo ou *in vitro* leva à diferenciação para as formas tripomastigotas metacíclicas (BONALDO et al., 1988; CONTRERAS et al., 1988b; KOLLIEN; SCHAUB, 2000). Além do estresse nutricional, condições de temperatura e de pH também parecem exercer influência na metaciclogênese *in vitro*. No trato intestinal do inseto vetor, o pH varia entre 5,9 e 8,9, de acordo com os períodos de jejum e de refeição de sangue (KOLLIEN; SCHAUB, 2000). Alguns dados mostram que cerca de dois meses após a alimentação, a excreta de triatomíneos é ácida e a população de parasitas nas excretas é principalmente constituída de tripomastigotas metacíclicos (TOMLINSON et al., 1995), confirmando a importância de estudos com relação às alterações de pH. Um estudo avaliando a exposição de formas epimastigotas a diferentes condições de estresse durante a metaciclogênese, demonstrou que diferentes tipos de estresse (meio TAU, meio LIT a 37°C ou meio LIT com pH 5,0) foram capazes de levar à diferenciação *in vitro* para as formas tripomastigotas metacíclicas, sendo que as obtidas em condições de estresse térmico e de pH tiveram a mesma capacidade infectiva que as formas obtidas após exposição ao estresse nutricional (MONTEIRO, 2008).

No processo de diferenciação *in vitro* das formas tripomastigotas metacíclicas para as formas amastigotas, denominada amastigogênese, a incubação dos parasitas a 37°C em um meio rico em proteínas é suficiente para promover a diferenciação e obter quantidade significativa de amastigotas com morfologia e propriedades biológicas e antigênicas similares àquelas de amastigotas intracelulares (CONTRERAS et al., 1988b). De modo semelhante, a incubação de tripomastigotas por 2 h em um meio com pH 5,0 leva à transformação em amastigotas com características equivalentes às formas isoladas *in vivo* (TOMLINSON et al., 1995).

A exposição a condições de estresse também parece ser relevante para os processos de diferenciação de outros tripanossomatídeos. Na diferenciação celular *in vitro* de formas sanguíneas para formas procíclicas de *T. brucei*, a incubação em meio com pH 5,5 a 37 °C por 2 horas não só acelerou a transformação das formas sanguíneas (presentes em mamíferos) longas para as curtas, mas também permitiu a obtenção de formas procíclicas (presentes no inseto) (ROLIN et al., 1998). O protozoário do gênero *Leishmania* também tem um ciclo de vida heteroxênico, envolvendo formas promastigotas extracelulares no aparelho digestivo do inseto vetor e formas amastigotas intracelulares no hospedeiro mamífero. As formas promastigotas são transmitidas pelo inseto ao mamífero, onde são rapidamente fagocitadas. Dentro do fagolisossomo, ou vacúolo parasitófago, podem sobreviver ao ambiente ácido desta organela e se transformar nas formas amastigotas (BURCHMORE; BARRETT, 2001). Foi verificado que a combinação de redução do pH e elevação da temperatura é capaz de induzir a transformação das formas promastigotas em amastigotas, além de alterar a expressão de vários genes nas formas promastigotas deste parasita (ZILBERSTEIN; SHAPIRA, 1994).

Estudos em larga escala permitem compreender a regulação e coordenação da expressão gênica, sendo um aspecto importante desses estudos a compreensão da resposta celular a cada mudança de ambiente pela reorganização de expressão gênica (GASCH; WERNER-WASHBURNE, 2002). Assim, estudos de reprogramação gênica gerada a cada novo ambiente, promovem descobertas de quando, onde e como cada gene é expresso, sugerindo possíveis mecanismos que a célula usa para sobreviver às mudanças ambientais.

### 1.9.1 Disponibilidade de nutrientes

De maneira geral a manutenção de epimastigotas de *T. cruzi* em meio axênico sob condições específicas de restrição de nutrientes ou em inanição tem importantes consequências no crescimento do parasita (PEREIRA et al., 2011), com modificações em seu metabolismo e a indução da metaciclogênese (FIGUEIREDO; ROSA; SOARES, 2000). O estresse nutricional induz a uma diminuição global na tradução, mediada pela fosforilação e inibição de eIF2. Em epimastigotas de *T. cruzi*, a fosforilação de eIF2 é induzida por incubação em meio pobre em nutrientes causando uma significativa redução de polissomas e diminuição da síntese proteica. Curiosamente em parasitas em que a fosforilação de eIF2 é prejudicada ocorre falha na diferenciação para tripomastigotas metacíclicos, indicando que a via de sinalização de eIF2 poderia regular a progressão do ciclo celular em *T. cruzi* (TONELLI et al., 2011).

A inanição também é um importante indutor de autofagia e reciclagem de organelas em diferentes células e poderia ser um mecanismo de remodelamento celular contribuindo para a diferenciação (YORIMITSU; KLIONSKY, 2005). Em epimastigotas, a inanição induz a formação de autofagossomos levando à transformação em formas tripomastigotas metacíclicas (ALVAREZ et al., 2008).

Surge então a questão: a inanição é uma situação fisiológica durante o ciclo de vida do *T. cruzi*? Em hospedeiros mamíferos existe uma abundância em nutriente, com alta concentração de glicose e aminoácidos, em contrapartida, em triatomíneos a ingestão de alimentos pode demorar aproximadamente 10 dias ou mais, sendo que no período de pouco aporte de nutrientes as condições químicas no intestino do inseto mudam drasticamente, afetando o desenvolvimento do parasita (KOLLIEN; SCHMIDT; SCHAUB, 1998). Embora a restrição de nutrientes seja um conhecido indutor de diferenciação *in vitro*, ainda se questiona se somente a ausência de componentes específicos impulsionaria os primeiros passos na diferenciação ou se fatores produzido pelo parasita sob estresse nutricional regulariam a transição ao próximo estágio de desenvolvimento.

*Quorum sensing* é um sistema de estímulos e respostas direcionadas conforme a densidade populacional do ambiente, sendo especialmente utilizado por diferentes espécies de bactéria para coordenar a expressão gênica em diferentes cenários sob esse aspecto (MILLER; BASSLER, 2001; NEALSON; HASTINGS, 1979). Mecanismos *quorum-sensing* são uma sugestão para a diferenciação, como ocorre em *T. brucei* (revisto por MONY; MATTHEWS, 2015). Nenhuma proteína que atuaria como mecanismo de *quorum sensing* foi identificada em *T. cruzi*, mas em epimastigotas a transição da fase exponencial para a estacionária ocorre uma determinada densidade celular constante, característica de cada cepa, independente da disponibilidade de nutrientes, apontando para a presença de um mecanismo relacionado que poderia ser gerado por restrição de nutrientes, mas não estritamente por ele causado (TYLER; ENGMAN, 2000).

Como já mencionado, o processo de metaciclogênese é dependente da fixação do flagelo a um substrato, tanto no vetor como *in vitro* (BONALDO et al., 1988; KOLLIEN; SCHMIDT; SCHAUB, 1998; BONALDO et al., 1988). A superfície de ligação é mediada em parte por proteínas glicosiladas, gp82 e gp90, pertencentes a família das transialidases, que são reguladas positivamente em formas metacíclicas sobre a diferenciação induzida por inanição, além disso ambas proteínas influenciam na infectividade do parasita (BAYER-SANTOS et al., 2013). É possível que a inanição induza alterações no perfil de expressão de moléculas de superfície que

por sua vez, medeiam a adesão e regulam a progressão do processo de diferenciação.

### 1.9.2 Mudança de temperatura

No inseto vetor a temperatura varia de 10 a 26 °C, flutuando diariamente dependendo do habitat do vetor. Após a invasão ao vertebrado, a mudança para uma temperatura altamente elevada faz com que o parasita desenvolva uma resposta ao estresse, caracterizada pelo aumento das proteínas de choque térmico (HSPs, do inglês *Heat Shock Proteins*) (PÉREZ-MORALES; OSTOA-SALOMA; ESPINOZA, 2009a). Um aumento similar ocorre em *Leishmania spp* na diferenciação de promastigotas para amastigotas (SAAR et al., 1998) e em promastigotas de *T. brucei*, no qual aparentemente não foram verificadas mudanças na quantidade total de mRNA de HSP70 nas formas procíclicas, somente nos níveis proteicos (HÄUSLER; CLAYTON, 1996).

As HSPs, também denominadas de chaperonas, são componentes chaves da resposta ao estresse térmico, prevenindo dobramentos errados e agregação proteica, também regulando localização e secreção de proteínas. Em tripanossomatídeos, as HSPs têm sido estudadas principalmente por análise genômica (FOLGUEIRA; REQUENA, 2007), mas a dinâmica de indução e o papel das chaperonas específicas durante o choque térmico estão longe de serem compreendidos. Epimastigotas quando expostos a 37°C demonstram um aumento de mRNA e do nível proteico das HSP70, HSP60 e HSP40, enquanto os níveis gerais de transcrição caem. Ainda quando incubadas com uma temperatura maior, 42°C, os níveis de mRNA da HSP70 diminuem, enquanto o nível de proteínas aumenta (DE CARVALHO et al., 1990). Além disso, no choque a 42°C ocorre tanto a inibição do *splicing* como a poliadenilação, enquanto os pré-mRNAs da HSP70 acumulam em polissomas (ENGMAN et al., 1995). A translocação do mRNA maduro ao núcleo e nucléolo (NÁZER; VERDÚN; SÁNCHEZ, 2012) e a redistribuição de proteína para a periferia das células (GIAMBIAGI-DEMARVAL; SOUTO-PADRÓN; RONDINELLI, 1996) também foram observados.

Em *T. cruzi*, a família homóloga da HSP40 tem apenas um membro, TcJ2, que mostrou um aumento de mRNA após o choque térmico (TIBBETTS et al., 1998). Os níveis de mRNA codificador da proteína HSP104 e dela própria estão aumentados em choque térmico (CAMPOS et al., 2012), além disso mRNAs de pequenas chaperoninas (HSP10 e HSP16) também estão aumentados em choque térmico (FERNANDES et al., 2005; PÉREZ-MORALES; OSTOA-

SALOMA; ESPINOZA, 2009b). Eletroforese de gel bidimensional e análises proteômicas de 24 pontos diferenciais de epimastigotas submetidos a 42°C apresentaram um aumento de um pequeno número de proteínas relacionadas com o estresse, incluindo HSP70 e HSP40, mas não foram observadas grandes alterações na expressão de proteínas sob estas condições (PÉREZ-MORALES et al., 2012).

O mecanismo pelo qual a HSP70 e possivelmente outras HSPs são reguladas positivamente dependem da estabilização dos mRNAs. Em tripanossomatídeos, a estabilidade e degradação de mRNA é controlada por elementos cis-atuantes na região UTR-3' (CLAYTON; SHAPIRA, 2007). Foi demonstrado que a meia-vida dos mRNAs da HSP70 é de 60 minutos a 29°C e 127 minutos a 37°C. Esse efeito é mediado por elementos ricos em uridina na região UTR-3' e sítios aceptores de *trans-splicing* na UTR-5' (RODRIGUES et al., 2010). Uma proteína de dedos de zinco em *T. brucei*, ZC3H11, induzida por choque térmico, se liga especificamente a regiões ricas em AU na UTR-3', estabilizando os mRNAs de várias HSPs e outras proteínas relacionadas ao estresse (DROLL et al., 2013). Assim é razoável especular que proteínas semelhantes possam estar presentes em *T. cruzi*.

Um aspecto da mudança de temperatura pouco estudado é o seu efeito sobre a dinâmica e a composição lipídica nas membranas, e como essas modificações afetam as respostas celulares. A fim de manter a fluidez constante e preservar as funções das proteínas, as células respondem a mudança na temperatura alterando a sua composição da membrana. Isso é chamada de adaptação homeoviscosa e é um passo fundamental na resposta celular ao estresse térmico em todos os organismos (ALOIA; RAISON, 1989; BUDA et al., 1994; SINENSKY, 1974). A troca de temperatura que ocorre na natureza entre as formas epimastigotas para metacíclicas, de 28 a 37°C, leva ao aumento da proporção de esterol/fosfolipídeos, após 24 a 48 horas de choque quente. Ao contrário de outras células, eles aumentam o conteúdo de ácidos graxos insaturados relacionados com esteróis neutros e triglicerídeos, o que sugere que um interruptor de ácidos graxos pode ocorrer (FLORIN-CHRISTENSEN et al., 1997). As consequências funcionais da adaptação homeoviscosa em tripanossomatídeos durante a adaptação térmica ainda não foram determinadas. Em bactérias (NAGY et al., 2007; SHIGAPOVA et al., 2005) e plantas (MITTLER; FINKA; GOLOUBINOFF, 2012), um aumento da temperatura resulta na fluidificação transitória da membrana e a ativação da entrada de $Ca^{2+}$ no plasma. O aumento do $Ca^{2+}$ ativa fatores de choque térmico regulando a expressão de proteínas HSPs, desencadeando vias de sinalização. Além do $Ca^{2+}$, a proteína Hsf (fatores de choque térmico, do inglês *Heat shock factors*) controla a expressão gênica de proteínas HSPs

e gatilhos que desencadeiam várias cascatas de sinalização (BALOGH et al., 2013). Em tripanossomatídeos, ainda não foram relatadas evidências proteicas da existência de Hsf, o que não surpreende uma vez que o controle das proteínas HSPs é pós-traducional. Então como o parasita detecta mudanças de temperatura e desencadeia respostas compensatórias? Uma possibilidade seria a existência de RNAs que atuariam como sensores devido a sua capacidade de sofrer alterações conformacionais induzidas pela temperatura. Poucos exemplos têm sido descritos em bactérias e células de mamíferos, nas quais a eficiência de tradução para genes de estresse e relacionados à virulência pode ser controlada por termosensores de RNA (JOHANSSON et al., 2002; SHAPIRO; COWEN, 2012).

Outra possibilidade seria a mudança nas interações lipídio-proteína e na dinâmica da membrana lipídica como transdutores de sinais do estresse térmico. A mudança de temperatura levaria à reorganização da estrutura lipídica, adaptando-se a temperatura e promovendo a troca das balsas lipídicas ricas em colesterol por balsas lipídicas ricas em ceramida, formando um domínio de membrana mais rígido e levando ao aumento da densidade de receptores e moléculas de sinalização necessários para a comunicação intracelular de estímulos externos (BALOGH et al., 2013). As balsas lipídicas são abundantes nas membranas flagelares de *T. cruzi* (MARIC et al., 2011) e *T. brucei* (TYLER et al., 2009), dirigindo a localização de moléculas de sinalização, como moléculas relacionadas ao AMPc e canais de $Ca^{2+}$ (MARIC; EPTING; ENGMAN, 2010; OBERHOLZER et al., 2011). O flagelo tem sido descrito como uma estrutura sensível em tripanossomatídeos, assim a reorganização lipídica em resposta a uma mudança de temperatura poderia ser uma das maneiras de gerar sinais direcionados a partir do flagelo ao corpo celular como forma de desencadear respostas adaptativas ao parasita. Além disso, essa modificação na densidade de canais de $Ca^{2+}$ levaria a uma intensa resposta biológica, uma vez que o $Ca^{2+}$ tem um importante papel na diferenciação e invasão de *T. cruzi* (CALER et al., 2000; LAMMEL et al., 1996).

## 2 GENÔMICA FUNCIONAL

As diversas modificações morfológicas, funcionais e bioquímicas que ocorrem no parasita ao longo do seu ciclo de vida refletem uma adaptação às distintas condições biológicas encontradas no interior dos hospedeiros (TYLER & ENGMAN, 2001). O estudo dos aspectos celulares, bem como dos mecanismos de regulação da expressão gênica envolvidos nesses processos foi auxiliado pela possibilidade de obtenção *in vitro* de maior quantidade de parasitas

em diferentes formas evolutivas e em vários estágios de diferenciação, e principalmente pela evolução tecnológica que tem ocorrido nos últimos anos, especificamente importante para o nosso trabalho, o sequenciamento em larga escala.

Trabalhos que utilizam a genômica funcional para avaliar a expressão gênica de um organismo em determinada condição também são definidos como estudos em larga escala (MCGETTIGAN, 2013). O estudo do conjunto completo de moléculas de RNA de uma célula é chamado de transcritômica (DONG; CHEN, 2013) e o estudo do conjunto completo de proteínas de proteômica (GILMORE; WASHBURN, 2010).

## 2.1 Transcriptômica

Desde que foram introduzidas no mercado em 2004 as tecnologias de sequenciamento de DNA de segunda geração impulsionaram os estudos em larga escala. Quatro equipamentos consolidados no mercado [454 GenomeSequencer FLX (Roche Applied Science), Illumina Genome Analyser, SOLiD (Applied Biosystems) e Ion Torrent Technology (Life Technologies)] tiveram suas respectivas vantagens e desvantagens revisadas recentemente (revisto por METZKER, 2010; revisto por BUERMANS; DEN DUNNEN, 2014; revisto por NGUYEN; BURNETT, 2014). Entre as principais vantagens encontradas nas estratégias de sequenciamento de segunda geração, em relação ao sequenciamento clássico de Sanger, podem ser citadas a ausência do laborioso processo de clonagem *in vivo*; o alto grau de paralelismo devido a sequenciamento em células de fluxo; a utilização de volumes reduzidos de reagentes e maior produtividade de dados (revisto por SHENDURE; JI, 2008).

Os sistemas de sequenciamento de segunda geração variam em detalhes técnicos, mas com o mesmo objetivo de realizar o sequenciamento massivo ou em larga escala. De maneira detalhada, a base da aplicação são as leituras pequenas para determinar o sítio de origem da sequência no genoma de referência sem a necessidade de sequenciar a totalidade de cada molécula presente na amostra inicial. Cerca de 30 nucleotídeos (tag) no caso do SOLiD, já possibilitam identificação através do alinhamento. Desta forma, o número de leituras que mapeiam em uma determinada região do genoma correlaciona-se com a abundância da mesma na amostra original (WOLD & MYERS, 2008). Esse método propiciou uma nova maneira de analisar transcritomas (RNA-Seq), sítios genômicos de ligação de proteínas (CHIP-Seq) e padrões de metilação de genoma (Metil-Seq) (WOLD & MYERS, 2008; MOROZOVA & MARRA, 2008).

O desenvolvimento de tecnologias de sequenciamento de DNA de terceira geração

[Pacific Biosciences Technologie (PacBio) e Nanopore Technologies (em fase de testes)] utilizam o sequenciamento de moléculas únicas, não sendo necessária a amplificação das amostras como nas tecnologias de segunda geração, possuem um baixo custo, simples preparação do material, tempos de corrida bem menores e leituras longas (revisto por BUERMANS; EN DUNNEN, 2014). O novo desafio é a análise e interpretação da grande quantidade de dados gerados (MARDIS, 2010).

## 2.2 Proteômica

A proteômica teve seu início desde o final da década de 1970 quando pesquisadores iniciaram a formação de bancos de dados de proteínas utilizando a técnica de eletroforese de gel bidimensional, tecnologia disponível na época (O'FARRELL, 1975). O desenvolvimento de novas tecnologias para o estudo do conjunto de proteínas de um certo organismo passaram a ser denominadas instrumentos da proteômica (AEBERSOLD; HOOD; WATTS, 2000).

A espectrometria de massas (MS) é uma das mais importantes ferramentas analíticas disponíveis e desde a década de 90 tem se tornado um método muito poderoso, e atualmente o mais usado na caracterização de proteínas, principalmente com o desenvolvimento de novas técnicas de ionização que permitem a transferência destas biomoléculas da fase líquida para fase gasosa (VAN RIPER et al., 2013).

Avanços da MS possibilitaram análises globais do proteoma celular, com a identificação e quantificação de milhares de proteínas em diferentes modelos biológicos (DE GODOY et al., 2008; LUNDBY et al., 2012). A abordagem de escolha para MS normalmente é a técnica conhecida por *shotgun* na qual as proteínas de uma amostra são digeridas por uma protease específica e os peptídeos provenientes desta digestão são analisados. O conhecimento prévio da protease permite que a predição dos peptídeos seja realizada através do seu confronto com bancos de dados teóricos. Abordagens de proteômica em que as proteínas não precisam ser digeridas (proteômica *top-down*) ou que são digeridas por proteases de reconhecimento de sítios raros geram peptídeos maiores (proteômica *middle-down*) são utilizada para aplicações mais específicas (TAYLOR et al., 2003; WU et al., 2012). Estas abordagens normalmente exigem espectrômetros com alta resolução e são utilizadas em amostras menos complexas, para diferenciar isoformas proteicas ou identificar modificações pós-traducionais.

## 2 OBJETIVOS

O objetivo do estudo foi analisar a modulação da expressão gênica da forma epimastigotas da cepa Dm28c de *Trypanosoma cruzi* durante sua curva de crescimento em cultivo e em três condições de estresse nutricional. O trabalho foi dividido em três capítulos, as quais possuem os objetivos específicos abaixo:

Capítulo 1: *Trypanosoma cruzi* transcriptome during axenic epimastigote growth curve

- Avaliar o perfil de crescimento dos parasitas e a existência de diferentes fases da curva de crescimento.
- Avaliar o comportamento do parasita em relação as fases do ciclo celular e a viabilidade celular ao longo da curva.
- Avaliar o perfil polissomal e formação de complexos de RNA durante as fases da curva de crescimento.
- Analisar o perfil de expressão gênica, por RNA-seq, em epimastigotas por 10 dias consecutivos das frações de RNA total e polissomal.

Capítulo 2: Proteome of *Trypanosoma cruzi* growth curve

- Analisar o perfil de expressão proteica em epimastigotas durante 8 dias consecutivos da sua curva de crescimento usando a metodologia LC-MS/MS.

Capítulo 3: *Trypanosoma cruzi* stationary epimastigote transcriptome response to nutritional deprivation

- Analisar o perfil de expressão gênica, por RNA-seq, em epimastigotas de fase estacionária inicial em diferentes condições de meio pobre em nutrientes (PBS, TAU e TAU3AAG) durante 1, 2, 4, 6 e 24 horas.

## 3 CAPÍTULO 1

Artigo científico em preparação para ser enviado para a revista *Parasitology*.

# *TRYPANOSOMA CRUZI* TRANSCRIPTOME DURING AXENIC EPIMASTIGOTE GROWTH CURVE

Cyndia Mara Bezerra dos Santos[1,2], Adriana Ludwig[2,3,], Rafael Luis Kessler[2,3]; Rita de Cássia Pontello Rampazzo[3], Alexandre Haruo Inoue[2], Marco Aurélio Krieger[1,2,3], Daniela Parada Pavoni[1,2], Christian Macagnan Probst[1,2]

[1] Programa de Pós-Graduação em Biologia Celular e Molecular, Centro Politécnico, Universidade Federal do Paraná, Curitiba, Paraná, Brazil.

[2] Instituto Carlos Chagas/Fiocruz-PR, Curitiba, Paraná, Brazil.

[3] Instituto de Biologia Molecular do Paraná, Curitiba, Paraná, Brazil.

*Corresponding author: Email: cprosbt@fiocruz.br

Curitiba/PR, Brazil, Tel.: +55 41 3316 3230; Fax: +55 41 3316 3267

**Key words:** *Trypanosoma cruzi*, Chagas disease, growth curve, RNA-seq, polysomes.

## SUMMARY

An important step to understand the *Trypanosoma cruzi* biology is the study of cellular and molecular features presented during its growth curve. Here, we show a global view of gene expression profile for total and polysomal RNA fractions along 10 days of the *T. cruzi* epimastigote growth curve *in vitro*. A total of 2491 differential expressed genes (DEGs) were identified using RNA-Seq approach, of which 768 were modulated in both fractions. According to the modulation pattern, these DEGs were grouped into 13 clusters and some of them show enrichment of important GO terms. In most clusters there was remarkable overlapped modulation between each RNA fraction. However, the polysomal profile might reveal mRNAs that are being translated or storaged and their expression pattern could be different from the total RNA fraction. Moreover, at the stationary phase the polysomal content greatly declined while the RNA granules seemed to increase. This leads us to conclude that most mRNAs isolated from the sucrose cushion at late growth stages were associated with granules instead of polyribosomes. We highlight some views on the *T. cruzi* growth curve, mainly related to the stationary phase and the response to glucose depletion.


## INTRODUCTION

There is a notable interest to understand the cell biology of *Trypanosoma cruzi*, the protozoan parasite causative of Chagas disease, an endemic illness affecting 6 to 7 million people worldwide, mostly in Latin America (WHO, 2016). *T. cruzi* belongs to the Trypanosomatidae family that encompasses also other human pathogens, such as *T. brucei* (causing African Trypanosomiasis) and *Leishmania spp*. (causing Leishmaniasis).

*T. cruzi* exhibits at least four stages in its complex life cycle, which involves an alternation between two distinct hosts: epimastigotes (replicative) and metacyclic trypomastigotes (non-replicative and infective) found in the insect vector and amastigotes (replicative) and blood trypomastigotes (non-replicative and infective) found in the mammalian hosts (BRENER, 1973). All *T. cruzi* life cycle forms can be obtained *in vitro* (CONTRERAS A.; DE LIMA R.; NAVARRO A., 2006). Epimastigotes, naturally found in the gut of infected insect vectors, can be maintained in laboratory through cultivation in a rich medium, refreshed when the culture reaches a high cell density (CAMARGO, 1964a). Parasites multiply exponentially until they reach a stationary phase, when they respond to several stresses, such

as nutrient depletion, by ceasing growth and entering a nonproliferating quiescent state (HERNÁNDEZ et al., 2012; TYLER; ENGMAN, 2000). Moreover, a small proportion of cells in the stationary phase might undergo metacyclogenesis, giving rise to metacyclic trypomastigotes (CAMARGO, 1964a; CONTRERAS et al., 1985). Several cellular changes occur during *T. cruzi* exponential to stationary phase transition, such as the elongation of both the cell body and the flagellum (TYLER; ENGMAN, 2000), a reduction and eventual nucleolus disassembly and a decrease of transcription and translation rates (HERNÁNDEZ et al., 2012; NEPOMUCENO-MEJÍA et al., 2010). Thus, the study of epimastigote growth on culture can help unveil several aspects of *T. cruzi* biology, from cell biology to gene expression regulation. Trypanosomatids have a singular gene expression control (CAMPBELL; THOMAS; STURM, 2003; CLAYTON; SHAPIRA, 2007; TEIXEIRA, 1998). These parasites transcribe long polycistronic arrays containing dozens of genes with no functional relationship among them (AGABIAN, 1990). Polycistronic RNA is then processed by concerted trans-splicing and polyadenylation reactions to produce mature mRNAs that always contain the same 39 nucleotides species-specific spliced leader (SL), or mini-exon, at the 5' end (LIANG et al., 2003). With the exception for the SL precursor gene, no RNA polymerase II promoter was detected in the upstream regions of polycistronic gene units in trypanosomatid genomes (BERRIMAN et al., 2005; EL-SAYED et al., 2005; IVENS et al., 2005b). Interestingly, genes of the same polycistronic unit may show large differences in expression level (CAPEWELL et al., 2013; HAILE; PAPADOPOULOU, 2007; MARTÍNEZ-CALVILLO et al., 2010). It is believed that polycistrons are transcribed and processed constitutively (MARTÍNEZ-CALVILLO et al., 2010) and gene expression is mainly regulated post-transcriptionally, by selective transport to the cytoplasm, mRNA stability and polysomal mobilization (CLAYTON; SHAPIRA, 2007).

In the present work, we presented an RNA-Seq transcriptomic analysis of *T. cruzi* epimastigotes life cycle stage, comparing total and polysomal RNA during the entire growth curve. Our data provide insights into how the epimastigote regulates its gene expression during the transition from the exponential to the stationary phase. Polysomal profile analysis shows great decrease on polysome formation at the stationary phase while, RNA granules seem to increase. Clusterization and gene ontology analysis of RNA deep sequencing allowed us to observe the similarities and differences between total and polysomal RNA fractions giving us

support to explore and discuss possible mechanisms that underlie the epimastigote life events during the axenic growth curve.

## MATERIALS AND METHODS

*Trypanosoma cruzi maintenance and growth curve samples*

Epimastigotes of *T. cruzi* Dm28c strain (CONTRERAS et al., 1988b) were maintained in axenic conditions at 28°C in liver infusion tryptose (LIT) medium supplemented with 10% heat-inactivated fetal bovine serum (CAMARGO, 1964a), in logarithmic growth by continuous subculturing $10^6$ cells/ml each three days. For RNA-seq analysis of epimastigote growth curve, 10 consecutive days were evaluated in biological triplicates. To obtain enough parasite samples, for each replicate, the same original epimastigote culture was used to prepare 30 flasks (250 ml) with 100 ml of LIT containing $10^6$ cells/ml, ensuring biological similarity. Daily, three culture flasks were used to determine cell density, using an automatic counter (Z2Coulter® – Beckman Coulter) to obtain the epimastigote growth curve. Based on the same cell counting, enough flasks to obtain $10^8$ and $10^9$ cells were used each day for extraction of total and polysomal RNA, respectively. Differential counting analysis was performed by light microscopy, using a Neubauer chamber to access the percent of metacyclic trypomastigotes arising from cultures.

*FACS analysis*

Cell cycle and cell viability analyses were performed in a FACSCanto II flow cytometer (flow cytometry facility RPT08L PDTIS / Carlos Chagas Institute - Fiocruz Paraná). For cell cycle assay, $2x10^6$ cells were harvested and fixed with 70% methanol at days 1, 3, 6 and 9 of growth curve. After this step, cells were harvested, washed in PBS and resuspended in 500 µl of a DNA staining solution containing 0.425 mM Tris-HCl, 15 µg/ml propidium iodide, 0.0125% NP40 detergent, 1.25 mM NaCl and 8.75 U/L of RNase A. These cells were kept on ice until flow cytometry quantification. A total of 20,000 events were acquired and data analysis was performed using FlowJo software (Treestar software). All experiments were done at least in duplicate. Data analysis was done in FL2-Widht×FL2-Area gated cells to exclude debris and doublets. The Dean-Jett-Fox algorithm of FlowJo software was used to estimate percentage of cells in G0/G1, S and G2/M phases of cell cycle. For cell viability, all experiments were done at least in triplicate using the same analysis patterns mentioned above. At days 1 to 10 of growth

curve, $2x10^6$ cells were harvested, washed and incubated for 10 minutes at 28ºC in 5 µg/ml propidium iodide (PI) in PBS.

*Polyribosome isolation and analysis*

Polysomes were purified using sucrose cushions (modified from Goldenberg *et al.*, 1985). An amount of $10^9$ cells was incubated with 10 mg/ml cycloheximide directly in culture medium and kept at 28°C for 10 minutes. After centrifugation at 7,000 x g for 5 minutes, cells were washed two times with NKM buffer (140mM NaCl, 5mM KCl and 1.5mM $MgCl_2$) supplemented with Hepes (10 mM) and cycloheximide (10 µm/ml). The cell pellet was resuspended in 50 ml of NKM buffer supplemented with 10 mM Hepes, 10 µm/ml cycloheximide, 10 µm/ml heparin and 5 mM Beta-mercaptoethanol. The suspension was transferred to a new tube containing 10 ml of lysis buffer (NKM supplemented with 1% NP-40 and 250 mM 2 M sucrose to final concentration), with continuous homogenization by pipeting. The lysate was centrifuged at 10,000 x g at 4 °C for 30 minutes. Cleared supernatant was carefully layered onto 2 M sucrose cushion and ultracentrifuged at 4 °C for 2 hours at 270,000 x g in a Beckman SW40 rotor. Polysomal fraction was recovered from the final pellet.

For polysome profile analysis, $10^9$ parasites were treated with 100 µg/ml cycloheximide for 10 minutes at 28°C and then harvested by centrifugation at 5,000 g at 4°C for 5 minutes and next washed with cold TKM buffer (10 mM Tris-HCl pH 7.4, 10 mM $MgCl_2$, 300 mM KCl), supplemented with cycloheximide (100 µg/ml). Cells were suspended in 900 µl TKM supplemented with 100 µg/ml cycloheximide, 10 µg/ml heparin and 10 µM and the suspension was transferred in a new tube with 100 µl TKM buffer containing 10% (v/v) NP-40 and 2 M sucrose. The lysate was centrifuged at 16,000 g at 4 °C for 10 minutes. Cleared supernatant was gently applied on a linear 15-55% (w/v) sucrose gradient and centrifuged at 4 °C for 2 hours at 39,000 rpm in a Beckman SW40 rotor. The sucrose gradient was collected at a rate of 1 ml per minute, and analyzed spectrophotometrically (254 nm) on "ISCO Foxy JR system". Aliquots of 30 µl of each collected fraction were analyzed by electrophoresis in SDS-PAGE, followed by Western blotting with antibodies against *T. cruzi* ribosomal protein S7 (1:500). After washing, the membrane was incubated with IRDye® 680RD secondary antibodies (LI-COR) for 1 hour at room temperature. The membrane was washed three times with PBS containing 0.1% Tween-20 and antibody binding was detected using the Odyssey Infrared Imaging System (LI-COR).

*Localization of mRNA in T. cruzi*

Parasites were harvested by centrifugation, washed in PBS (pH 7.4), fixed by incubation in 4% paraformaldehyde and were adhered to poly-L-lysine-coated slides for 10 minutes. The slides were washed in PBS and the parasites were permeabilized by incubation with 0.2 M HCl diluted in PBS for 10 minutes. The cells were incubated with prehybridization buffer containing 35% formamide, 0.02% BSA in 2X SSC buffer, 25 μg/ml tRNA, 1 mg/ml salmon sperm DNA (Sigma-Aldrich) and 40 U/ml RNaseOUT (Invitrogen) for 30 minutes at 37°C. For detection of poly(A)$^+$ RNA, digoxigenin-conjugated oligo(dT) probes (6 ng/μl) were diluted in prehybridization buffer and denatured by heating at 65°C for 3 minutes. As a control, 100 μg/ml RNase A was added to the pretreatment buffer before probe hybridization. Hybridization was performed for 16 hours at 37°C. Probe binding was detected by indirect immunofluorescence analysis with mouse monoclonal anti-digoxigenin antibody (Sigma-Aldrich, 1:300 dilution) and Alexa Fluor 488-conjugated goat anti-mouse IgG secondary antibody (Invitrogen, 1:600 dilution). DNA was stained by incubation with 5 μg/ml DAPI for 15 minutes. Slides were analyzed in inverted microscopy (Leica DMI6000B) associated with deconvolution software Leica AF6000 (microscope facility RPT07C PDTIS / Carlos Chagas Institute - Fiocruz Paraná).

*RNA isolation*

Total and polysomal RNA were isolated using the RNeasy mini kit (Qiagen), and treated with RNase free DNase I (Qiagen). RNA samples were quantified by absorbance at 260 nm using the Nanodrop ND-1000 (Thermo Scientific) and the RNA integrity and quality was checked with a bionalyzer RNA 6000 Pico Kit (Agilent 2100). mRNA was selected by oligo-dT chromatography using PolyATtract® mRNA Isolation kit (Promega).

*RNA-seq*

Samples were prepared for RNA sequencing using the SOLiD™ Total RNA-Seq Kit (Life Technologies, #4445374) accordingly to manufacturer instructions. Briefly, RNA was fragmented using RNase III and cleaned up with Invitrogen RiboMinus™ Concentration Module. Strand-specific adaptors were hybridized and ligated to both extremities of RNA in an overnight reaction, followed by first strand cDNA synthesis with reverse transcriptase. cDNA was purified using MinElute® PCR Purification Kit (Qiagen) and gel-based size selected using a Novex TBE-Urea 6% gel (#EC6865BOX). On-gel cDNA was amplified by PCR using

SOLiD™ RNA barcoding kit primers (Life Technologies, #4427046 and #4453189) and purified with Invitrogen PureLink® PCR Micro Kit. Amplified DNA was quantified with Qubit® 2.0 Fluorometer and the Qubit® dsDNA HS Assay Kit. Equal mass of each sample, containing specific barcodes, were pooled together and the mixtures used as DNA template for emulsion PCR on Applied Biosystems SOLiD® EZ Bead™ E80 system (#4453095). Barcoded libraries were sequenced on a SOLiD™ 4 system using multiplex fragment sequencing protocol.

*RNA-Seq Data processing*

Raw single reads of 50 nucleotides were subject to quality-filtered using the standard SOLiDTM WT Analysis Pipeline tool. Reads were mapped to *T. cruzi* CL Brener genome (EL-SAYED et al., 2005), using SHRIMP2 (DAVID et al., 2011). In order to exclude redundancy in *T. cruzi* gene annotation and read counts, clusters of orthologous genes were determined based on nucleotide sequence similarity and named as Supra Genes (SG) . SG are groups consisting of genes that contain nucleotide sequences with high similarity, which eliminates redundancy in the transcriptome profile by allowing for multiple mapping positions of a single read. SG read counts were obtained by summing the number of reads aligned to each coding sequence (CDS) of all members of SGs using perl programming language script. SG read counts was used for the analysis of differential expression. Read counts were normalized and analyzed for differential expression in edgerR package (ROBINSON; MCCARTHY; SMYTH, 2009), considering different levels of statistical significance,false discovery rate (FDR) (BENJAMINI; HOCHBERG, 1995), with maximum value of 10% and the second filter $\log_2$-fold-change $\geq 1.0$ ($\log_2$ FC). Non-linear regression data analysis was performed using Lowess in R program to obtain an average measure of expression, considering variance inter replicas and inter days.

*Clusterization of gene expression patterns*

Expression level (normalized RNA-Seq counts) of differentially expressed genes were normalized between samples using the Z value [(counts - mean counts)/counts standard deviation] in order to put all genes in the same scale with mean of zero and standard deviation of one. The transformed profiles were then clustered with the fuzzy c-means (FCM) clustering algorithm (FUTSCHIK; CARLISLE, 2005), which is based on the open-source programming language R Bioconductor (bioconductor.org). The main parameters (c = number of clusters and m = fuzzification parameter) were derived by the iterative refinement procedure as described

by Futschik and Carlisle (FUTSCHIK; CARLISLE, 2005). The final clustering was done with the c = 13 and m = 2.4. Only genes with membership value higher than 0.5 were considered for following GO analysis.

*Gene Ontology*

Better annotation of the identified proteins and Gene Ontology (GO) classification were achivied using Blast2GO software (CONESA et al., 2005), using default parameters. Overrepresentation of GO terms on specific gene sets was evaluated using Fisher's exact test with an FDR of 0.01 and looking for most specific terms.

*Analyses of genes related to glucose sensing pathways*

To get insights into the glucose response pathway in *T. cruzi* , we searched in *T. cruzi* genome for homologous genes that are known to have a role on this process in *Saccharomyces cerevisiae*. The sequences of *S. cerevisiae* proteins were obtained on UniprotKB and used as query on blastP searches against *T. cruzi* CL Brener Esmeraldo-like genome. We used an initial e-value cutoff of $1e^{-10}$. However, due to the long evolutionary distance between these species, hits above this threshold were also analyzed, checking for similar protein domains and structure. To corroborate homology inference, we performed reciprocal blastP against *S. cerevisiae*.

## RESULTS

*T. cruzi epimastigotes (Dm28c) growth curve pattern*

The epimastigote growth curve was initiated from 1 x $10^6$ cell/ml and was followed during 10 days (Fig. 1A). We observed a typical growth curve with distinguishable phases: I) a smaller proliferation in the beginning of the growth curve until day 2, designated lag phase; II) an exponential or log phase from days 3 to 5 reaching 9.64 x $10^7$ ± 4.63 x $10^6$ cells/ml; III) an early stationary phase from days 5 to 7, when the cells continue dividing, nevertheless with a clearly reduced growth rate achieving 1.19 x $10^8$± 7.01 x $10^6$ cells/ml; IV) a stationary phase from days 8 to 10, reaching a virtually stable density. There was a small percentage of metacyclic trypomastigotes first detected at day 7 (1.73%; ± 1.24%) and gradually increasing until 10.66%± 2.35% at day 10 (Fig. 1B).

By microscopic examination, we verified normal epimastigote morphology and flagellar

motility, during almost the entire curve. At the stationary phase, however, parasites presented body and flagellar elongation and a high number of cells (45% at day 9), without motility (data not shown). We then verified whether such cells were still alive, by cell viability analysis during the growth curve. This analysis showed that the percentage of dead parasites was stable until day 8, with an average of 1.14%± 0.30% reaching 6.08% (± 1.44%) at day 10 (Fig. 1C and 1D). Thus, we assumed that the majority of immobile cells were still alive.

We analyzed the cell cycle on days 1, 3, 6 and 9, by flow cytometry (Fig. 1E and 1F). Most parasites (39.93%± 2.94%) were in G1 phase at the first day. This proportion increased along the growth curve, reaching 60.95% (± 4.34%) on day 6, virtually remaining stable. Oppositely, cells in S and G2/M phases were present in smaller fractions, 26.73% (± 1.30%) and 33.33% (± 4.03%) at day 1, respectively. These fractions decreased during the curve reaching 22.06% (± 0.48%) and 23.00% (± 2.24%) for S and to G2/M phases, respectively, at day 9.

*Polysome fraction decreases while mRNA granules increase at stationary phase*

In actively growing cells, the rate of translation seems to remain constant in the exponential phase. As a result, multiple ribosomes simultaneously engaged in translation are present in single mRNA molecules. We analyzed the polysome profile sedimentation on sucrose density of epimastigotes from days 3, 6 and 9, in order to evaluate when the translation is affected in the *T. cruzi* growth curve. Polysome formation was widely disrupted for parasites on days 6 and 9, demonstrating decreased translation since the early stationary phase (Fig. 2A, B and C).

During nutritional stress, *T. cruzi* increases the formation of P-body-like granules (Holetz et al., 2007). Since polysome content was decreased in the stationary phase, we analyzed the mRNA localization and the formation of RNA-containing granules. The pattern of mRNA distribution was altered along the growth curve. Parasites of day 3 showed a cytoplasmic mRNA localization enrichedt around the nucleus, while parasites at days 6 and 9 showed a higher number of RNA granules (arrows in Fig. 2D).

*RNA-seq analysis and identification of differentially expressed genes (DEG)*

We performed RNA-seq analyses to evaluate the spatiotemporal gene expression profiling, along the epimastigote growth curve. The experiments were performed in biological triplicate. For each of the 10 days, two libraries were constructed, one consisting of total RNA and the other of polysomal RNA. The total number of reads generated was 455 million for total

RNA library and 412 million for polysomal RNA library. The average number of reads per sample was 15.7 million and 19.6 million, for total and polysomal RNA, respectively (Additional file 2). After initial assembling, 8926 SGs were mapped in CL Brener genome (EL-SAYED et al., 2005) and multiple sample test analysis identified 2491 DEGs (FDR < 10%) during the growth curve, wherein 1792 were modulated in total RNA and 1467 in polysomal RNA fraction. Figure 3 shows the number and overlapping of DEGs between the analyzed RNA fractions for distinct FDR thresholds. Considering a FDR of 10%, 768 (30.83%) DEGs were modulated in both RNA fractions, 1024 (41.10%) weremodulated only in total RNA and 699 (28.06%) only in polysomal RNA fraction.

We also compared all experimental points to day 1 (reference point) by exact tests in edgeR software. Table 1 shows the number of DEGs in each day of the epimastigotes growth, for total and polysomal RNA samples. As expected, the number of DEGs increased with time, with a more representative amount of DEGs from day 5.

*Correlation of gene expression over time*

To understand the dynamics of gene expression between total and polysomal RNA fractions during the growth curve, we clustered the DEGs accordingly their expression patterns, using the Fuzzy c-means clustering. The optimal number of clusters was iteratively determined to be 13 (Additional file 3). Figure 4 shows the pattern expression of the 13 fuzzy clusters by centroid of each cluster and in Additional file 4 is represented the pattern with all DEGs presents in each cluster.

This analysis considered all DEGs in total and polysomal RNA fractions detected by multiple sample test. For those DEGs that are specific from one fraction, their respective expression data from the other RNA fraction was included. A total of 2,133 genes were successfully determined to a most probable expression profile cluster (membership value > 0.5); 1,703 (79.83%) of them showed a similar modulation patterns for both RNA fractions (Clusters 3, 4, 6, 8, 10, 11 and 12). Clusters 4 (157 genes), 6 (210 genes), 8 (299 genes) and 10 (267 genes) presents a constant increase of RNA expression in both RNA fractions, while clusters 3 (163 genes), 11 (212 genes) and 12 (395 genes) show a decreasing expression profile. Cluster 1 (95 genes) displays increasing RNA expression until day 7, when total RNA remain constant while polysomal RNA fraction decreases. Cluster 2 (56 genes) shows an interesting antagonic pattern between total and polysomal RNA fractions, respectively decreasing and increasing the RNA expression. Cluster 5 (128 genes) shows a reduction of gene expression for both fractions

until day 7, remaining almost stable in the total fraction and increasing in the polysomal fraction in the remaining days. Cluster 7 (48 genes) exhibits similar modulation of RNA fractions with an increase of gene expression followed by a decrease; nonetheless this pattern switched at day 4 in the total and at day 7 in the polysomal fraction. Cluster 13 (71 genes) shows an increase of RNA expression until day 5 in the total and until day 7 in the polysomal fraction; then it declined in the total and remained almost stable in the polysomal fraction. Clusters 7 and 13 presented similar modulation profiles for polysomal RNA, however for total RNA there is a decrease in RNA expression in cluster 7 from day 4 and in cluster 13, from day 5. Clusters 1, 5 and 12 showed change in gene expression profile in both fractions from day 7. Interestingly, for some genes a change in RNA expression pattern at day 7 occurred only for one RNA fraction, as we can see for total RNA in clusters 2 and 9 (32 genes), and for polysomal RNA in clusters 6, 7, 10 and 13. Latter observations could be explained by the stabilization of the stationary phase at day 7.

*Functional enrichment analysis*

To improve our understanding of gene expression clusters and give insights into functional properties, clusters compositions were used for GO enrichment analysis by Blast2GO (CONESA et al., 2005). To optimize GO analysis and the chance of finding enriched terms, we grouped clusters with similar expression patters (Fig. 5) due to the large proportion of hypothetical genes in *T. cruzi* (without GO anotation) that difficult the identification of statistically enriched GO terms. Thus, clusters that presented a similar modulation pattern were grouped, while singular ones remained isolated (Fig. 5). The first group was composed of clusters 4, 6, 8 and 10, since they have a upregulated pattern of gene expression for both RNA fractions. The second group was composed of clusters 3, 5, 11 and 12 as they have downregulated pattern of gene expression. Finally, the third group was composed of clusters 7 and 13 that presented a pattern of gene upregulation, followed by gene downregulation (Fig. 5).

GO terms were assigned for 1354 genes of 11 clusters (Fig. 6). Unfortunately, it was not possible to get significantly enriched GO terms for clusters 2 and 9, probably because they are smaller in number of genes.

For the upregulated group (clusters 4, 6, 8, and 10), eight GO terms were identified. Most genes codes for trans-sialidase superfamily that presented the following GO terms: carbohydrate metabolic process (GO:0005975); glycosphingolipid metabolic process (GO:0006687); exo-alpha-sialidase activity (GO:0004308); and pathogenesis (GO:0009405).

Another set of genes highly represented in these clusters are those encoding kinase proteins related to protein phosphorylation (GO:0006468); protein serine/threonine kinase activity (GO:0004674); serine family amino acid metabolic process (GO:0009069); and ATP binding (GO:0005524). The GO:0005975 and GO:0005524 also include proteins involved in the glycolytic process, as the important glycosomal phosphoenolpyruvate carboxykinase enzyme (TcCLB.508441.20).

Functional terms found for downregulated group (clusters 3, 11 and 12) were: ribosome biogenesis (GO:0042254); methylation (GO:0032259); methyltransferase activity (GO:0008168); gene expression (GO:0010467) including proteins mainly involved in translation process; intracellular organelle lumen (GO:0070013) embracing RNA polymerase genes and mitochondrial matrix related genes; RNA binding (GO:0003723); ribosome (GO:0005840); nucleolus (GO:0005730); and cellular nitrogen compound metabolic process (GO:0034641).

Clusters 7 and 13 are associated with 13 GO functional terms all related to cytoskeletal cellular components; however only a small fraction of genes (~16%) from these clusters had some GO term assigned.

Cluster 1 had only one category, which has the molecular function “protein binding” (GO:0005515), composed mainly by uncharacterized proteins. Analyzing cluster 5, we found only terms from the GO “cellular component” domain, including proteins involved in several cellular processes. Although GO enrichment terms were not found in clusters 2 and 9, which the gene expression between total and polysomal mRNAs had inverse expression pattern, the presence of proteins that may be involved in post transcriptional regulation were present, as RNA binding proteins.

*Identification of genes hypothetically regulated by glucose sensing pathways*

Because glucose has a major role in cell maintenance, analyses of possible genes involved in the nutrient sensing pathway were investigated. We explored possible proteins involved in this process according to trypanosomatid literature, however as few works contemplated this field, we also looked for candidates based on the data from the unicellular model organism *S. cerevisiae*. Several *S. cerevisiae* homologous genes were identified and some of them have their mRNA expression modulated in our data. Were modulated Snf1 (TcCLB.510861.140, TcCLB.510257.130 and TcCLB.464807.10), Sak1/Tos3/Elm1 (TcCLB.503613.10, TcCLB.506775.190, TcCLB.506801.120 and TcCLB.510759.40), Snf4 (TcCLB.503841.20), Sip2/Gal83 (TcCLB.504427.50), Glc7 (TcCLB.507757.50,

TcCLB.509633.60, and TcCLB.509633.50) and Hxk2 (TcCLB.508951.20). The results are summarized in (table 2).

## DISCUSSION

High throughput approaches have been widely used in recent years to study several biological aspects of organisms. RNA-Seq methods generated valuable information about gene expression regulation on an omics scale (MOROZOVA; HIRST; MARRA, 2009), accurately determine the levels of specific gene expression. Several transcriptome works were performed in trypanosomatids evaluating different aspects of the biology of these parasites, as life cycle stages, cell cycle and intracellular infection (ARCHER et al., 2011; FADDA et al., 2014; GREIF et al., 2013; KOLEV et al., 2010; LI et al., 2016; RASTROJO et al., 2013). Here, we discussed the results from a deep sequencing study of the *T. cruzi* Dm28c epimastigote growth curve.

*Evaluation of the T. cruzi growth curve*

We explored some cellular and biological aspects of the *T. cruzi* epimastigote *in vitro* growth curve during 10 consecutive days. Epimastigotes increase density by binary fission and show a typical *in vitro* growth curve with two major different phases, the exponential and the stationary phase. The exponential phase is a period characterized by a constant exponential growth rate, where the population density increases. The stationary phase occurs when cells arrest their growth, in response to starvation (WERNER-WASHBURNE et al., 1993). We also observed the existence of a possible lag phase during the two first days of the *T. cruzi* growth curve, thought to be a period when cells adapt to a new environment (YATES; SMOTZER, 2007). Moreover, we saw a transitory phase between exponential and stationary phases (day 5 to 7) with significant decrease of growth rate, before it virtually ceases. These observations are expected, since epimastigote growth seems to be controlled by nutritional depletion and cell density (CAMARGO, 1964a; TYLER; ENGMAN, 2000).

We observed a high number of parasites without motility at the stationary phase and cell viability analysis indicated that most of these cells were still alive. This observation corroborates the hypothesis that cells at the stationary phase reach a quiescent stage. For some microorganism, the stationary phase is represented mainly by cells arrested in G0 stage of the cell cycle (WERNER-WASHBURNE et al., 1993). In *T. cruzi*, we observed an increase of cell

percentage in G0/G1 phase, although approximately 40% seems to be dividing or arrested in S or G2/M. The regulation of cell cycle is still poorly understood in trypanosomatids, but several genes whose products seems to be involved in this process were identified (HAMMARTON; MONNERAT; MOTTRAM, 2007; POTENZA et al., 2012). Some of these genes were found modulated, in our data.

Specific molecules that regulate transition through different phases of cell cycle, as cyclins and Cdc2-related kinases (CRKs), have been studied in *T. brucei;* here we investigated the mRNA expression pattern of their homologous genes in *T. cruzi*. Six of 10 cyclins are upregulated during the growth curve (TcCLB.508385.30 - CYC2, TcCLB.508385.30 - CYC4 and TcCLB.508207.250 - CYC8, cluster 10; TcCLB.507677.150 - CYC5, TcCLB.503885.100 - CYC10 and TcCLB.503551.20 - CYC11, cluster 8). RNAi studies in *T. brucei* showed that CYC2 and CYC4 play a major and minor role in promoting G1/S transition, respectively (reviewed Li, 2012). Moreover, four of 11 CRKs also showed some modulation pattern (TcCLB.510609.70 - CRK2, TcCLB.509099.150 - CRK9, TcCLB.510329.70 - CRK10 and TcCLB.511751.50 - CRK11, clusters 8, 2, 10 and 1, respectively). CRK2 appears to be involved through G1/S transition and seems to interact with CYC2 (GOURGUECHON; SAVICH; WANG, 2007).

Among several constituents of the CMG complex (Cdc45/Mcm2-7/GINS) involved in DNA replication in eukaryotes and apparently conserved in *T. brucei* (reviewed by Li, 2012), we found three homologous genes in *T. cruzi* , downregulated along the growth curve (TcCLB.508647.140 - Mcm5, cluster 12; TcCLB.510283.150 - Psf2, cluster 11 and TcCLB.510087.100 - Psf3, cluster 3), suggesting that S phase progression could be harmed in old cultures.

Downregulation of selected genes via RNAi identified several *T. brucei* genes as essential to the cytokinesis process (reviewed in Hammarton *et al.*, 2007). Interestingly, we found that some of the homologous genes in *T. cruzi* are modulated during the growth curve, corresponding mainly to genes encoding flagellar related proteins and centrins (TcCLB.511729.60 - MORN repeat-containing protein 1, downregulated not clustered; TcCLB.509171.100 - Hydin, cluster 13; TcCLB.506887.20 - Parkin co-regulated protein, cluster 7; TcCLB.508323.60 - centrin 1, cluster 5; TcCLB.510763.100 - trypanin and TcCLB.506401.90 - centrin 2, cluster 2). Further work on these genes and others in *T. cruzi* can help to understand whether the cells presented in G2/M stage in the stationary phase are arrested by some cytokinesis failure or if there is a constant percentage of cells that pass from one stage to the next, even during stationary phase.

*Dynamic of mRNAs and their association to polyribosomes and granules during the growth curve*

As already mentioned, gene expression control in trypanosomatids occurs post-transcriptionally and the mature mRNAs exported to cytoplasm will be exposed to different ways of regulation that ultimately will lead to mRNA translation, RNA degradation or association to protein-RNA complexes (DE GAUDENZI et al., 2011). As for other eukaryotes, *T. cruzi* mRNAs can be compartmentalized in ribonucleoprotein complexes called P-bodies or stress granules. The presence of mRNA granules in *T. cruzi* was observed under nutritional stress (CASSOLA; GAUDENZI; FRASCH, 2007; HOLETZ et al., 2007). It has been suggested that the mRNAs can be protected in granules for posterior translation, as a strategy to cope with periods of starvation (CASSOLA; GAUDENZI; FRASCH, 2007). In this context, the transcriptome analysis of a complete set of mRNAs (total fraction) versus a set of mRNAs linked to polysomes or other complexes (polysomal RNA fraction) could give insights to better understand the mechanisms behind gene expression regulation.

We observed that the rate of translation seems to diminish at the stationary phase, since polysome formation was widely disrupted for parasites on days 6 and 9. Moreover, the increase of RNA-containing granules at this phase is consistent with the findings of other authors in a nutritional poor environment (HOLETZ et al., 2007). These observations lead us to suggest that at the stationary phase, most mRNAs isolated from sucrose cushion should be associated with granules instead with polyribosomes, which means they might have been saved for further translation.

*Biological processes and molecular functions implicated on the T. cruzi growth*

The comparison of RNA expression data revealed a very similar modulation pattern between total and polysomal RNA fractions. This is not entirely unexpected, since the polysomal portion is included in the total fraction. One of our goals was to identify possible differences on RNA fraction profiles that could reveal their regulation dynamics during the growth curve. We were able to recognize three clusters (named 2, 7 and 9) that present distinct total and polysomal modulation patterns leading to formulation of some hypotheses.

Cluster 2 genes, for example, show a modulation that suggests those mRNAs have a constant reduction on translation, since their expression is decreasing in polysomal fraction, in spite of their increase in total RNA fraction. Genes in this cluster mainly encode hypothetical proteins. Genes from cluster 7 also encode hypothetical proteins and some cytoskeletal cellular

components and seem to have a delay on protein production in relation to the mRNA synthesis, since their polysomal expression pattern is very similar to the total, but approximately three days delayed. There is also cluster 9 where total RNA expression decays, while polysomal RNA is increasing. This cluster pattern occurs when genes have translation level increased or their polysomes may be stocked for translation. There is no GO terms enrichment for this cluster.

The analyses of GO enrichment could help to identify important genes and processes involved in the major cellular and molecular changes that occur with epimastigotes, during the growth curve. Unfortunately, a great part of the modulated genes is annotated as hypothetical proteins, due to the lack of any information on its probable function. Yet, we were able to discuss relevant points on the *T. cruzi* growth curve, mainly in relation to the stationary phase. Many clusters showed a smooth change on their RNA expression in the 7th day of the growth curve, coinciding with the beginning of late stationary phase. These changes could be explained, in part, by the global RNA synthesis repression that is described for this stage (ELIAS et al., 2001), but some genes probably have important specific modulation.

Trans-sialidases are an important pathogenesis factor that mediates transfer of sialic acids from the host glycoconjugates, to the surface of the parasite (reviewed in Briones *et al.*, 1994). In our data, a great part of upregulated genes belongs to the trans-sialidases superfamily, corroborating the idea that the stationary epimastigote appears to be a predictive stage to become a metacyclic trypomastigote, since after metacyclogenesis the cell will have been prepared to interact with a new host (HERNÁNDEZ et al., 2012).

As mentioned, during the stationary phase, we observed flagellar elongation in the parasites, in accordance to Tyler and Engman (2000). Some genes encoding flagellar related proteins were modulated in our data and possibly had consequences on flagellar elongation, as the gene encoding the "paraflagellar rod protein" (TcCLB.509099.30), an important structural component of flagellum (PORTMAN; GULL, 2010) that is upregulated until day 7, the polysomal RNA level remaining constant from then (cluster 13). The modulation of other flagellar related genes could also explain the lack of parasite motility, as discussed above for possible cytokinesis failure. Another cellular consequence found in the *T. cruzi* stationary phase is a significant reduction of nucleoli area (NEPOMUCENO-MEJÍA et al., 2010). In accordance to this observation, we found an enrichment of nucleolus related genes in downregulated

clusters.

The glucose exhaustion is probably one of the causes to the events mentioned above (NEPOMUCENO-MEJÍA et al., 2010; TYLER; ENGMAN, 2000). In *T. cruzi* , the glycolysis pathway is compartmentalized in the glycosome, where the initial reactions occur. As in other eukaryotes, some metabolites produced in the glycolytic pathway are used by other paths in the cell, as the pentose phosphate pathway (PPP) and tricarboxylic acid cycle. Several genes encoding enzymes involved in energy metabolism are modulated in our data.

Some authors have shown that glucose depletion occurs from the 4$^{th}$ to the 7$^{th}$ day of growth in culture (DE LIMA et al., 2008; SHAW; KALEM; ZIMMER, 2016). The results may vary depending on the culture medium, the *T. cruzi* strain or the glucose estimation method. After glucose depletion, cells obtain energy by amino acid breakdown catabolism (URBINA, 1994b). The phosphoenol pyruvate carboxykinase (PEPCK) is involved in the gluconeogenesis from amino acids (MAUGERI; CANNATA; CAZZULO, 2011) and its gene was found upregulated in our data.

*RNA binding proteins*

The accurate gene regulation in kinetoplastids is partly controlled by RNA-binding proteins (RBPs), trans-acting factors that operates in several processes, from the initial mRNA processing to the mRNA decay (CLAYTON, 2013). A high number of RBP candidates genes were identified in trypanosomatids, including proteins containing the domains Alba, Pumilio, Zinc-finger or RNA recognition motif (RRM) (CLAYTON, 2013; DE GAUDENZI; FRASCH; CLAYTON, 2005) and several of the *T. cruzi* genes are modulated along the growth curve.

Some specific RBP genes that are modulated in our data are better studied and seems to have a role on the mRNA levels or translation in *T. brucei* (CLAYTON, 2013). For example, the genes encoding two pumilio-domain proteins were downregulated during the growth curve (TcCLB.511715.100 - pumilio/PUF 7, cluster 5; TcCLB.506773.130 – pumilio/PUF10, downregulated not clustered). *T. brucei* PUF7 and PUF10 are necessary for rRNA maturation in nucleolus and they act in combination with BoP1 and NRG1 proteins (SCHUMANN BURKARD et al., 2013). In our assay, the *T. cruzi* NRG1 homologous gene was also downregulated (TcCLB.507963.90 - hypothetical conserved protein, cluster 12).

Some Alba-domain proteins (ALBA1, 2, 3 and 4) can interact each other acting in the translation process (MANI et al., 2011). The mRNA levels of two *T. cruzi* Alba genes were also reduced (TcCLB.504089.60 – ALBA1, cluster 5; TcCLB.504089.70 – ALBA2, cluster 12).

Interestingly, ALBA2 in *T. brucei* was found associated with polyribosomes in sucrose

gradient analysis (MANI et al., 2011). In accordance to this observation, ALBA2 mRNA level was found decreasing together with the polysomes along the growth curve.

Of the RRM-containing proteins whose genes were upregulated, we can highlight the followings: RBP42 (TcCLB.509167.140, upregulated not clustered) that in *T. brucei* is partially associated with polysomes and has been involved with many mRNA target sites related with energy metabolism (DAS et al., 2012). RBP6 (TcCLB.506693.30, cluster 10) and RBP10 (TcCLB.510507.50, cluster 10) have been implicated in the *T. brucei* developmental progression, wherein the RBP6 promotes differentiation to epimastigote and trypomastigote metacyclic forms (KOLEV et al., 2012) and the RBP10 probably prevents the expression of procyclic form specific regulatory proteins (WURST et al., 2012).

Three important *T. brucei* Zinc-finger proteins have their homologous genes modulated during the *T. cruzi* growth curve: ZFP1 (TcCLB.511511.3, cluster 10) is specific to procyclic stage and plays an important role in the differentiation from bloodstream to procyclic form (HENDRIKS; MATTHEWS, 2005); ZC3H20 (TcCLB.506859.204, cluster 13) is required for growth in procyclic forms (LING; TROTTER; HENDRIKS, 2011); and ZC3H11 (TcCLB.504929.5, cluster 8) is a post-transcriptional regulator that binds several chaperone mRNAs for stabilization after heat shock in procyclic forms (DROLL et al., 2013). Moreover, several others Zinc-finger proteins identified in *T. cruzi* (KRAMER; KIMBLIN; CARRINGTON, 2010) were found modulated in this study.

Few *T. cruzi* RBPs are well characterized and the attempt to correlate then to their functions in *T. brucei* is a challenge. The distinct patterns of modulation found in this work for many RBPs mRNAs indicate that they may have diverse roles in the control of gene expression probably triggering important cellular and molecular processes during the growth curve. In this context, our work can provide early insights into how these genes work in the epimastigote form.

*Several genes involved in glucose response are modulated during the T. cruzi growth curve*

As previously mentioned, glucose is the preferential carbon source in *T. cruzi* (CANNATA; CAZZULO, 1984). Consequently, the glucose concentration decrease along the exponential phase of growth (DE LIMA et al., 2008; SHAW; KALEM; ZIMMER, 2016). We suggest there is a possible sensing control in *T. cruzi* that responds when glucose concentration is significantly depleted in the medium. We then hypothesize the first part of this pathway,

indicating candidate genes involved (Fig. 7).

The glucose entrance in cells is mediated by facilitated transport via transmembrane proteins. In *T. cruzi* , only one gene was identified to encode a glucose transporter, the *TcrHT* gene (genbank accession U05588) (DOS SANTOS et al., 2012; TETAUD et al., 1994). In our data, *TcrHT* was found to increase along the growth curve, supposedly concomitant to glucose depletion.

A major gene involved in the glucose suppression signaling pathway is the Snf1 kinase, a member of the SNF1/AMPK family, highly conserved among eukaryotes (HEDBACKER; CARLSON, 2008). In *S. cerevisiae,* it is activated by phosphorylation in low glucose conditions, triggering different biological process as respiratory metabolism and gluconeogenesis (CONRAD et al., 2014). Several genes from SNF1/AMPK family seem to be found in *T. cruzi* . Two of them (TcCLB.510861.140 and TcCLB.464807.10) were found in cluster 10, presenting an increasing of RNA expression during the growth curve. Snf1 is phosphorylated by three homologous redundant upstream kinases, Sak1, Tos3, and Elm1 in yeast (CONRAD et al., 2014). We found four possible homologous genes in *T. cruzi* (TcCLB.503613.10, TcCLB.506775.190, TcCLB.506801.120, TcCLB.510759.40) that are modulated in different clusters (clusters 13, 8, 1 and 6, respectively), increasing the RNA expression during the exponential phase. Snf1 acts as a heterotrimeric protein complex composed by an α-subunit with the catalytic kinase from N-terminal portion of Snf1, a regulatory γ-subunit provided by the Snf4 protein and a β-subunit that regulates subcellular location (Sip1 - vacuole, Sip2 - cytosol or Gal83 - nucleus) (JIANG; CARLSON, 1997). Analyses of the *T. cruzi* genome indicate that these other components of the Snf1 complex are not highly conserved, as the Snf1. The TcCLB.503841.20 gene is probably homologous to Snf4 and the TcCLB.504427.50 gene to Sip2/Gal83. The proteins encoded for these genes presented limited similarity to the yeast counterparts, however the presence of the same protein domains and reciprocal blastp searches suggest homology. We were not able to find additional genes corresponding to another β-subunit in *T. cruzi* , suggesting that in this parasite there is no such compartmentalization of distinct complexes. The Snf4 homologous gene is not modulated in our expression data, while the Sip2/Gal83 homologous gene presents a pattern of constant increasing.

The Snf1/Snf4/Gal83 complex in *S. cerevisiae,* activates different transcription factors (eg. Adr1, Sip4, Cat8) and inactivates the repressor Mig1/Hxk2, leading to the expression of a large set of genes involved in the use of alternative carbon sources (CONRAD et al., 2014).

Sip2 seems to complement the GAL83 function when this is deleted (ZHANG; OLSSON; NIELSEN, 2010). We were not able to find any of these downstream action genes in *T. cruzi* , which is expected since this parasite, in general, do not have transcriptional control at the initiation level. The downstream process of glucose depletion response in *T. cruzi* is still unknown. Nevertheless, it is plausible that this complex is acting in posttranscriptional regulation mechanisms.

The presence of glucose, conversely, leads to the activation of Glc7-Reg1 complex by the Hxk2, which inactivates Snf1 by dephosphorylation (CONRAD et al., 2014). No Reg1 homologous gene was found in *T. cruzi* genome, while Glc7 presents three candidates (TcCLB.507757.50, TcCLB.509633.60 and TcCLB.509633.50) with an increasing RNA expression pattern. An Hxk2 homologous gene is also found in *T. cruzi* (TcCLB.508951.20), with upregulated expression. These proteins are possibly involved in other pathways and their gene activation is achieved by post translational modification, rather than by protein amount.

We do not intend to exhaust or finish the point. This is an attempt to obtain a primary picture of glucose depletion response for *T. cruzi* .

## CONCLUSION

This work represents the first assessment of gene expression modulation in the growth curve of a kinetoplastid protozoa. We have discussed some aspects of the *T. cruzi* growth curve, mainly related to the stationary phase and the response to glucose depletion. Yet, we provided a high amount of data that are available to the scientific community to give insights into critical processes during the epimastigote development.

## REFERENCES

**Agabian, N.** (1990). Trans splicing of nuclear pre-mRNAs. *Cell* **61**, 1157–1160. doi:10.1016/0092-8674(90)90674-4.

**Archer, S. K., Inchaustegui, D., Queiroz, R. and Clayton, C.** (2011). The cell cycle regulated transcriptome of Trypanosoma brucei. *PLoS ONE* **6**,. doi:10.1371/journal.pone.0018425.

**Benjamini, Y. and Hochberg, Y.** (1995). Benjamini Y, Hochberg Y. Controlling the false discovery rate: a practical and powerful approach to multiple testing. *Journal of the Royal Statistical Society B* **57**, 289–300. doi:10.2307/2346101.

**Berriman, M., Ghedin, E., Hertz-Fowler, C., Blandin, G., Renauld, H., Bartholomeu, D. C., Lennard, N. J., Caler, E., Hamlin, N. E., Haas, B., Böhme, U., Hannick, L., Aslett, M. A., Shallom, J., Marcello, L., Hou, L., Wickstead, B., Alsmark, U. C. M., Arrowsmith, C., Atkin, R. J., Barron, A. J., Bringaud, F., Brooks, K., Carrington, M., Cherevach, I., Chillingworth, T.-J., Churcher, C., Clark, L. N., Corton, C. H., Cronin, A., Davies, R. M., Doggett, J., Djikeng, A., Feldblyum, T., Field, M. C., Fraser, A., Goodhead, I., Hance, Z., Harper, D., Harris, B. R., Hauser, H., Hostetler, J., Ivens, A., Jagels, K., Johnson, D., Johnson, J., Jones, K., Kerhornou, X., Koo, H., Larke, N., Landfear, S., Larkin, C., Leech, V., Line, A., Lord, A., Macleod, A., Mooney, P. J., Moule, S., Martin, D. M. A., Morgan, G. W., Mungall, K., Norbertczak, H., Ormond, D., Pai, G., Peacock, C. S., Peterson, J., Quail, M. A., Rabbinowitsch, E., Rajandream, M.-A., Reitter, C., Salzberg, S. L., Sanders, M., Schobel, S., Sharp, S., Simmonds, M., Simpson, A. J., Tallon, L., Turner, C. M. R., Tait, A., Tivey, A. R., Van Aken, S., Walker, D., Wanless, D., Wang, S., White, B., White, O., Whitehead, S., Woodward, J., Wortman, J., Adams, M. D., Embley, T. M., Gull, K., Ullu, E., Barry, J. D., Fairlamb, A. H., Opperdoes, F., Barrell, B. G., Donelson, J. E., et al.** (2005). The genome of the African trypanosome Trypanosoma brucei. *Science (New York, N.Y.)* 309, 416–22. doi:10.1126/science.1112642.

**Brener, Z.** (1973). Biology of *Trypanosoma cruzi*. *Annual review of microbiology* **27**, 347– 382. doi:10.1146/annurev.mi.27.100173.002023.

**Briones, M. R. S., Egima, C. M., Acosta, A. and Schenkman, S.** (1994). Trans-Sialidase and sialic acid acceptors from insect to mammalian stages of *Trypanosoma cruzi. Experimental Parasitology* **79**, 211–214. doi:10.1006/expr.1994.1083.

**Camargo, E. P.** (1964). Growth and differentiation in *trypanosoma cruzi*. I. Origin of metacyclic trypanosomes in liquid media.

*Revista do Instituto de Medicina Tropical de São Paulo* **6**, 93–100.

**Campbell, D. A., Thomas, S. and Sturm, N. R.** (2003). Transcription in kinetoplastid protozoa: Why be normal? *Microbes and Infection* **5**, 1231–1240. doi:10.1016/j.micinf.2003.09.005.

**Cannata, J. J. and Cazzulo, J. J.** (1984). The aerobic fermentation of glucose by *Trypanosoma cruzi*. *Comparative biochemistry and physiology. B, Comparative biochemistry* **79**, 297–308. doi:10.1016/0305-0491(84)90380-8.

**Capewell, P., Monk, S., Ivens, A., MacGregor, P., Fenn, K., Walrad, P., Bringaud, F., Smith, T. K. and Matthews, K. R.** (2013). Regulation of Trypanosoma brucei Total and Polysomal mRNA during Development within Its Mammalian Host. *PLoS ONE* **8**, e67069. doi:10.1371/journal.pone.0067069.

**Cassola, A., Gaudenzi, J. G. De and Frasch, A. C.** (2007). Recruitment of mRNAs to cytoplasmic ribonucleoprotein granules in trypanosomes. **65**, 655–670. doi:10.1111/j.1365-2958.2007.05833.x.

**Clayton, C.** (2013). The Regulation of Trypanosome Gene Expression by RNA-Binding Proteins. *PLoS Pathogens* **9**, 9–12. doi:10.1371/journal.ppat.1003680.

**Clayton, C. and Shapira, M.** (2007). Post-transcriptional regulation of gene expression in trypanosomes and leishmanias. *Molecular and Biochemical Parasitology* **156**, 93–101. doi:10.1016/j.molbiopara.2007.07.007.

**Conesa, A., Götz, S., García-Gómez, J. M., Terol, J., Talón, M. and Robles, M.** (2005). Blast2GO: A universal tool for annotation, visualization and analysis in functional genomics research. *Bioinformatics* **21**, 3674–3676. doi:10.1093/bioinformatics/bti610.

**Conrad, M., Schothorst, J., Kankipati, H. N., Van Zeebroeck, G., Rubio-Texeira, M. and Thevelein, J. M.** (2014). Nutrient sensing and signaling in the yeast Saccharomyces cerevisiae. *FEMS Microbiology Reviews* **38**, 254–299. doi:10.1111/1574-6976.12065.

**Contreras, V. T., Salles, J. M., Thomas, N., Morel, C. M. and Goldenberg, S.** (1985). In

vitro differentiation of *Trypanosoma cruzi* under chemically defined conditions. *Molecular and biochemical parasitology* **16**, 315–327. doi:10.1016/0166- 6851(85)90073-8.

**Contreras, V. T., Araujo-Jorge, T. C., Bonaldo, M. C., Thomaz, N., Barbosa, H. S., Meirelles, M. de N. and Goldenberg, S.** (1988). Biological aspects of the Dm 28c clone of *Trypanosoma cruzi* after metacyclogenesis in chemically defined media. *Memórias do Instituto Oswaldo Cruz* **83**, 123–33. doi:S0074-02761988000100016 [pii].

**Contreras A., V. T., De Lima R., A. R. and Navarro A., M. C.** (2006). Para La Diferenciación in Vitro *Trypanosoma cruzi* Morphogenesis : Relevant Factors for in Vitro Differentiation. *Acta Biol. Venez.* **26**, 49–60.

**Das, A., Morales, R., Banday, M., Garcia, S., Hao, L. L., Cross, G. A. M., Estevez, A. M. and Bellofatto, V.** (2012). *The essential polysome-associated RNA-binding protein RBP42 targets mRNAs involved in Trypanosoma brucei energy metabolism*. doi:10.1261/rna.033829.112.

**David, M., Dzamba, M., Lister, D., Ilie, L. and Brudno, M.** (2011). SHRiMP2: Sensitive yet Practical Short Read Mapping. *Bioinformatics* **27**, 1011–1012. doi:10.1093/bioinformatics/btr046.

**De Gaudenzi, J., Frasch, A. C. and Clayton, C.** (2005). RNA-Binding Domain Proteins in Kinetoplastids: a Comparative Analysis. *Eukaryotic Cell* **4**, 2106–2114. doi:10.1128/EC.4.12.2106-2114.2005.

**De Gaudenzi, J. G., Noé, G., Campo, V. a., Frasch, A. C. and Cassola, A.** (2011). Gene expression regulation in trypanosomatids. *Essays in biochemistry* **51**, 31–46. doi:10.1042/bse0510031.

**De Lima, A. R., Navarro, M. C., Arteaga, R. Y. and Contreras, V. T.** (2008). Cultivation of *Trypanosoma cruzi* epimastigotes in low glucose axenic media shifts its competence to differentiate at metacyclic trypomastigotes. *Experimental Parasitology* **119**, 336–342. doi:10.1016/j.exppara.2008.03.003.

**dos Santos, P. F., Ruiz, J. C., Soares, R. P. P., Moreira, D. S., Rezende, A. M., Folador, E. L., Oliveira, G., Romanha, A. J. and Murta, S. M. F.** (2012). Molecular characterization of the hexose transporter gene in benznidazole resistant and susceptible populations of *Trypanosoma cruzi* . *Parasites & Vectors* **5**, 161. doi:10.1186/1756-3305-5-161.

**Droll, D., Minia, I., Fadda, A., Singh, A., Stewart, M., Queiroz, R. and Clayton, C.** (2013). Post-Transcriptional Regulation of the Trypanosome Heat Shock Response by a Zinc Finger Protein. *PLoS Pathogens* **9**,. doi:10.1371/journal.ppat.1003286.

**El-sayed, N. M., Myler, P. J., Bartholomeu, D. C., Nilsson, D., Aggarwal, G., Tran, A.- N., Ghedin, E., Worthey, E. a, Delcher, A. L., Blandin, G., Westenberger, S. J., Caler, E.,**

**Cerqueira, G. C., Branche, C., Haas, B., Anupama, A., Arner, E., Aslund, L., Attipoe, P., Bontempi, E., Bringaud, F., Burton, P., Cadag, E., Campbell, D. a, Carrington, M., Crabtree, J., Darban, H., da Silveira, J. F., de Jong, P., Edwards, K., Englund, P. T., Fazelina, G., Feldblyum, T., Ferella, M., Frasch, A. C., Gull, K., Horn, D., Hou, L., Huang, Y., Kindlund, E., Klingbeil, M., Kluge, S., Koo, H., Lacerda, D., Levin, M. J., Lorenzi, H., Louie, T., Machado, C. R., McCulloch, R., Mckenna, A., Mizuno, Y., Mottram, J. C., Nelson, S., Ochaya, S., Osoegawa, K., Pai, G., Parsons, M., Pentony, M., Pettersson, U., Pop, M., Ramirez, J. L., Rinta, J., Robertson, L., Salzberg, S. L., Sanchez, D. O., Seyler, A., Sharma, R., Shetty, J., Simpson, A. J., Sisk, E., Tammi, M. T., Tarleton, R., Teixeira, S., Van Aken, S., Vogt, C., Ward, P. N., Wickstead, B., Wortman, J., White, O., Fraser, C. M., Stuart, K. D., Andersson, B., Tran, A.-N., Ghedin, E., Worthey, E. a, Delcher, A. L., Caler, E., Cerqueira, G. C., Branche, C., Haas, B., Anupama, A., Arner, E., Lena, A., Burton, P., Cadag, E., Campbell, D. a, Attipoe, P., Bontempi, E., et al.** (2005). The genome sequence of *Trypanosoma cruzi* , etiologic agent of Chagas disease. *Science (New York, N.Y.)* 309, 409–15. doi:10.1126/science.1112631.

**Elias, M. C. Q. B., Marques-Porto, R., Freym??ller, E. and Schenkman, S.** (2001). Transcription rate modulation through the *Trypanosoma cruzi* life cycle occurs in parallel with changes in nuclear organisation. *Molecular and Biochemical Parasitology* **112**, 79–90. doi:10.1016/S0166-6851(00)00349-2.

**Fadda, A., Ryten, M., Droll, D., Rojas, F., Färber, V., Haanstra, J. R., Merce, C., Bakker, B. M., Matthews, K. and Clayton, C.** (2014). Transcriptome-wide analysis of trypanosome mRNA decay reveals complex degradation kinetics and suggests a role for co-transcriptional degradation in determining mRNA levels. *Molecular Microbiology* **94**, 307–326. doi:10.1111/mmi.12764.

**Futschik, M. E. and Carlisle, B.** (2005). Noise-robust soft clustering of gene expression time-course data. *Journal of bioinformatics and computational biology* **3**, 965–88. doi:10.1142/S0219720005001375.

**Goldenberg, S., Salles, J. M., Contreras, V. T., Franco, M. P. L., Katzin, A. M., Colli, W. and Morel, C. M.** (1985). Characterization of messenger RNA from epimastigotes and metacyclic trypomastigotes of *Trypanosoma cruzi* . *FEBS Letters* **180**, 265–270. doi:10.1016/0014-5793(85)81083-8.

**Gourguechon, S., Savich, J. M. and Wang, C. C.** (2007). The Multiple Roles of cyclin E1 in Controlling Cell Cycle Progression and Cellular Morphology of Trypanosoma brucei. *Journal*

*of Molecular Biology* **368**, 939–950. doi:10.1016/j.jmb.2007.02.050.

**Greif, G., Ponce de Leon, M., Lamolle, G., Rodriguez, M., Piñeyro, D., Tavares- Marques, L. M., Reyna-Bello, A., Robello, C. and Alvarez-Valin, F.** (2013). Transcriptome analysis of the bloodstream stage from the parasite Trypanosoma vivax. *BMC genomics* **14**, 149. doi:10.1186/1471-2164-14-149.

**Haile, S. and Papadopoulou, B.** (2007). Developmental regulation of gene expression in trypanosomatid parasitic protozoa. *Current Opinion in Microbiology* **10**, 569–577. doi:10.1016/j.mib.2007.10.001.

**Hammarton, T. C., Monnerat, S. and Mottram, J. C.** (2007). Cytokinesis in trypanosomatids. *Current Opinion in Microbiology* **10**, 520–527. doi:10.1016/j.mib.2007.10.005.

**Hedbacker, K. and Carlson, M.** (2008). SNF1/AMPK pathways in yeast. *Frontiers in bioscience : a journal and virtual library* **13**, 2408–20. doi:2854 [pii].

**Hendriks, E. F. and Matthews, K. R.** (2005). Disruption of the developmental programme of Trypanosoma brucei by genetic ablation of TbZFP1, a differentiation-enriched CCCH protein. *Molecular Microbiology* **57**, 706–716. doi:10.1111/j.1365-2958.2005.04679.x.

**Hernández, R., Cevallos, A. M., Nepomuceno-mejía, T. and López-villaseñor, I.** (2012). Stationary phase in *Trypanosoma cruzi* epimastigotes as a preadaptive stage for metacyclogenesis. *Parasitology Research* **111**, 509–514. doi:10.1007/s00436-012-2974- y.

**Holetz, F. B., Correa, A., Ávila, A. R., Nakamura, C. V., Krieger, M. A. and Goldenberg, S.** (2007). Evidence of P-body-like structures in *Trypanosoma cruzi* . Biochemical and Biophysical Research Communications 356, 1062–1067.doi:10.1016/j.bbrc.2007.03.104.

**Ivens, A. C., Peacock, C. S., Worthey, E. A., Murphy, L., Aggarwal, G., Berriman, M., Sisk, E., Rajandream, M.-A. A., Adlem, E., Aert, R., Anupama, A., Apostolou, Z., Attipoe, P., Bason, N., Bauser, C., Beck, A., Beverley, S. M., Bianchettin, G., Borzym, K., Bothe, G., Bruschi, C. V, Collins, M., Cadag, E., Ciarloni, L., Clayton, C., Coulson, R. M. R., Cronin, A., Cruz, A. K., Davies, R. M., De Gaudenzi, J., Dobson, D. E., Duesterhoeft, A., Fazelina, G., Fosker, N., Frasch, A. C., Fraser, A., Fuchs, M., Gabel, C., Goble, A., Goffeau, A., Harris, D., Hertz-Fowler, C., Hilbert, H., Horn, D., Huang, Y., Klages, S., Knights, A., Kube, M., Larke, N., Litvin, L., Lord, A., Louie, T., Marra, M., Masuy, D., Matthews, K., Michaeli, S., Mottram, J. C., Müller-Auer, S., Munden, H., Nelson, S., Norbertczak, H., Oliver, K., O'neil, S., Pentony, M., Pohl, T. M., Price, C., Purnelle, B., Quail, M. A., Rabbinowitsch, E., Reinhardt, R., Rieger, M., Rinta, J., Robben, J., Robertson, L., Ruiz, J. C., Rutter, S., Saunders, D., Schäfer, M., Schein, J., Schwartz, D. C., Seeger, K., Seyler, A., Sharp, S., Shin, H., Sivam, D., Squares, R., Squares, S., Tosato,**

**V., Vogt, C., Volckaert, G., Wambutt, R., Warren, T., Wedler, H., Woodward, J., Zhou, S., Zimmermann, W., Smith, D. F., Blackwell, J. M., et al**. (2005). The genome of the kinetoplastid parasite, Leishmania major. *Science (New York, N.Y.)* 309, 436–42. doi:10.1126/science.1112680.

**Jiang, R. and Carlson, M.** (1997). The Snf1 protein kinase and its activating subunit, Snf4, interact with distinct domains of the Sip1/Sip2/Gal83 component in the kinase complex. *Molecular and cellular biology* **17**, 2099–2106.

**Kolev, N. G., Franklin, J. B., Carmi, S., Shi, H., Michaeli, S. and Tschudi, C.** (2010). The transcriptome of the human pathogen Trypanosoma brucei at single-nucleotide resolution. *PLoS Pathogens* **6**, 1–15. doi:10.1371/journal.ppat.1001090.

**Kolev, N. G., Ramey-Butler, K., Cross, G. A. M., Ullu, E. and Tschudi, C.** (2012). Developmental Progression to Infectivity in Trypanosoma brucei Triggered by an RNA-Binding Protein. *Science* **338**, 1352–1353. doi:10.1126/science.1229641.

**Kramer, S., Kimblin, N. C. and Carrington, M.** (2010). Genome-wide in silico screen for CCCH-type zinc finger proteins of Trypanosoma brucei, *Trypanosoma cruzi* and Leishmania major. *BMC Genomics* **11**, 283. doi:10.1186/1471-2164-11-283.

**Li, Z.** (2012). Regulation of the cell division cycle in Trypanosoma brucei. *Eukaryotic Cell* **11**, 1180–1190. doi:10.1128/EC.00145-12.

**Li, Y., Shah-Simpson, S., Okrah, K., Belew, A. T., Choi, J., Caradonna, K. L., Padmanabhan, P., Ndegwa, D. M., Temanni, M. R., Corrada Bravo, H., El-Sayed, N. M. and Burleigh, B. A.** (2016). Transcriptome Remodeling in *Trypanosoma cruzi* and Human Cells during Intracellular Infection. *PLoS pathogens* 12, e1005511. doi:10.1371/journal.ppat.1005511.

**Liang, X. H., Haritan, A., Uliel, S. and Michaeli, S.** (2003). trans and cis splicing in trypanosomatids: Mechanism, factors, and regulation. *Eukaryotic Cell* **2**, 830–840. doi:10.1128/EC.2.5.830-840.2003.

**Ling, A. S., Trotter, J. R. and Hendriks, E. F.** (2011). A Zinc Finger Protein, TbZC3H20, Stabilizes Two Developmentally Regulated mRNAs in Trypanosomes. *Journal of Biological Chemistry* **286**, 20152–20162. doi:10.1074/jbc.M110.139261.

**Mani, J., Güttinger, A., Schimanski, B., Heller, M., Acosta-Serrano, A., Pescher, P., Späth, G. and Roditi, I.** (2011). Alba-Domain Proteins of Trypanosoma brucei Are Cytoplasmic RNA-Binding Proteins That Interact with the Translation Machinery. *PLoS ONE* **6**, e22463. doi:10.1371/journal.pone.0022463.

**Martínez-Calvillo, S., Vizuet-de-Rueda, J. C., Florencio-Martínez, L. E., Manning-Cela, R. G. and Figueroa-Angulo, E. E.** (2010). Gene expression in trypanosomatid parasites. Journal of biomedicine & biotechnology 2010, 525241. doi:10.1155/2010/525241.

**Maugeri, D. A., Cannata, J. J. B. and Cazzulo, J.-J.** (2011). Glucose metabolism in *Trypanosoma cruzi* . *Essays in biochemistry* **51**, 15–30. doi:10.1042/bse0510015.

**Morozova, O., Hirst, M. and Marra, M. A.** (2009). Applications of New Sequencing Technologies for Transcriptome Analysis. *Annu. Rev. Genomics Hum. Genet* **10**, 135– 51. doi:10.1146/annurev-genom-082908-145957.

**Nepomuceno-Mejía, T., Lara-Martínez, R., Cevallos, A. M., López-Villaseñor, I., Jiménez-García, L. F. and Hernández, R.** (2010). The *Trypanosoma cruzi* nucleolus: a morphometrical analysis of cultured epimastigotes in the exponential and stationary phases. *FEMS microbiology letters* **313**, 41–6. doi:10.1111/j.1574-6968.2010.02117.x.

**Portman, N. and Gull, K.** (2010). The paraflagellar rod of kinetoplastid parasites: From structure to components and function. *International Journal for Parasitology* **40**, 135– 148. doi:10.1016/j.ijpara.2009.10.005.

**Potenza, M., Schenkman, S., Laverrière, M. and Tellez-Iñón, M. T.** (2012). Functional characterization of TcCYC2 cyclin from *Trypanosoma cruzi* . *Experimental Parasitology* **132**, 537–545. doi:10.1016/j.exppara.2012.09.002.

**Rastrojo, A., Carrasco-Ramiro, F., Martín, D., Crespillo, A., Reguera, R. M., Aguado, B. and Requena, J. M.** (2013). The transcriptome of Leishmania major in the axenic promastigote stage: transcript annotation and relative expression levels by RNA-seq. *BMC genomics* **14**, 223. doi:10.1186/1471-2164-14-223.

**Robinson, M. D., McCarthy, D. J. and Smyth, G. K.** (2009). edgeR: A Bioconductor package for differential expression analysis of digital gene expression data. *Bioinformatics* **26**, 139–140. doi:10.1093/bioinformatics/btp616.

**Schumann Burkard, G., Käser, S., de Araújo, P. R., Schimanski, B., Naguleswaran, A., Knüsel, S., Heller, M. and Roditi, I.** (2013). Nucleolar proteins regulate stage-specific gene expression and ribosomal RNA maturation in Trypanosoma brucei. *Molecular Microbiology* **88**, 827–840. doi:10.1111/mmi.12227.

**Shaw, A. K., Kalem, M. C. and Zimmer, S. L.** (2016). Mitochondrial Gene Expression Is Responsive to Starvation Stress and Developmental Transition in *Trypanosoma cruzi* . **1**,. doi:10.1128/mSphere.00051-16.Editor.

**Teixeira, S. M.** (1998). Control of gene expression in Trypanosomatidae. *Brazilian journal of medical and biological research* **31**, 1503–16.

**Tetaud, E., Bringaud, F., Chabas, S., Barrett, M. P. and Baltz, T.** (1994). Characterization of glucose transport and cloning of a hexose transporter gene in *Trypanosoma cruzi* . *Proceedings of the National Academy of Sciences of the United States of America* **91**, 8278–82.

**Tyler, K. M. and Engman, D. M.** (2000). Flagellar elongation induced by glucose limitation is preadaptive for *Trypanosoma cruzi* differentiation. *Cell Motility and the Cytoskeleton* **46**, 269–278. doi:10.1002/1097-0169(200008)46:4<269::AID-CM4>3.0.CO;2-V.

**Urbina, J. A.** (1994). Intermediary Metabolism of *Trypanosoma cruzi* . *Parasitology today* **I**, 107–110.

**Werner-Washburne, M., Braun, E., Johnston, G. C. and Singer, R. a** (1993). Stationary phase in the yeast Saccharomyces cerevisiae. *Microbiology and Molecular Biology Reviews* **57**, 383–401. doi:10.1093/nar/gkr782.

**WHO** (2016). Chagas disease (American trypanosomiasis).

**Wurst, M., Seliger, B., Jha, B. A., Klein, C., Queiroz, R. and Clayton, C.** (2012). Expression of the RNA recognition motif protein RBP10 promotes a bloodstream-form transcript pattern in Trypanosoma brucei. *Molecular Microbiology* **83**, 1048–1063. doi:10.1111/j.1365-2958.2012.07988.x.

**Yates, G. T. and Smotzer, T.** (2007). On the lag phase and initial decline of microbial growth curves. *Journal of Theoretical Biology* **244**, 511–517. doi:10.1016/j.jtbi.2006.08.017.

**Zhang, J., Olsson, L. and Nielsen, J.** (2010). The beta-subunits of the Snf1 kinase in Saccharomyces cerevisiae, Gal83 and Sip2, but not Sip1, are redundant in glucose derepression and regulation of sterol biosynthesis. *Molecular Microbiology* **77**, 371–383. doi:10.1111/j.1365-2958.2010.07209.x.

## TABLES

Table 1. The Number of DEGs in each day of the epimastigotes growth. All exprimental points were compared to the first day of culture using edgeR package (exact test function) with 10% FDR, for total and polysomal RNA samples.

| Days of growth | Total | Polysomal |
|---|---|---|
| 2 | 0 | 0 |
| 3 | 1 | 0 |
| 4 | 1 | 5 |
| 5 | 570 | 33 |
| 6 | 145 | 600 |
| 7 | 1170 | 51 |
| 8 | 737 | 577 |
| 9 | 1510 | 280 |
| 10 | 1564 | 193 |

Table 2: Information concerning the searches of *S. cerevisiae* homolog genes related to glucose sensing in *T. cruzi*.

| **Name** | **Gene ID in *T. cruzi*** | **% sim/ext** | **e-value** | **Cluster** |
|---|---|---|---|---|
| Snf1 | TcCLB.510861.140 | 63/46 | 4.00E-78 | 10 |
| | TcCLB.510257.130 | 55/60 | 1.00E-61 | - |
| | TcCLB.464807.10 | 65/35 | 7.00E-72 | 10 |
| Sak1/Tos3/Elm1 | TcCLB.503613.10 | 48/38 | 1.00E-42 | 13 |
| | TcCLB.506775.190 | 50/30 | 5.00E-40 | 8 |
| | TcCLB.506801.120 | 49/29 | 1.00E-35 | 1 |
| | TcCLB.510759.40 | 51/25 | 4.00E-36 | 6 |
| Snf4 | TcCLB.503841.20 | 54/31 | 3.00E-07 | - |
| Sip2/Gal83 | TcCLB.504427.50 | 52/16 | 0.002 | 4 |
| Glc7 | TcCLB.507757.50 | 86/88 | 3.00E-146 | - |
| | TcCLB.509633.60 | 79/93 | 4.00E-136 | 8 |
| | TcCLB.509633.50 | 78/94 | 1.00E-135 | 8 |
| Hxk2 | TcCLB.508951.20 | 53/95 | 4.00E-76 | - |

## FIGURES

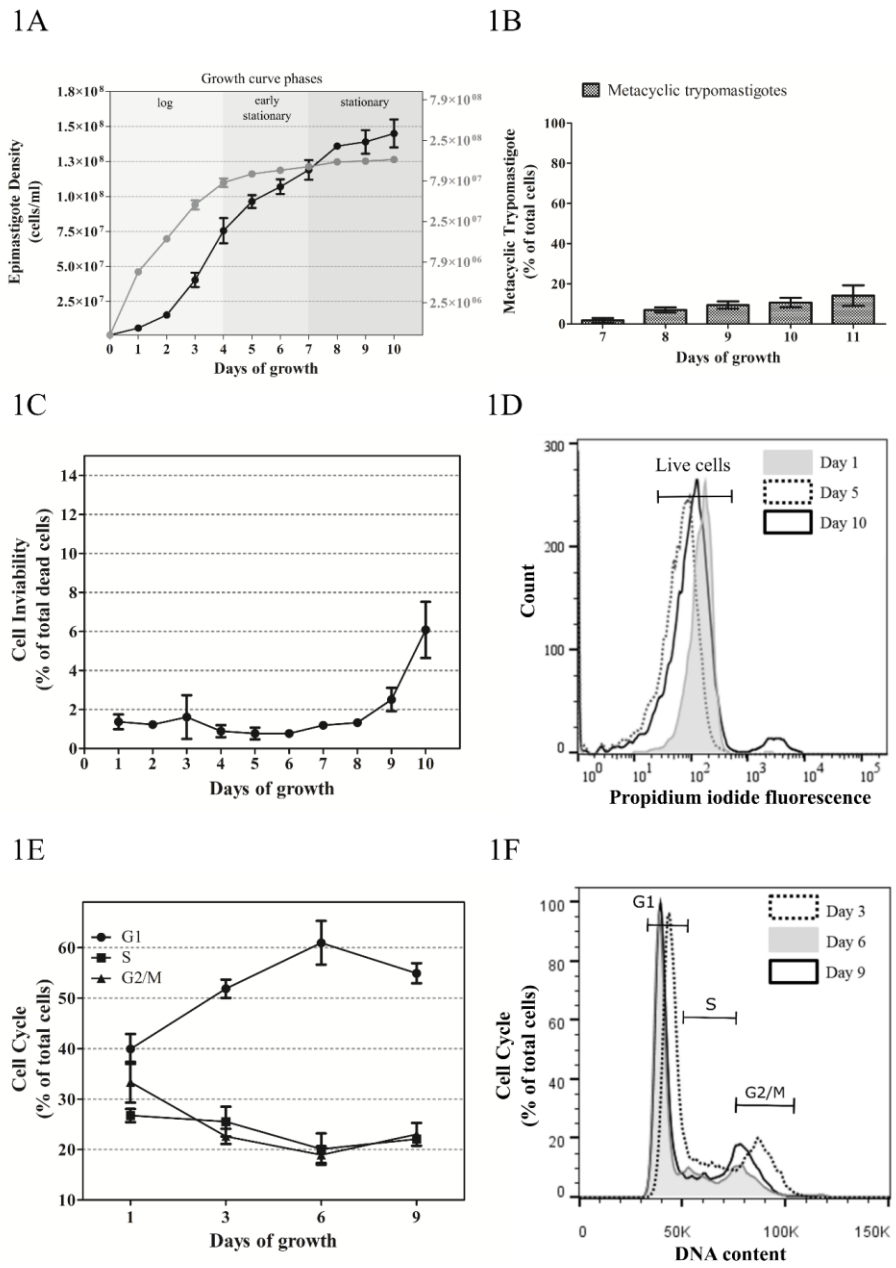


Fig. 1. Analysis of axenic epimastigotes growth. (A) Parasite growth in culture were measured daily over 10-day period and the cell densities were plotted against time showing the growth curve. Left y axis: linear scale, right y axis: logarithmic scale; (B) Percentage of metacyclic trypomastigotes during the epimastigotes culture; (C) Cell inviability were measured daily by PI staining over 10-day period and plotted against time; (D) Cell viability profiles of epimastigote cells with PI fluorescence (indicating live vs dead cells) at day 1, 3 and 9; (E) Cell cycle were measured at day 1, 3, 6 and 9 of epimastigote growth and plotted against time; and (F) flow cytometry profiles of epimastigote cells with propidium iodide fluorescence (indicating DNA content) at day 1, 3 and 9. Data points are expressed as mean ± S.D. of three biological replicates.

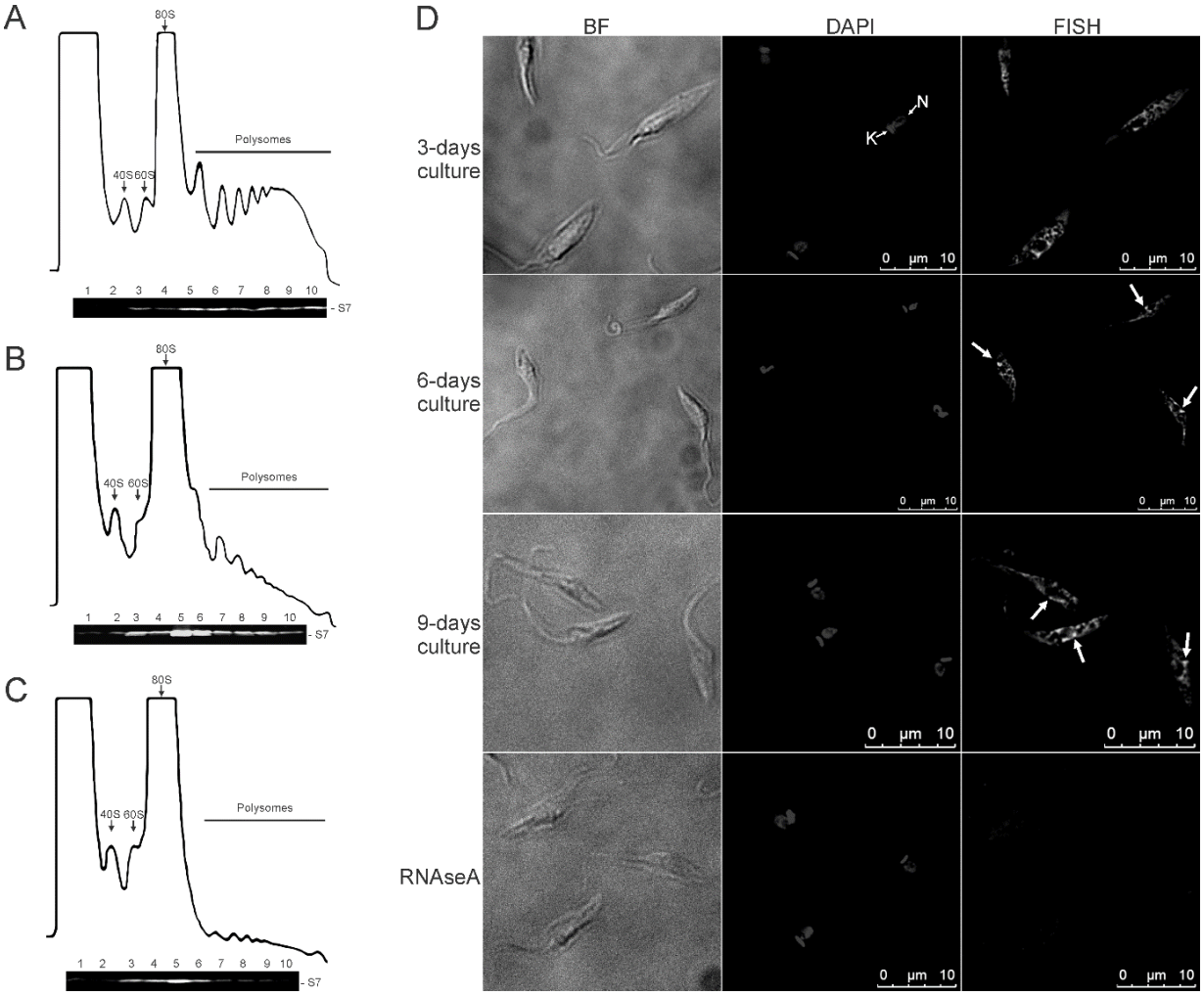


Fig. 2. Polysomes and mRNA granules analysis. (A-C) Profile sedimentation profile on sucrose density gradient (15-55%) of 3 (A), 6 (B) and 9 (C) -days culture of the *T. cruzi* growth curve treated with 100 µg/ml cicloheximide. Fractions (1-10) were analyzed by Western-blot using an antibody against S7 ribosomal protein, a small ribosomal subunit protein. 40S and 60S ribosomal subunits, the 80S ribosome monomer and polysomes are indicated in (A-C). (D) Localization of mRNA by fluorescent in situ hybridization (FISH) assay using specific oligo(dT) probe conjugated with digoxigenin. Probe detection was performed by indirect immunofluorescence with anti-DIG goat antibodies (Sigma-Aldrich, 1:300 dilution) followed by secondary Alexa Fluor 488-conjugated antibodies (1:600 dilution). As a control, 100 mg/ml RNase A was incubated with the parasites before probe hybridization (RNase A) or the probe was not incubated for hybridization (No probe). BF = Bright field. DAPI = DNA stained with DAPI. N = nucleus. K = kinetoplast. Arrows = parasites with accumulation of mRNA in granules. Bar = 5 µm.

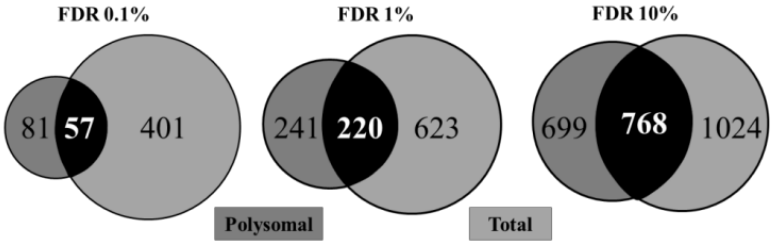


Fig. 3. Comparison between total and polysomal RNA numbers of differential expressed genes (DEG) identified during growth curve using Euler diagram. DEGs with 0.1, 1.0 and 10% FDR analysis were considered.

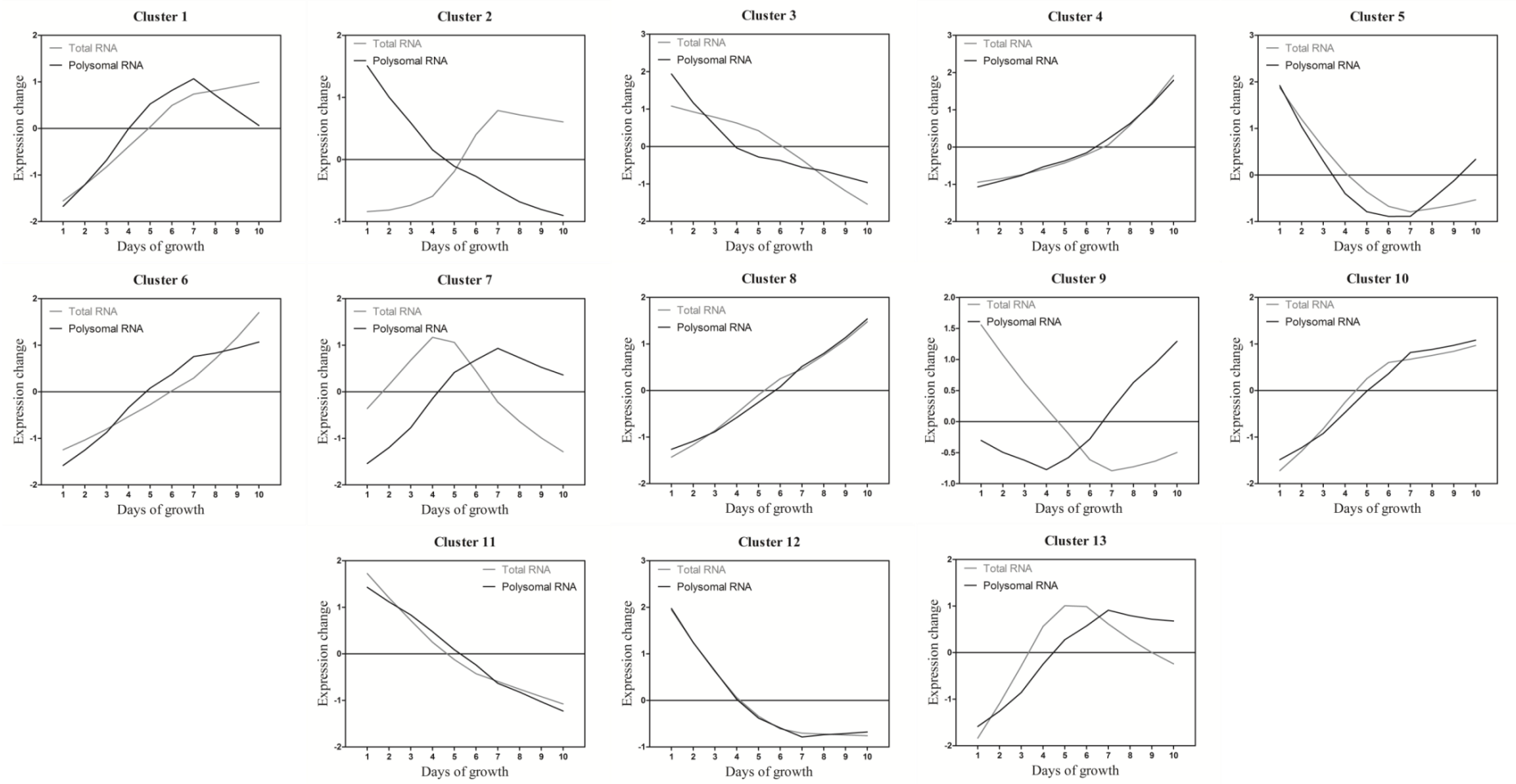


Fig. 4. Temporal patterns of gene expression during the *T. cruzi* growth curve identified by Fuzzy c-means clustering. Only the centroides are shown. Thirteen clusters showed different profile.

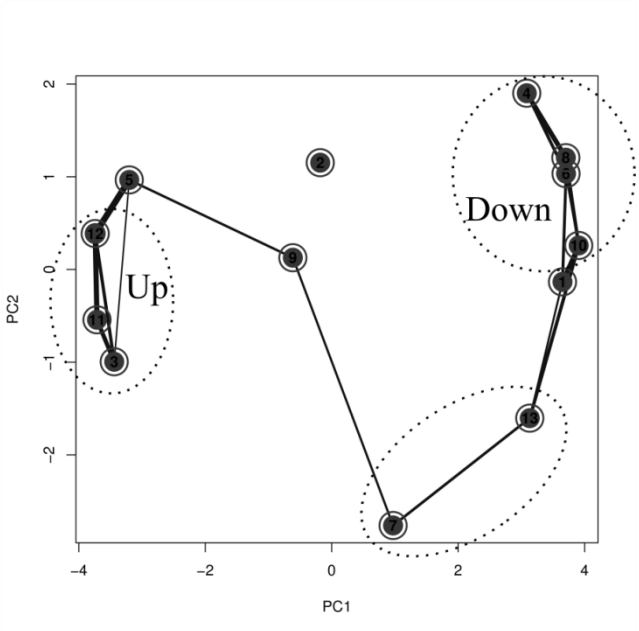


Fig. 5. Principal component analysis (PCA) showing the distance between each cluster of DEGs. The width of lines connecting the points represents the number of genes shared between groups during the fuzzy clusterization iterations. Dotted ellipses represent clusters with similar expression patterns that were grouped for GO analysis (see text). This graph was ploted by the "overlap.plot" function of fuzzy-c-means algorithm.

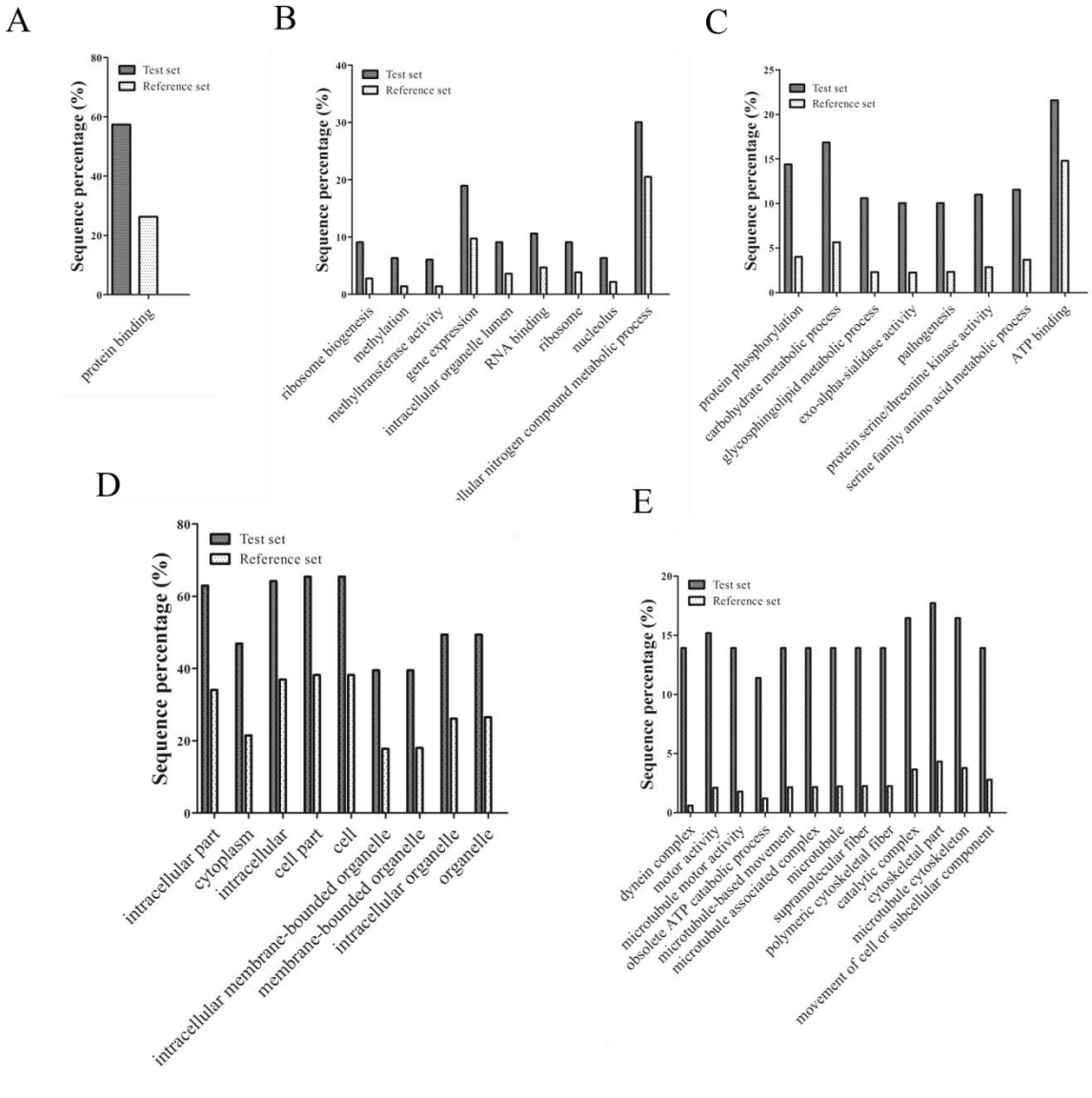


Fig. 6. Enriched categories of GO terms for the different clusters. A) Cluster 1; B) Cluster 5; C) Clusters 7 and 13; D) Clusters 3, 11 and 12; E) Clusters 4, 6, 8 and 10.

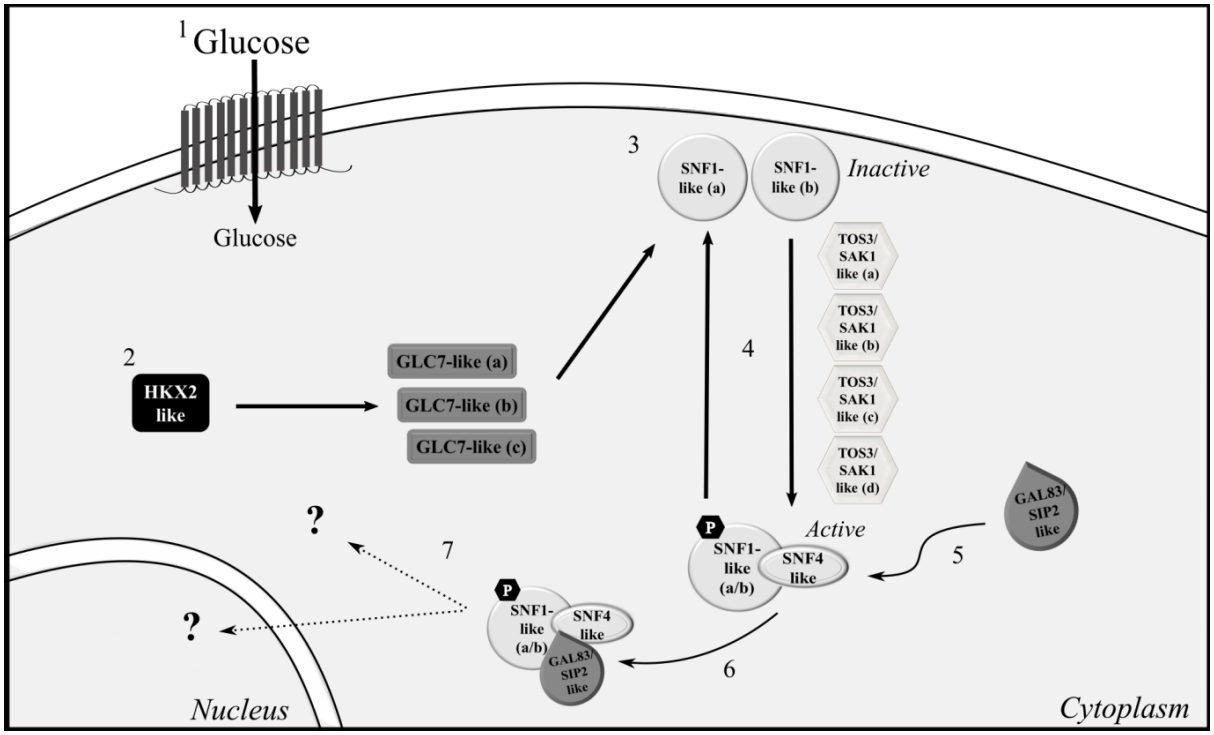


Fig. 7. Hypothetical model of glucose sensing pathway in *Trypanosoma cruzi* . 1) Glucose uptake in cell by only one type of glucose transporter gene that encodes a predicted protein with 12 transmembrane domains (TcrHT gene). In presence of glucose: 2) HXK2-like could play an important role, possibly stimulates one or more of the homologous Glc7-like phosphatases (a, b and c) to dephosphorylate Snf1-like. In absence of glucose: (3) One or moreSnf1-like protein kinases (two of the three possible *T. cruzi* homologous were represented) could be a major protein sense of glucose repression pathway (4) being phosphorylated by four possible homologous proteins, named Tos3/Sak1-like proteins (a, b, c and d). Phosphorylated Snf1-like probable acts as a heterotrimeric protein complex binding to Snf4-like, and to (5) a third protein, Gal83/Sip2-like forming the active complex (6). Thus, the complex might act (7) in cytoplasm and/or nucleus possible influencing the expression of specific genes in a posttranslational manner.

## ADDITIONAL FILES

Additional file 1

Additional Table 1. RNA total sequencing date from SOLiD platform. Total number of reads generated, mapped genes and percentage ratio between reads number and mapped genes.

| Sample | Reads | Mapped genes | % |
|---|---|---|---|
| R1 d1 | 25.914.424 | 3.761.994 | 14,5% |
| R2 d1 | 14.423.190 | 4.365.746 | 30,3% |
| R3 d1 | 15.193.196 | 5.667.094 | 37,3% |
| R1 d2 | 8.009.108 | 1.267.551 | 15,8% |
| R2 d2 | 13.567.040 | 4,399,547 | 32,4% |
| R3 d2 | 13.511.044 | 4.939.298 | 36,6% |
| R1 d3 | 28.114.654 | 8.124.908 | 28,9% |
| R2 d3 | 9.197.397 | 2.038.984 | 22,2% |
| R3 d3 | 27.552.854 | 9.998.374 | 36,3% |
| R1 d4 | 7.240.263 | 1.358.227 | 18,8% |
| R2 d4 | 10.431.269 | 1.378.185 | 13,2% |
| R3 d4 | 13.559.166 | 5.273.825 | 38,9% |
| R1 d5 | 11.054.831 | 1.297.336 | 11,7% |
| R2 d5 | 9.393.150 | 3.480.423 | 37,1% |
| R1 d6 | 7.028.547 | 802.985 | 11,4% |
| R2 d6 | 12.316.046 | 1.685.044 | 13,7% |
| R3 d6 | 19.433.111 | 7.036.615 | 36,2% |
| R1 d7 | 18.592.523 | 6.771.367 | 36,4% |
| R2 d7 | 12.108.683 | 2.809.495 | 23,2% |
| R3 d7 | 14.299.758 | 4.879.346 | 34,1% |
| R1 d8 | 10.979.175 | 4.552.584 | 41,5% |
| R2 d8 | 11.003.776 | 4.593.353 | 41,7% |
| R3 d8 | 31.069.371 | 8.087.033 | 26,0% |
| R1 d9 | 6.491.121 | 2.277.764 | 35,1% |
| R2 d9 | 28.091.980 | 8,322,228 | 29,6% |
| R3 d9 | 12.397.971 | 2.787.894 | 22,5% |
| R1 d10 | 7.418.750 | 2.580.280 | 34,8% |
| R2 d10 | 26.134.377 | 9.344.508 | 35,8% |
| R3 d10 | 30.624.996 | 9.392.500 | 30,7% |

Note: R- biological replicates; d- day of growth.

Additional Table 2. RNA polysomal sequencing date from SOLiD platform. Total number of reads generated, mapped genes and percentage ratio between reads number and mapped genes.

| Sample | Reads | Mapped genes | % |
|---|---|---|---|
| R1 d1 | 26.629.052 | 625.439 | 2,3% |
| R2 d1 | 13.035.689 | 5.478.569 | 42,0% |
| R3 d1 | 14.258.745 | 5.500.564 | 38,6% |
| R1 d2 | 11.878.544 | 4.395.924 | 37,0% |
| R2 d2 | 15.400.642 | 5.638.885 | 36,6% |
| R2 d3 | 12773.805 | 4.825.063 | 37,8% |
| R3 d3 | 15.798.712 | 5.993.916 | 37,9% |
| R1 d4 | 14.532.722 | 5.333.752 | 36,7% |
| R3 d4 | 11.200.086 | 4.544.160 | 40,6% |
| R1 d5 | 15.657.212 | 5.886.898 | 37,6% |
| R3 d5 | 18.145.506 | 6.714.337 | 37,0% |
| R2 d6 | 18.175.237 | 7.579.212 | 41,7% |
| R1 d7 | 15.231.345 | 5.503.538 | 36,1% |
| R2 d7 | 12.802.809 | 5.180.039 | 40,5% |
| R3 d7 | 9.215.150 | 209.266 | 2,3% |
| R1 d8 | 14.418.080 | 5.437.061 | 37,7% |
| R2 d8 | 16.996.317 | 5.620.611 | 33,1% |
| R3 d8 | 15.719.249 | 6.584.459 | 41,9% |
| R2 d9 | 15.817.710 | 6.548.630 | 41,4% |
| R3 d9 | 110.269.949 | 43.012.501 | 39,0% |
| R3 d10 | 14.189.340 | 5.386.171 | 38,0% |

Note: R- biological replicates; d- day of growth.

Additional Figure 1.

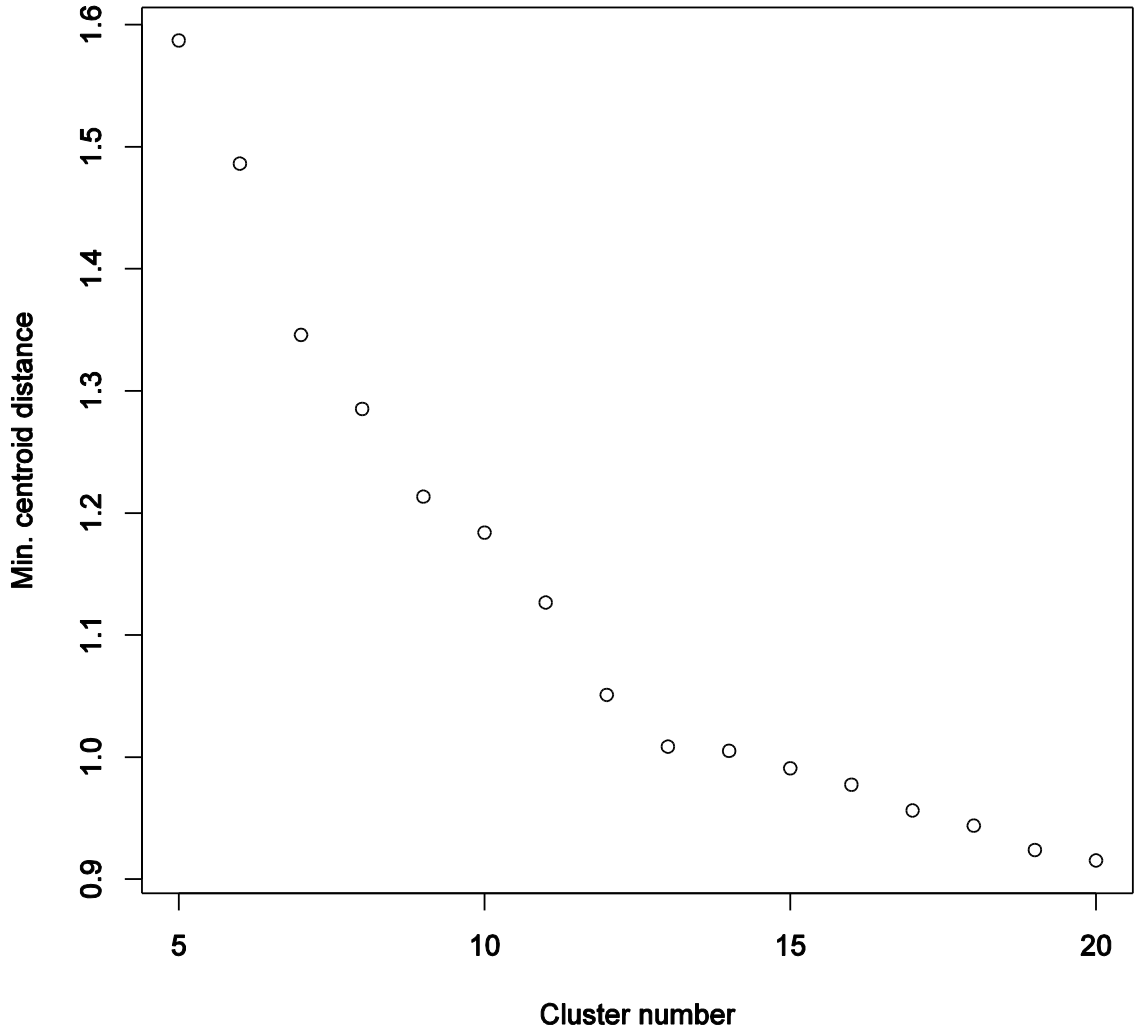


Additional Figure 1. Global clustering structure generated by Fuzzy. Three clusterings for c = 12, 13, 14 were analyzed and compared.

# Additional file 3

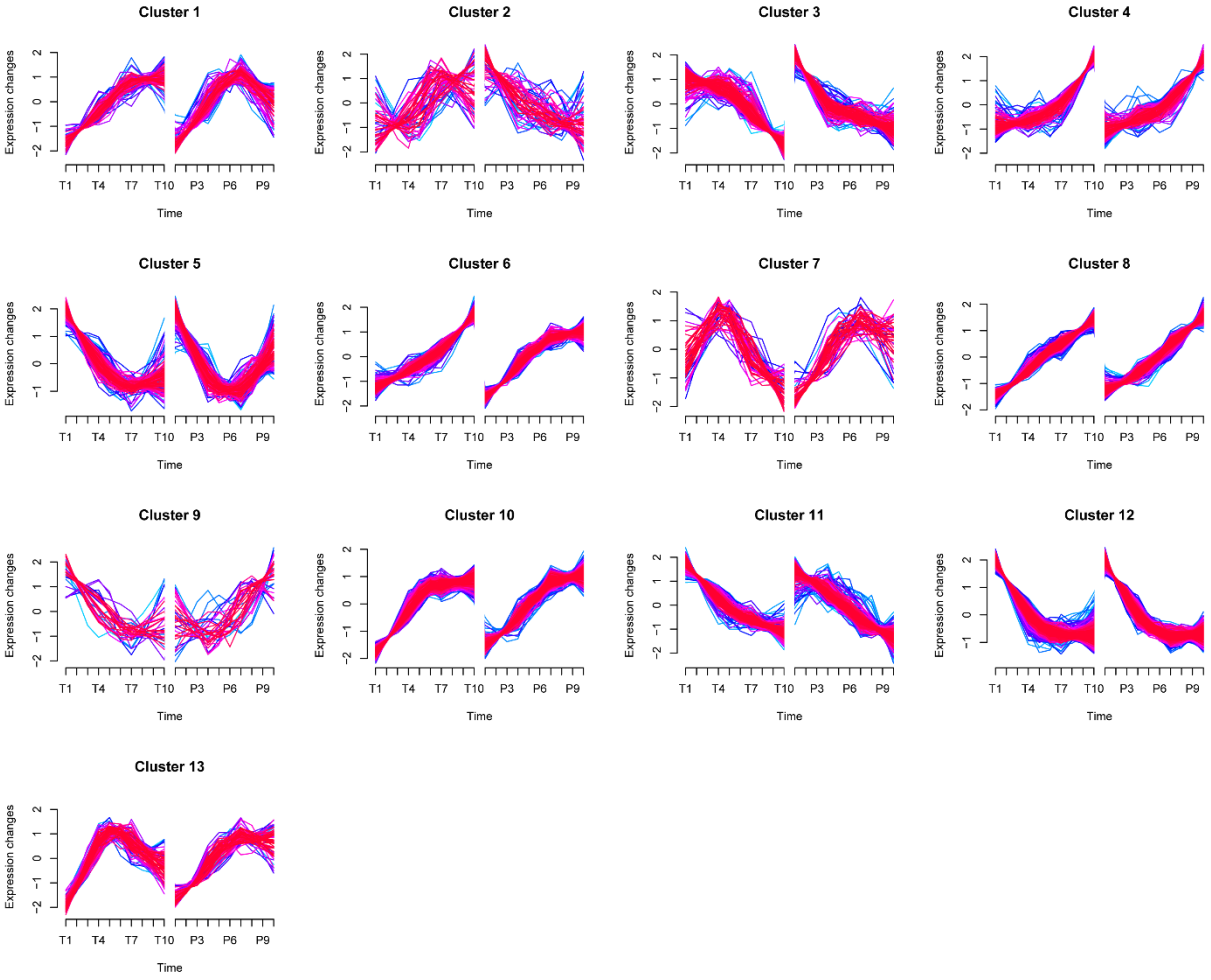

# 4 CAPÍTULO 2

Artigo científico em preparação para ser enviado para a revista Journal of Proteomics*

* Os dados analisados até o momento são preliminares, pois nem todas as corridas previstas foram concluídas.

## PROTEOME OF *TRYPANOSOMA CRUZI* GROWTH CURVE

Cyndia M. B. dos Santos[1,2ǂ]; Juliana C. Amorim[1ǂ]; Marco A. Krieger[1,2,3]; Daniela Parada Pavoni[1,2]; Fabricio K. Marchini[1,3]; Christian M. Probst[1,2*]

1 Laboratório de Genômica Funcional, Instituto Carlos Chagas – Fiocruz, R. Prof. Algacyr Munhoz Mader, 3775, Curitiba - PR - Brazil, 81350-010
2 Programa de Pós-Graduação em Biologia Celular e Molecular, Centro Politécnico, Universidade Federal do Paraná, Curitiba, Paraná, Brazil.
3 Instituto de Biologia Molecular do Paraná, Curitiba, Paraná, Brazil.

*Corresponding author: Email: cprosbt@fiocruz.br
Curitiba/PR, Brazil, Tel.: +55 41 3316 3230; Fax: +55 41 3316 3267

ǂ These authors contributed equally to this work

**Key words:** proteome, growth, trypanosomatid.

**ABSTRACT**

*Trypanosoma cruzi* is the causative agent of Chagas disease, an important illness in Latin America affecting eight millions of people. The study of many aspects of the parasite growth curve in culture is an important step to understand their basic biology, and their behavior in an environment that varies over a time course. We performed a LC-MS/MS approach during eight days of the *T. cruzi* epimastigote growth curve and this study is a complementary a substantial transcriptomic analysis of *T. cruzi* epimastigote growth curve that allowed us to better comprehend their gene expression dynamics. We identified 2,766 protein groups with a false discovery rate of 1% and 1301 proteins by quantitative proteomics, which 92 differentially expressed proteins (DEPs) from the two biological replicates. The Fisher's exact test showed a great percentage of growth, cell division, mRNA binding proteins between all identified proteins. This work will provide important information concerning the epimastigote growth.

## INTRODUCTION

The *Trypanosoma cruzi* is the flagellated protozoa causative of Chagas disease which is an endemic illness with essentially chronic clinical course. This disease, the protozoa and its insect vector were discovery by the Brazilian physician Carlos Chagas in 1909 (CHAGAS, 1909). However, after more than one hundred years of parasite discovery little is known about many aspects of its cellular and molecular biology. Parasite life is essentially connected with growth and this phenomenon can be scientifically studied from growth curve that is represented by the relation between cell number in vitro culture at different times. Growth curve analysis were used in *T. cruzi* to evaluate growth factors as essential components of culture medium (ENDERS; BRAUNS; ZWISLER, 1977) and in Leishmania braziliensis to verify the efficiency of adaption in new medium (CELESTE; GUIMARÃES, 1988).

The complex life cycle of *T. cruzi* is heteroxenic involving a vertebrate and an invertebrate host, achieving at least four different stages: epimastigote and metacyclic trypomastigote are present in triatomine vector; and amastigote and bloodstream trypomastigote present in mammalian (TYLER; ENGMAN, 2001). The epimastigote is a proliferative and non-infective form found in the insect gut. When it reaches the midgut terminal portion, a decrease in nutritional conditions leads to physiological stress and the parasite undergoes a process of differentiation to metacyclic trypomastigote. The metacyclic

trypomastigote is the infective stage and its natural transmission occurs when the triatomine vector bites the mammalian host to feed on blood. This leads to gut engorgement that causes immediate excretion, containing the parasites (ALVES; COLLI, 2007; BONALDO et al., 1988; TYLER; ENGMAN, 2001).

The understanding of in vitro cultivation of *T. cruzi* epimastigote forms allowed considerable advance on biochemistry and physiology aspects of this evolutionary stage. As long as the parasites grow and multiply along the growth curve, high cell density leads to nutrient depletion and the cells enter the stationary phase, where they present some morphological changes and seem to adopt an intermediate form between the exponential epimastigote and the metacyclic trypomastigote cells (HERNÁNDEZ et al., 2012). Thus, studies of the epimastigote growth curve and the effects of ambient factors on growth become an important way to understand how this parasite behaves in environments that change over time. In this sense, omics studies can provide insights into the molecular components and processes involved in the growth curve, as well as in their regulation.

Unicellular organisms have the ability to adapt to the different environmental situations; therefore, they can survive to several adverse conditions. These alterations are possible by gene expression modulation, achieved mainly by transcription start control. However, trypanosomatids have a small number of RNA Polymerase II transcription regions characterized to date. Gene expression in these parasites occurs in polycistronic units at the same rate, encode proteins with unrelated functions. Control of gene expression occurs by post-transcriptional mechanisms, regulated in different ways, as the mRNA processing and export from the nucleus; mRNA cytoplasmic degradation; association with the translational machinery and protein stability (TEIXEIRA, 1998; VANHAMME; PAYS, 1995). Data of transcriptomic analysis has shown to be a simple resource to comprehend gene expression dynamics in *T. cruzi* epimastigotes based on the wide time relation associated with the analyses of several different points of culture along the growth curve (SANTOS et al., 2016). Moreover, we have demonstrated that at the stationary phase of *T. cruzi* epimastigote, seems to occur a mechanism of translational decrease, where the polysome content is greatly disrupted while the number mRNA granules increases. As we found interesting patterns of mRNA modulation at the stationary phase, proteomic analysis along the growth curve can help to better understand the mRNA dynamics occurring between polysomes and RNA granules at this quiescent stage, shedding light on which proteins are being translated and which genes may have been maintained in granules. Here we present a proteomic analysis from the *T. cruzi* growth curve.

Proteomic analysis during growth curve will contribute to expand the knowledge about behavior the *T. cruzi* on natural stress that occurs in vitro, such a starving and high density population.

## MATERIAL AND METHODS

### *Parasite cultures and protein extraction*

Parasites culture: exponentially growing epimastigotes form of *T. cruzi* Dm28c (CONTRERAS et al., 1988a) were cultured in liver LIT medium (5.4 mM KCl, 150 mM NaCl, 24 mM glucose, 5% (v/v) liver extract, 0.025% (w/v) hemin, 2% (w/v) yeast extract, 1.5% (w/v) tryptose, 10% heat-inactivated fetal bovine) at 28 °C (CAMARGO, 1964b). Growth curve was followed by eight consecutive days in culture (density of ~ 3 x 107 – 1 x 108 parasites/ mL) were obtained by centrifugation at 3000×g for 10 min at 25 °C.

Protein extraction: 100 µg of total protein were extract with lysis buffer (0.1 M Tris-HCl, pH 7.5, 0.1 M DTT and 4% SDS), incubated at 95 °C for 5 min and sonicated at duty cycle 20% and output control 3 (Cole Parmer 500-Watt Ultrasonic Homogenizer) (SCHELTEMA et al., 2014). Cell debris was removed by centrifugation at 14,000×g for 10 min and supernatants were collected and stored at −80 ºC until use.

### *Shotgun Proteomics*

Sample preparation: *T. cruzi* proteome were evaluated by GeLC-MS/MS method. First, 28 µg of total parasite extract were separated by one-dimension SDS-PAGE in 10% polyacrylamide gel and then stained with Coomassie blue. Each gel lane was sliced to small pieces of about 1 mm3; destained with 50% ethanol, 25 mM ammonium bicarbonate (ABC), and dehydrated with 100% ethanol. Proteins in the gel pieces were reduced with 10 mM DTT, 50 mM ABC, and alkylated with 50 mM iodacetamide, 50 mM ABC. Then, gels were washed with 50 mM ABC and dehydrated with 100% ethanol and this step was repeated. At that time, gels were incubated with a 12.5 ng/ml trypsin (Promega) solution in 50 mM ABC at 37 °C for 18 hours. After trypsin digestion, trifluoroacetic acid (TFA) was added at a final concentration of 0.5%. Peptides were extracted from gel matrix through incubation twice with 30% MeCN, 3% TFA, and twice with

100% MeCN. Extracted peptides were dried and desalted with homemade C18 spin columns. Peptides were eluted from C18 columns and resuspended in 25 µl 0.1% formic acid, 5% DMSO. Ten microliters were separated by on-line C18 reversed phase chromatography and injected into a Thermo LTQ-Orbitrap XL ETD (RAPPSILBER; ISHIHAMA; MANN, 2003).

NanoLC-MS/MS runs: runs were conducted on mass spectrometry facility RPT02H PDTIS/ Carlos Chagas Institute /FIOCRUZ-PR. Peptide mixtures were separated by online RP nanoLC and analyzed by electrospray tandem mass spectrometry. The experiments were performed on an Agilent 1000 nanoflow system connected to an LTQ Orbitrap XL ETD mass spectrometer (Agilent Technologies, Palo Alto, CA) equipped with a nanoelectrospray ion source (Proxeon Biosystems, Odense, Denmark). Peptides were separated in a 15-cm fused silica column (75 µm inner diameter from Proxeon Biosystems, Odense, Denmark) in-house packed with reversed-phase ReproSil-Pur C18-AQ 3.0 µm resin (Dr. Maisch GmbH, Ammerbuch-Entringen, Germany) and heated at 60°C. Peptides were analyzed with a flow rate of 250 nL/min with gradient of 5 to 40% MeCN in 0.1% formic acid, 5% DMSO in a 240 min. Examination of full-scan MS spectra (at 300 – 1,600 m/z range) were developed in the Orbitrap analyzer with resolution of 60,000 at 400 m/z (after accumulation to a target value of 1,000,000 in the C-trap). The mass spectrometer operated in a data-dependent mode to automatically switch between MS and MS/MS (MS2) acquisition. The ten most intense ions were sequentially isolated and fragmented in the linear ion trap using collision-induced dissociation at a target value of 30,000. The general conditions for mass spectrometric were: spray voltage, 2.7 kV; no cover and auxiliary gas flow; ion transfer tube temperature, 100 ºC; collision gas pressure, 1.3 mTorr; normalized collision energy using wide-band activation mode 35% for MS2. Ion selection thresholds were 250 counts for MS2. An activation q = 0.25 and activation time of 30 ms was applied in MS2 acquisitions. The “lock mass” option was enabled in all full scans to improve mass accuracy of precursor ions (OLSEN et al., 2005).

Data analysis: MaxQuant platform (version 1.5.2.8) (COX; MANN, 2008), with Andromeda algorithm for database searching (COX et al., 2011), was used for label-free protein quantification. Proteins were searched against a decoy database, prepared by reversing the sequence of each entry of the *T. cruzi* protein sequence database (containing 11,346 protein sequences, downloaded in April 2016 from UniprotKB (http://www.uniprot.org/). And this database was added to the frequently contaminants (porcine trypsin, Achromobacter lyticus

lysyl endopeptidase and human keratins) and their reversed sequences. Carbamidomethylation of cysteine was set as a fixed modification; oxidation of methionines and N-terminal acetylation were allowed as variable modifications. For validation of the identifications, a minimum of six amino acids for peptide length and two peptides per protein was defined. MS tolerance was fixed of 7 ppm, MS/MS tolerance of 0.5 Da and for trypsin specific digestion two missed cleavages were allowed.

Data was analyzed using Perseus version 1.5.5.3 (http://www.perseus-framework.org/) (TYANOVA et al., 2016). On this tool was conducted filter, log transformation and general annotation of experiment design, that permits the clusterization of the general intensity of protein with hierarchical-k-means clustering and differential expression determination. Further information on the identified, quantified and differential expressed proteins were acquired using Blast2GO software(CONESA et al., 2005) and TriTrypDB (http://www.tritrypdb.org) (ASLETT et al., 2009). Differentially expressed proteins (DEP) was determined comparing LFQ intensity values by multiple sample test; ANOVA variance test (p-values <0.01) and Benjamini-Hochberg (q-value <0.01) were denominate as differential expressed events. Fisher exact test was performed in the identified proteins after subjecting the quantitative value of the spectra to the embedded normalization.

## RESULTS AND DISCUSSION

*Trypanosoma cruzi* belongs to Trypanosomatidae Family that include other species that also cause important diseases in humans, Trypanosoma brucei is the agent sleeping sickness and Leishmania spp. causing cutaneous and visceral leishmaniasis. The incidence of Chagas disease is mainly due to the economic and social level of the region and is a major public health problem in Latin America affecting eight million of people. Proteomics studies of these parasites can provide important information about the protein content and contribute to better understand their biology.

Although some growth curve proteomic studies have been conducted in other organism (CONCEIC, 2010), this is the first study in a member of Kinetoplastida order. Another important point in this study is the use of several points along the growth curve that cover the two main phases, exponential and stationary. Until now a few large-scale studies have been conducted in this sense. Comprehension of how the *T. cruzi* modulated its transitions between the different phases and its adaptation to the growth conditions is an important step to understand its biology. Previously, our group characterized the growth curve of *T. cruzi*

epimastigotes (Dm28c) and studied their transcriptome modulation. Despite literature show poor correlation between mRNA and protein expression levels, this work can provide a great step towards understanding the regulation of a singular parasite.

*Growth cell curve*

Growth curve was monitored during eight consecutive days and showed a normal growth pattern consistent with previous studies (CAMARGO, 1964b; SANTOS *et al*., 2016) (Fig. 1A). According to Santos *et al*. (2016) (Capítulo 1), the growth curves present lag (days 1-2), exponential (days 3-5), early stationary (days 6-7) and stationary (days 8-10) phases. The exponential phase reaches 8.5 x 107 cells/ml at day 5 and the parasites showed normal morphology at this phase. A representation of the complete experimental study design is shown in Fig. 2. Two biological replicates were maintained in separate flasks and every day the cultures were monitored and an amount of cells were collected to compose the samples for each day along the growth curve. After protein extraction processing for all samples, we verified the profile of samples by gradient gel electrophoresis and all of them had an uniform pattern (Fig. 1B). All samples were processed using Gel-LCMS/MS, two runs for each sample of both biological replicate were processed in the mass spectrometry, totalizing 30 runs. Here we present the first proteomic analysis of the *T. cruzi* epimastigote forms growth curve under in vitro conditions.

*General proteomic analysis*

The wide-reaching identifications rate was 441,700 MS/MS spectra (43.11% of the total acquired) corresponding to 19,898 non-redundant peptide sequences belonging to 30 runs and 2,766 protein groups with a false discovery rate of 1% (supplementary tables 1, 2 and 3). When peptides could be assigned to more than one protein, this set of proteins was denominated a protein group. Then, the protein groups identified were distributed into three categories represented by (1) one protein per group (97.9%, 3,180 groups), (2) two proteins per group (1.5%, 50 groups) or (3) more than two proteins per group (0.6%, 19 groups). From total protein groups expressed along the time, 1,774 (54.6%) were annotated as uncharacterized protein reflecting the high proportion of genes with unknown function in the trypanosomatid genome. The Fisher's exact test applied to the 2,766 proteins identified showed a great percentage of proteins related with metabolic process and translation. The ten terms of gene ontology with smaller p-value founded were: cytosol (GO:0005829), protein complex (GO:0043234), cellular amino acid metabolic process (GO:0006520), oxidoreductase activity (GO:0016491),

mitochondrion (GO:0005739), catabolic process (GO:0009056), translation (GO:0006412), generation of precursor metabolites and energy (GO:0006091), ribosome (GO:0005840) and cofactor metabolic process (GO:0051186). As expected, terms related with growth and cell division were widely found.

Based on elimination of "missing values" parameters and considering only proteins that have intensity to apply the statistical test, we were able to quantified 1,301 proteins.

*Differential expression proteins (DEPs)*

For analysis of comparative proteomic data, the intensity changes of cell growth points were classified by their Multiple sample test results (p-value and q-value) and fold-changes. Biological terms and domains annotated were followed by Fisher exactly test and clusterization analysis for proteins known to show differential regulation between lifecycle stages. During in vitro cell growth was obtained 92 DEPs (Table 1), and the Principal Component Analysis (PCA) of these DEPs demonstrated a very good reproducibility between two replicates.

Among 92 DEPs identified, 50 (~54%) own functional description and 42 (~46%) were uncharacterized protein. These is expected once in *T. cruzi* almost half of the genome is formed by hypothetical protein gene, thus missing of any information on its probable function, complicating possible analysis of biological processes. Among the DEPs 57 (~62%) were down-regulated, showing that most proteins are reduced to their synthesis. Four dynein heavy chain proteins (V5BZ77, V5BQC6, V5BNR1 and V5BFL3) are downregulated, they are related of cytoskeletal motor that provide forces and displacements important in mitosis, and drives the beat of flagella and promoting the retrograde transport. Thus, as the parasites reach the stationary phase has been demonstrated that they decrease the flagellar movement. Our attention is also drawn to the presence of two calmodulin (V5BMR3 and V5B5Q5), that mediates the control of a large number of enzymes, ion channels and other proteins by Ca2+. Among the enzymes to be stimulated by the calmodulin-Ca2+ complex are a number of protein kinases and phosphatases. We believe that most DEPs are downregulated probably to controls energy expenditure, since the cell prepares to enter a starving period.

Thrity-five proteins were upregulated along the growth curve. Three proteins: glutamamyl carboxypeptidase (V5D9A3), arginine kinase (V5BUA6) and aminopeptidase (V5BWE3) are related with arginine biosynthetic process. Arginine kinase is one of the key enzymes, responsible for the parasites' metabolic plasticity, which maintains the cell energy homeostasis during environment changes. Besides, it is an important component in resistance mechanisms to different stress factors, such as reactive oxygen species, pH and starvation.

Another upregulated DEP is the paraflagellar rod protein 3 (V5BDW8), that is related to molecular processes associated with the motility of the parasite, which could be involved in increasing the flagella during stationary phase.

Four terms by gene ontology were founded in DEPs: cilium (GO:0005929), cellular amino acid metabolic process (GO:0006520), biosynthetic process (GO:0009058) and oxidoreductase activity (GO:0016491).

*Clusterization*

Hierarchical clustering showed that regulated proteins could be grouped in seven clusters (Fig. 3). Cluster 1, 2 and 3 with increased proteins along the growth curve, and cluster 3 with increasing from days 2 and 3, showing a regulation after leaving the lag phase. Clusters 4, 5, 6 and 7 with decreased proteins, which cluster 6 had a higher protein levels from the 5th and 6th day. Within cluster 6, paraflagellar rod component par 4 (V5BJE7) and paraflagellar rod component (V5BDF9) were present, it may be related to flagellar increase that occurs in stationary phase.

*Comparison between transcriptomic and proteomic analysis*

Growth curve has already been studied in *T. cruzi* followed by transcriptome analyses and despite the general low correlation between transcriptome and proteome data, we observed some matches (SANTOS *et al.*, 2016). Considering all different phases, we founded 13 proteins that were modulated in transcriptome data too. We founded nine correlations among transcriptomic and proteomic data, seven proteins were increased, which four also had increase in it mRNA levels at the same time of the curve (V5D8K9, V5ASA0, V5B7R2, V5BUA6, V5D5L9, V5D9A3 and V5BM81). Another two proteins were diminished between phases and when compared to transcriptomic data it their mRNA levels also were decreased and the other two had increased in it mRNA level (V5BNL9 and V5BGF4).

We founded two proteins regulated in transcriptomic data with increased of it mRNA level that are diminish in proteomic study (V5DBK9 and V5BL75). An explanation for this would be that these mRNAs were in stress granules and therefore not being translated or that such proteins would have a very short half-life, leading to a decrease in the proteome. The proteins level of V5BEA8 and V5BWE3 were diminished while its mRNA levels were increased in this growth curve time. Surprisingly, these proteins are increased even with the total and polysomal mRNA levels decreased along the curve.

## CONCLUSION

This is the first study of growth curve proteome in *T. cruzi*. The results showed here provides a comprehensive understanding of the molecular basis of *T. cruzi* growth curve, showing various proteins and potential pathways directly related to the parasite's behavior in vitro conditions. The proteins shown here may be explaining events that could be regulate biochemical processes and provide information about events that occurring in the epimastigote growth and metacyclogenesis.

**REFERENCES**

[1] C. Chagas, Nova tripanozomiaze humana: Estudos sobre a morfolojia e o ciclo evolutivo do Schizotrypanum cruzi n. gen., n. sp., ajente etiolojico de nova entidade morbida do homem, Mem. Inst. Oswaldo Cruz. 1 (1909) 159–218. doi:10.1590/S0074- 02761909000200008.

[2] B. Enders, F. Brauns, O. Zwisler, Biochemical and technical considerations regarding the mass production of certain parasitic protozoa, Bull. World Health Organ. 55 (1977) 393–402.

[3] B.J. Celeste, M.C. Guimarães, Growth curves of Leishmania braziliensis braziliensis promastigotes and surface antigen expression before and after adaptation to Schneider's Drosophila medium as assessed by anti-Leishmania human sera., Rev. Inst. Med. Trop. Sao Paulo. 30 (1988) 63–67. doi:10.1590/S0036-46651988000200001.

[4] K.M. Tyler, D.M. Engman, The life cycle of *Trypanosoma cruzi* revisited, Int. J. Parasitol. 31 (2001) 472–481. doi:10.1016/S0020-7519(01)00153-9.

[5] M.C. Bonaldo, T. Souto-Padron, W. de Souza, S. Goldenberg, Cell-substrate adhesion during *Trypanosoma cruzi* differentiation., J. Cell Biol. 106 (1988) 1349–58. doi:10.1083/jcb.106.4.1349.

[6] M.J.M. Alves, W. Colli, *Trypanosoma cruzi*: adhesion to the host cell and intracellular survival., IUBMB Life. 59 (2007) 274–279. doi:10.1080/15216540701200084.

[7] R. Hernández, A.M. Cevallos, T. Nepomuceno-mejía, I. López-villaseñor, Stationary phase in *Trypanosoma cruzi* epimastigotes as a preadaptive stage for metacyclogenesis, Parasitol. Res. 111 (2012) 509–514. doi:10.1007/s00436-012-2974-y.

[8] L. Vanhamme, E. Pays, Control of gene expression in trypanosomes., Microbiol. Rev. 59 (1995) 223–240.

[9] S.M. Teixeira, Control of gene expression in Trypanosomatidae., Brazilian J. Med. Biol. Res. 31 (1998) 1503–16. http://www.ncbi.nlm.nih.gov/pubmed/12917811.

[10] CMB. Santos, A. Ludwig, R. Kessler, R. Rampazzo, A. Inoue, M. Krieger, D. Pavoni, C. Probst, *Trypanosoma cruzi* transcriptome during axenic epimastigote growth curve, Parasitology. (2016). In preparation.

[11] V. Contreras, T.A. Jorge, M.C.. Bonaldo, N. Thomaz, H.S.. Barbosa, M. de N.S.L.. Meirelles, S. Goldenberg, Biological aspects of the DM28C clone of *Trypanosoma cruzi* after metacyclogenesis in chemically denined media, Mem. Inst.Oswaldo Cruz. 83 (1988) 123–133.

[12] E.P. Camargo, Growth and differentiation in *Trypanosoma cruzi*, (1964) 93–100.

[13] R.A. Scheltema, J. Hauschild, O. Lange, D. Hornburg, E. Denisov, A. Kuehn, A. Makarov, M. Mann, The Q Exactive HF , a Benchtop Mass Spectrometer with a Pre- filter , High Performance Quadrupole and an Ultra- High Field Orbitrap Analyzer, (2014) 1–29.

[14] J. Rappsilber, Y. Ishihama, M. Mann, Stop and Go Extraction Tips for Matrix-Assisted Laser Desorption/Ionization, Nanoelectrospray, and LC/MS Sample Pretreatment in Proteomics, Anal. Chem. 75 (2003) 663–670. doi:10.1021/ac026117i.

[15] J. V Olsen, L.M.F. de Godoy, G. Li, B. Macek, P. Mortensen, R. Pesch, A. Makarov, O. Lange, S. Horning, M. Mann, Parts per million mass accuracy on an Orbitrap mass spectrometer via lock mass injection into a C-trap., Mol. Cell. Proteomics. 4 (2005) 2010–21. doi:10.1074/mcp.T500030-MCP200.

[16] J. Cox, M. Mann, MaxQuant enables high peptide identification rates, individualized p.p.b.-range mass accuracies and proteome-wide protein quantification., Nat. Biotechnol. 26 (2008) 1367–72. doi:10.1038/nbt.1511.

[17] J. Cox, N. Neuhauser, A. Michalski, R. a Scheltema, J. V Olsen, M. Mann, Andromeda: a peptide search engine integrated into the MaxQuant environment., J. Proteome Res. 10 (2011) 1794–805. doi:10.1021/pr101065j.

[18] S. Tyanova, T. Temu, P. Sinitcyn, A. Carlson, M.Y. Hein, T. Geiger, M. Mann, J. Cox, The Perseus computational platform for comprehensive analysis of (prote)omics data, Nat. Methods. (2016). doi:10.1038/nmeth.3901.

[19] A. Conesa, S. G??tz, J.M. Garc??a-G??mez, J. Terol, M. Tal??n, M. Robles, Blast2GO: A universal tool for annotation, visualization and analysis in functional genomics research, Bioinformatics. 21 (2005) 3674–3676. doi:10.1093/bioinformatics/bti610.

[20] M. Aslett, C. Aurrecoechea, M. Berriman, J. Brestelli, B.P. Brunk, M. Carrington, D.P. Depledge, S. Fischer, B. Gajria, X. Gao, M.J. Gardner, A. Gingle, G. Grant, O.S. Harb, M. Heiges, C. Hertz-Fowler, R. Houston, F. Innamorato, J. Iodice, J.C. Kissinger, E. Kraemer, W. Li, F.J. Logan, J.A. Miller, S. Mitra, P.J. Myler, V. Nayak, C. Pennington, I. Phan, D.F. Pinney, G. Ramasamy, M.B. Rogers, D.S. Roos, C. Ross, D. Sivam, D.F. Smith, G. Srinivasamoorthy, C.J. Stoeckert, S. Subramanian, R. Thibodeau, A. Tivey, C. Treatman, G. Velarde, H. Wang, TriTrypDB: A functional genomic resource for the Trypanosomatidae, Nucleic Acids Res. 38 (2009) 457–462. doi:10.1093/nar/gkp851.

[21] L.E.C. Conceic, A reference growth curve for nutritional experiments in zebrafish ( Danio rerio ) and changes in whole body proteome during development, (2010) 1199– 1215. doi:10.1007/s10695-010-9400-0.

Table 1: Differential expressed proteins found during the growth curve

| UNIPROTKB ID | PROTEIN NAME | ANOVA p value |
|---|---|---|
| V5AC55 | Uncharacterized protein | 3,19E-04 |
| V5AJP3 | Retrotransposon hot spot (RHS) protein | 2,04E-04 |
| V5ASA0 | Threonyl-tRNA synthetase | 1,65E-04 |
| V5ASS7 | Uncharacterized protein | 4.90E+09 |
| V5AWC6 | Dynein heavy chain | 2.18E+08 |
| V5AWV1 | Sphingosine 1-phosphate lyase | 4,78E-04 |
| V5AXK4 | Glycerate kinase | 2.22E+09 |
| V5AXR7 | Uncharacterized protein | 3,64E-04 |
| V5B1R9 | Uncharacterized protein | 4,18E-04 |
| V5B262 | Uncharacterized protein | 4.28E+09 |
| V5B2A2 | Uncharacterized protein | 5,25E-04 |
| V5B3M4 | Retrotransposon hot spot (RHS) protein | 4,78E-04 |
| V5B517 | Uncharacterized protein | 6.23E+05 |
| V5B5E7 | Surface protease GP63 | 2,17E-04 |
| V5B5Q5 | Calmodulin | 8.94E+09 |
| V5B654 | 1,2-Dihydroxy-3-keto-5-methylthiopentene dioxygenase | 1,02E-04 |
| V5B6L5 | Uncharacterized protein | 7.54E+07 |
| V5B6W3 | Uncharacterized protein | 2.27E+09 |
| V5B7R2 | Nitrate reductase | 8.72E+08 |
| V5B7W6 | Trifunctional enzyme alpha subunit | 2.38E+09 |
| V5B944 | Uncharacterized protein | 2.88E+09 |
| V5B9J8 | Uncharacterized protein | 2,30E-04 |
| V5BA06 | Uncharacterized protein | 5.14E+07 |
| V5BBE7 | Uncharacterized protein | 7.20E+09 |
| V5BBR9 | Uncharacterized protein | 1.68E+09 |
| V5BC28 | Serine/threonine-protein kinase a | 1,74E-04 |
| V5BDF9 | Paraflagellar rod component | 2.09E+08 |
| V5BDW8 | Paraflagellar rod protein 3 | 3.63E+09 |
| V5BEA8 | 2-amino-3-ketobutyrate coenzyme A ligase | 4,52E-04 |
| V5BF65 | Cytochrome c oxidase subunit IV | 1.08E+08 |
| V5BFG1 | Uncharacterized protein | 1,73E-04 |
| V5BFL3 | Dynein heavy chain | 1.42E+09 |
| V5BG00 | Uncharacterized protein | 4.64E+07 |
| V5BGF4 | ATP-dependent DEAD/H RNA helicase | 5,75E-04 |
| V5BGP9 | Uncharacterized protein | 2,34E-04 |
| V5BGU1 | Bystin | 3,45E-04 |
| V5BH98 | Adenylate kinase | 2,80E-04 |
| V5BHK4 | Uncharacterized protein | 2,19E-04 |
| V5BHQ7 | Uncharacterized protein | 6.51E+08 |
| V5BIC8 | Regulatory subunit of protein kinase a-like protein | 1,43E-04 |
| V5BIH6 | Leucine-rich repeat protein | 2,01E-04 |
| V5BIM1 | Uncharacterized protein | 8.92E+08 |

| | | |
|---|---|---|
| V5BJ29 | Uncharacterized protein | 4,85E-04 |
| V5BJE7 | Paraflagellar rod component par4 | 1.62E+09 |
| V5BJF5 | RNA cytidine acetyltransferase | 3,20E-04 |
| V5BJP2 | Uncharacterized protein | 3.32E+09 |
| V5BK17 | Uncharacterized protein | 1.14E+09 |
| V5BK66 | Thiolase protein-like protein | 4,11E-04 |
| V5BL75 | Membrane-bound acid phosphatase | 6.10E+06 |
| V5BLI8 | Uncharacterized protein | 1.70E+09 |
| V5BLS6 | Uncharacterized protein | 7.17E+08 |
| V5BM81 | Uncharacterized protein | 8.59E+08 |
| V5BMR3 | Calmodulin | 5,18E-04 |
| V5BNL9 | Mercaptopyruvate sulfurtransferase | 3,90E-04 |
| V5BNR1 | Dynein heavy chain | 4,59E-04 |
| V5BPS0 | Short chain 3-hydroxyacyl-CoA dehydrogenase | 6,59E-04 |
| V5BPZ7 | Uncharacterized protein | 4,20E-04 |
| V5BQC6 | Dynein heavy chain | 3,42E-04 |
| V5BQK5 | Arginyl-tRNA synthetase | 9.32E+08 |
| V5BRQ8 | Alcohol dehydrogenase | 1,31E-04 |
| V5BS76 | Uncharacterized protein | 4.11E+09 |
| V5BSB7 | Lanosterol 14-alpha-demethylase | 5.74E+07 |
| V5BTG8 | Uncharacterized protein | 3.14E+09 |
| V5BUA6 | Arginine kinase | 1.62E+08 |
| V5BUG5 | Uncharacterized protein | 5,81E-04 |
| V5BWC7 | Citrate synthase | 4,42E-04 |
| V5BWE3 | Aminopeptidase | 2,45E-04 |
| V5BX24 | Phosphoglycerate kinase | 1,63E-04 |
| V5BXN2 | Uncharacterized protein | 5.87E+09 |
| V5BZ77 | Dynein heavy chain | 5.03E+09 |
| V5C1B4 | Uncharacterized protein | 3,30E-04 |
| V5D560 | Axoneme central apparatus protein | 1,44E-04 |
| V5D5L9 | Fatty acid desaturase | 1.21E+08 |
| V5D8K9 | Methyltransferase | 9.45E+09 |
| V5D9A3 | Glutamamyl carboxypeptidase | 6.14E+09 |
| V5D9G5 | Uncharacterized protein | 8.05E+08 |
| V5DA09 | Mitogen-activated protein kinase | 7,02E-04 |
| V5DA42 | Uncharacterized protein | 2.54E+07 |
| V5DAE9 | Uncharacterized protein | 5,74E-04 |
| V5DBK9 | Uncharacterized protein | 1,76E-04 |
| V5DCU5 | 2-oxoglutarate dehydrogenase | 2,75E-04 |
| V5DEC0 | Eukaryotic translation initiation factor 2 subunit | 1,52E-04 |
| V5DIG4 | Uncharacterized protein | 8.40E+08 |
| V5DIG8 | Serine/threonine-protein phosphatase | 5.25E+09 |
| V5DL68 | Solanesyl-diphosphate synthase | 5.64E+07 |
| V5DLD7 | Uncharacterized protein | 4.63E+09 |
| V5DLP2 | Uncharacterized protein | 1,92E-04 |
| V5DMU2 | Dynein heavy chain | 6,60E-04 |

| | | |
|---|---|---|
| V5DSY9 | Pumilio | 1,87E-04 |
| V5DT29 | Uncharacterized protein | 1,11E-04 |
| V5DT33 | Uncharacterized protein | 1,70E-04 |
| V5DU12 | Uncharacterized protein | 9.46E+09 |

Table 2. Comparison of transcriptome and proteomic data analyzed during the growth curve.

| ID | Protein | Transcriptome | Proteome |
|---|---|---|---|
| V5D8K9 | Methyltransferase | increase | Increase |
| V5ASA0 | threonyl-tRNA synthetase | increase | Increase |
| V5B7R2 | nitrate reductase | increase | Increase |
| V5BL75 | membrane-bound acid phosphatase | increase | Decrease |
| V5BUA6 | arginine kinase | increase | Increase |
| V5D5L9 | fatty acid desaturase | increase | Increase |
| V5D9A3 | glutamamyl carboxypeptidase | increase | Increase |
| V5DBK9 | hypothetical protein | increase | Decrease |
| V5BM81 | hypothetical protein | increase | increase |
| V5BNL9 | mercaptopyruvate sulfurtransferase | decrease | decrease |
| V5BEA8 | 2-amino-3-ketobutyrate coenzyme A ligase | decrease | increase |
| V5BGF4 | ATP-dependent DEAD/H RNA helicase | decrease | decrease |
| V5BWE3 | Aminopeptidase | decrease | increase |

**FIGURES**

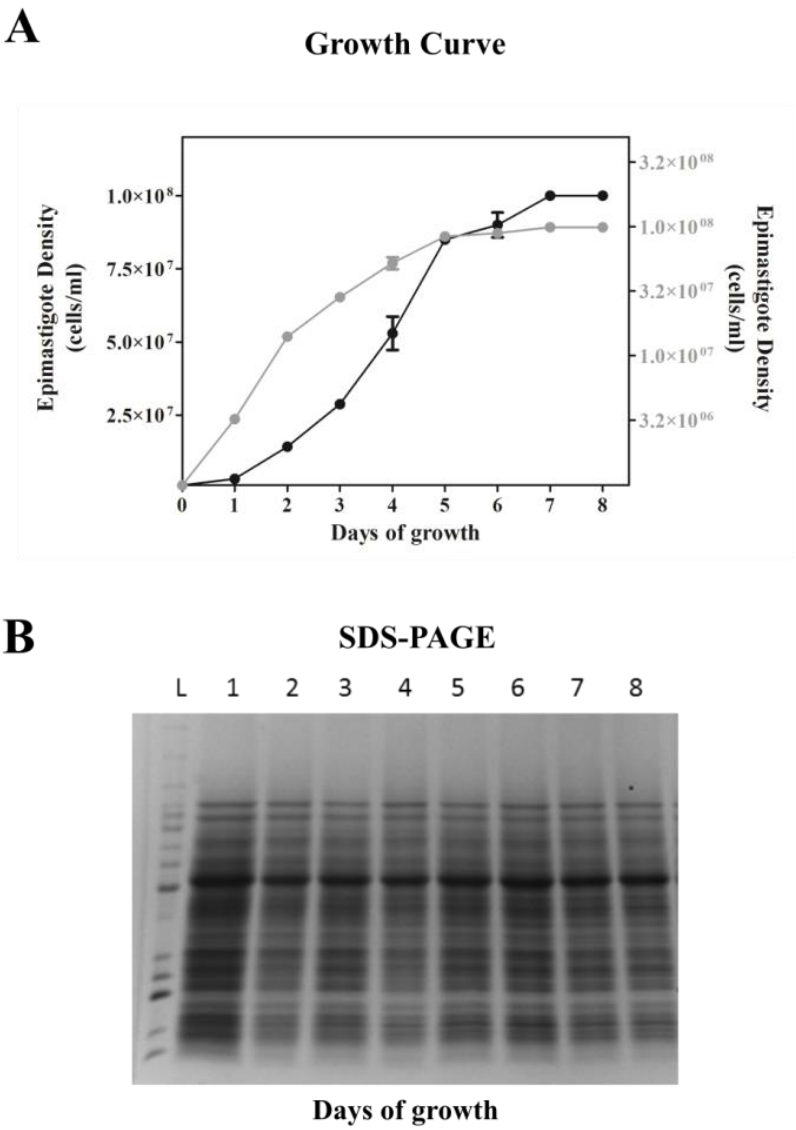


Fig. 1: Growth curve performance and protein samples A) Parasite density in culture measured by eight consecutive days of growth curve. The cell density was plotted against time. Data points represent means and standard deviation of the means (SEM). B) Protein samples extracted from each day of the growth curve were separated by gradient sodium dodecyl sulfate polyacrylamide gel electrophoresis (SDS-PAGE) after staining with Coomassie blue. Lane 1: BenchMark; lane 2: sample day 1; lane 3: sample day 2; lane 4: sample day 3; lane 5: sample day 4; lane 6: sample day 5; lane 7: sample day 6; lane 8: sample day 7 and lane 9: sample day 8.

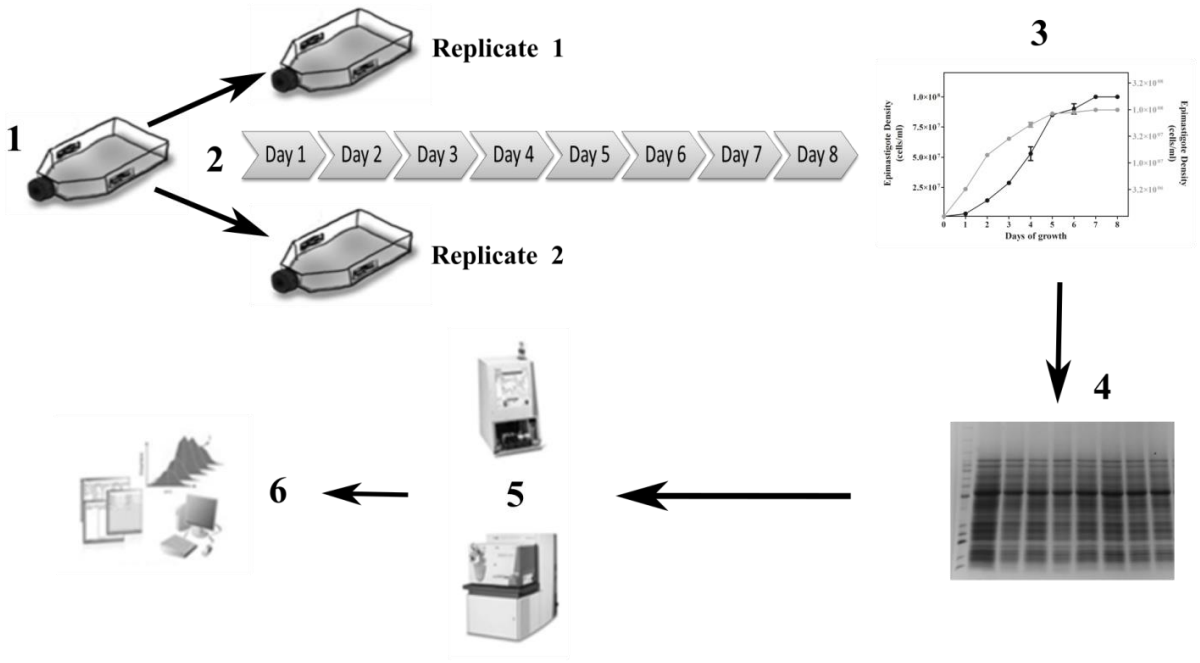


Fig. 2: Graphical representation of the complete experimental design of the study. 1) From one culture the biological replicates were prepared; 2) Two biological replicates were sampled by eight days 3) Growth curve was obtained 4) After cells were lysed, they were separated in a electrophoresis gel 5) LCMS/MS procedure 6) Data analysis.

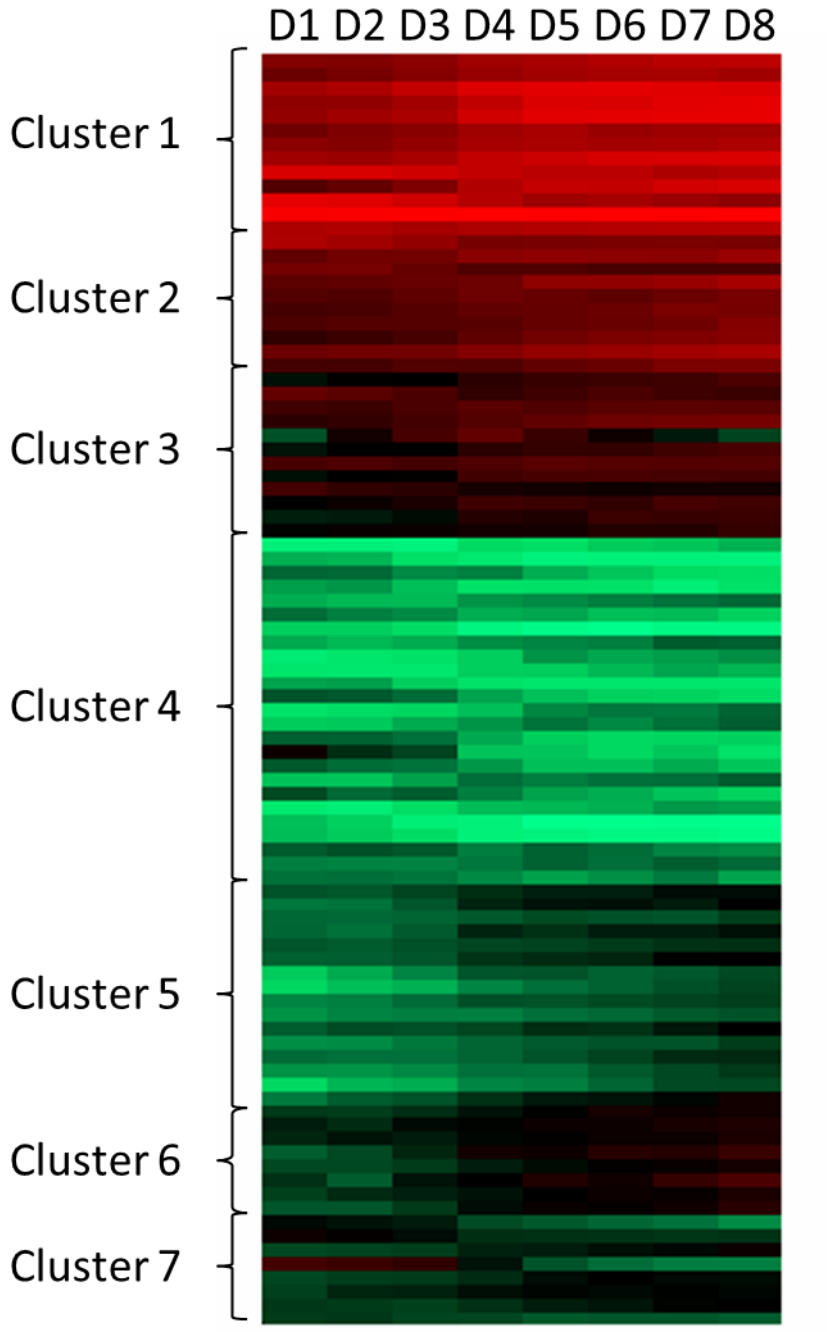


Fig. 3: Heat map of protein modulation patterns for 92 DEPs separated in seven clusters. Each column represents the days analyzed along the growth curve (D: day).

# 5 CAPÍTULO 3

Artigo científico em preparação.

## *TRYPANOSOMA CRUZI* STATIONARY EPIMASTIGOTE TRANSCRIPTOME RESPONSE TO NUTRITIONAL DEPRIVATION

Short title: TrypanosOmics: nutritional stress transcriptomics

Cyndia Mara Bezerra[1,3ǂ], Daniela Parada Pavoni[1,3], Marco Aurelio Krieger[1,3], Christian Macagnan Probst[1,2,3*ǂ]

1 Laboratório de Genômica Funcional, Instituto Carlos Chagas, FIOCRUZ-PR, Curitiba, Paraná, Brasil
2 Laboratório de Bioinformática e Biologia Computacional, Instituto Carlos Chagas, FIOCRUZ-PR, Curitiba, Paraná, Brasil
3 Programa de Pós-Graduação em Biologia Celular e Molecular, Centro Politécnico, Universidade Federal do Paraná, Curitiba, Paraná, Brazil.

* Corresponding author
E-mail: cprobst@fiocruz.br (CMP)

ǂ These authors contributed equally to this work

**Key-words:** RNA-seq, stress, nutritional deprivation

## ABSTRACT

*Trypanosoma cruzi* is the causative agent of Chagas disease, still an important illness with significant socio-economic impact in South America. It is a flagellated protist, which has distinct biological characteristics from other eukaryotes, chiefly the mechanism of gene expression regulation, which occurs mostly at the post-transcriptional level. In an effort to increase our understanding of the gene expression regulation network of this parasite, the TrypanosOmics initiative was devised, applying diverse methods are applied to produce large scale data sets that are integrated to obtain a general overview of *T. cruzi* Systems Biology. One major cornerstone of the TrypanosOmics initiative is to construct a broadly database of mRNA transcriptome quantification, in a large number of distinct biological situations. *T. cruzi* has a complex life cycle, alternating between two distinct host environments, a mammalian and an insect of the reduviidae family, dealing with extreme conditions as low pH, immune system components, alterations in osmolarity and nutritional deprivation, among others. This last extreme condition is also relevant as it is considered as an important factor in the differentiation processes of this parasite, mainly metacyclogenesis, the transformation of the insect replicative form, epimastigote, in the insect infective form, metacyclic trypomastigotes. An in vitro protocol for metacyclogenesis was developed and consists briefly in stressing stationary-phase epimastigotes by culturing them in nutrient deficient medium. Taking all this into consideration, we have performed a transcriptomic analysis of stationary epimastigotes submitted to three different poor media (PBS, TAU, TAU3AAG) up to 24h in order to: a) increase our coverage of the transcriptional landscape; b) provide important biological understanding of the adaptation to starvation and c) understand the initial steps in the metacyclogenesis process. We have identified 612, 804 and 941 differentially expressed supra-genes for PBS, TAU and TAU3AAG treatments, respectivley. The majority of modulated supra-genes were common to all three conditions, and the degree of modulation increased across the time. Up-regulated supra-genes were enriched in RNA binding proteins, whereas down-regulated supra-genes had mainly metabolic function. Supra-gene modulation associated with a specific treatment was generally restricted to a specific time-point, where for the other time points and conditions there was no (or low) modulation. Taken together, this study represents the first initiative to quantify the transcriptome response to nutritional deprivation in *T. cruzi*.

## INTRODUCTION

*Trypanosoma cruzi* is a protozoan eukaryote, which has diverged early from the main eukaryote evolutionary branch. It is the causative agent of Chagas disease, a still important illness in Latin America, with an estimated prevalence of 8 million people. It has a complex life cycle, alternating between two distinct hosts, a mammalian and a reduviidae insect, passing through morphological modifications.

It is an interesting model for biological studies, mainly related to differentiation and gene expression regulation. It has several distinct aspects, as mitochondrial RNA editing, post transcriptional regulation, kinetoplast, glycosomes, acidocalcisome, flagellum, among others. But a side effect of its large evolutionary distance from other eukaryote model organisms is that very little is known about the function for most of its genes.

Aiming to diminish this gap, we have started the TrypanosOmics initiative (1), whose major goals are to use the functional genomics approach, applying several large scale techniques, to enable gene function annotation and to identify the gene expression regulation network of *T. cruzi*. One of the main parts of the TrypanosOmics initiative is to build an extensive view of the transcriptional landscape of *T. cruzi* , by means of collecting mRNA modulation data across a vast number of distinct biological conditions.

*Trypanosoma cruzi* suffers metabolic changes due to its complex life cycle, dealing with very distinct environments in both hosts, as for instance, nutritional deprivation inside the reduviidae insect mid-gut. This process is believed to induce the differentiation process of metacyclogenesis, which involves several biochemical and morphological changes of the parasite. An in vitro model of metacyclogenesis was developed, which includes nutritional deprivation for 2 hours in a medium called TAU (triatomine artificial urine) and 48h~96h of incubation in TAU3AAG medium, which has very limited sources of carbon and nitrogen energy.

In the present work, we evaluated the transcriptome response of *T. cruzi* by RNA-Seq to three distinct low-nutrient media (PBS, TAU and TAU3AAG) to obtain important insights regarding nutritional stress response and increase our profiling of *T. cruzi* transcriptome landscape.

## RESULTS

We obtained transcriptome data for all experimental samples (n=48, supplementary table S1) with the exception of one replicate of TAU 24h (no sequencing) and TAU 3AAG 24h (low number of mapped reads). The number of differentially expressed supra-genes (DESG) are displayed in supplementary table S2, considering several FDR (false-discovery rate) thresholds. In general, the figures are very similar for each stress, with TAU 3AAG containing more DESG, especially for the lower FDR thresholds. For the posterior analyzes, we applied 5% FDR and 1.5 fold change thresholds.

Using these criteria, 611, 803 and 940 DESG were selected for PBS, TAU and TAU3AAG, respectively. For these, 278 (core set) and 1,385 (complete set) DESG passed the thresholds for all or for any of the three conditions, respectively. The pattern of modulation for the core and the complete set are in supplementary figures S2 and S3, respectively. In general, the pattern of modulation is very similar when comparing three conditions, even for the complete set, showing that the differences in the number of selected genes are more related to small deviations that impact the final assessment of significance, than differences in gene expression modulation between the conditions. There is a higher proportion of down- regulated DESG; and most of the DESG increased the modulation degree during time course, with few interesting exceptions (see below). Interestingly, there is a large number of genes that showed a peak of decrease at 6h for PBS and 24h for TAU and TAU3AAG, indicating a temporal difference between these conditions.

Instead of comparing the three conditions as a bipartite selection of DESG and non-DESG, we have selected all SG that passed the thresholds for any condition (n=1,385) and applied euclidean distance to have a better understanding of similarity between the modulations occurring in all conditions, and mainly to identify DESG whose expression differed between the conditions. Figure 1 shows the correspondence between the three conditions, regarding the euclidean distance between the gene expression profile. As expected from the analysis of supplementary figures S1 and S2, the vast majority of the complete set are in the region of high similarity between the three conditions (arbitrarily chosen to be an euclidean distance < 1); the supra-genes whose expression is distinct in PBS (n=193), TAU (n=93) and TAU3AAG (n=89) are depicted in supplementary file 8, 9 and 10 (S8, S9, S10), respectively.

### *Analysis of modulation in PBS*

SOM clustering of the 612 DEGS in PBS is represented in figure 2 and a detailed view of each cluster is in supplementary file S3. According to the classification of the main distinctive aspect of each cluster, 414 DEGS have decreased expression (67.7%), being 251 (60.6%) hypothetical conserved and 30 (7.2%) hypothetical; and 159 DEGS have increased expression (26.0%), being 82 hypothetical conserved (51.6%) and 24 hypothetical (15.1%).

Considering SG with functional annotation, there was decreased and increased expression of genes related in Table 1. Considering the large number of constituents of each families, they are not significantly enriched, but for some specific reason, these members behave distinctively.

*Analysis of modulation in TAU*

SOM clustering of the 804 DEGS in PBS is represented in Figure 3 and a detailed view of each cluster is in supplementary file S4. According to the classification of the main distinctive aspect of each cluster, 675 DEGS have decreased expression (84.0%), a significant difference from PBS. Among them, 432 (64.0%) are hypothetical conserved and 46 (6.8%) hypothetical, very similar to PBS. 114 DEGS have increased expression (14.2%), being 56 hypothetical conserved (49.1%) and 24 hypothetical (13.5%), figures similar to PBS.

Considering SG with functional annotation, there was decreased and increased expression of genes related in Table 2. Considering the large number of constituents of each family, they are not significantly enriched, but for some specific reason, these members behave distinctively, and there is other SG selected only in TAU, increasing the number of multi-genic SG modulated.

*Analysis of modulation in TAU3AAG*

SOM clustering of the 941 DEGS in TAU3AAG is represented in figure 4 and a detailed view of each cluster is in supplemental file S5. According to the classification of the main distinctive aspect of each cluster, 732 DEGS have decreased expression (77.8%), intermediary between PBS and TAU. Among them, 435 (59.4%) are hypothetical conserved and 48 (6.5%) hypothetical, figures similar to PBS and TAU. 208 DEGS have increased expression (22.1%), being 103 hypothetical conserved (49.5%) and 19 hypothetical (9.1%), figures also similar to PBS and TAU.

Considering SG with functional annotation, there was decreased and increased expression of genes related in Table 3.

*Functional analysis of modulated supra-genes shared between conditions*

Considering the results displayed in figure 1, an arbitrary threshold for the euclidean distance was established at one, selecting those supra-genes whose distance between PBS and TAU, and between PBS and TAU3AAG were below one.These supra-genes are displayed in supplemental file S7, ranked in increasing degree of distance; the main purpose of this file is to analyze specific supra-genes to see how similar the pattern of modulation is between the three conditions.

*Functional analysis of modulated supra-genes specific to PBS*

Considering the 193 supra-genes that were differently modulated in PBS (supplemental file S8), the vast majority of them are hypothetical conserved. Only one SG presented a higher increase of expression in PBS in relation to TAU and TAU3AAG (SGdmA6922, hypothetical protein).

All remaining SG showed: A) a decrease expression in TAU and TAU3AAG, where PBS generally presented an expression profile similar to stationary epimastigote: hypothetical protein conserved (SGdmA6558, SGdmA4854, SGdmA2580, SGdmA5601, SGdmA1529, SGdmA7662, SGDmA3326, SGdmA1069, SGdmA4856, SGdmA7460, SGdmA4707, SGdmA7330, SGdmA4971, SGdmA4987, SGdmA4949, SGdmA0924, SGdmA0353, SGdmA6711, SGdmA0350), hypothetical protein (SGdmA4116, SGdmA3977), ARP2/3 complex subunit (SGdmA5906), histone H1 (SGdmA1365), POMP37 (SGdmA1240), cytochrome B5 (SGdm5066), prefoldin subunit (SGdmA1110), ADG1-like (SGdmA3232), endonuclease III (SGdmA1877), monothiol glutaredoxin (SGdmA1189), pterin-4-alpha-carbinolamine dehydratase (SGdmA4168), DNA repair and recombination protein RAD54 (SGdmA7326), DNA/RNA non-specific endonuclease (SGdmA0860); B) a specific decrease in expression just in one time point of PBS: there are examples for 1h (hypothetical protein conserved (SGdmA0932, SGdmA0934, SGdmA0519), hypothetical protein (SGdmA0518, SGdmA0606), cation transporter (SGdmA0327), calpain−like cysteine peptidase (SGdmA0435, SGdmA0436), for 2h (hypothetical protein conserved (SGdmA1887, SGdmA6057, SGdmA0517, SGdmA0878, SG7343), polypeptide deformylase-like protein (SGdmA6371); for 4h, hypothetical protein conserved (SGdmA6692, SGdmA6722, SGdmA0736, SGdmA7039, SGdmA2899, SGdmA0600, SGdmA1659), hypothetical protein (SGdmA0825); for 6h, hypothetical protein conserved (SGdmA3432, SGdmA0802, SGdmA04500, SGdmA5635, SGdmA1701, SGdmA3939, SGdmA3750, SGdmA0921), hypothetical protein (SGdmA5186), map-kinase 4 (SGdmA0921), dynein light chain 2b,

cytoplasmic (SGdmA3161), vacuolar transporter chaperone (SGdmA3067), ARF-like 2 binding protein (SGdmA6582); for 24h: hypothetical protein conserved (SGdmA3644, SGdmA3503, SGdmA3989).

*Functional analysis of modulated supra-genes specific to TAU*

Considering the 93 supra-genes that were differently modulated in TAU (supplemental file S9), the vast majority of them are hypothetical conserved, as for PBS. Also, no SG presented a higher increase of expression in TAU in relation to PBS and TAU3AAG.

The major distinct aspect of the SG set is that most of them are down-regulated specifically in TAU at 24h (hypothetical protein conserved (SGdmA3654, SGdmA4074, SGdm0845, SGdmA1290, SGdmA2459, SGdmA1771, SGdmA4619, SGdmA3788, SGdmA1647, SGdmA7420, SGdmA3022, SGdmA2886, SGdmA3832, SGdmA4132, SGdmA5940SGdmA4402, SGdmA1604, SGdmA6670, SGdmA6362, SGdmA0275), hypothetical protein (SGdmA2718, ubiquinone biosynthesis protein (SGdmA2907), mitochondrial carrier protein (SGdmA7644), dephospho-CoA kinase (SGdmA2953), DNA-directed RNA polymerase I (SGdmA0847), histone deacetylase 1 (SGdmA3642), triglyceride lipase (SGdmA0919), RNA triphosphatase (SGdmA4395), origin recognition complex subunit 1 (ORC1, SGdmA4138)). Few are down regulated specifically at 6h (hypothetical protein conserved (SGdmA5370, SGdmA6919, SGdmA2817, SGdmA1134)). And another small subset has an expression profile similar to stationary epimastigotes when the other conditions show down-regulation: at 6h (zinc-binding protein (Yippee, SGdmA1847), cytochrome c (SGdmA5581), hypothetical protein (SGdmA2867)) and 24h – hypothetical protein conserved (SGdmA4403)).

*Functional analysis of modulated supra-genes specific to TAU3AAG*

Considering the 89 supra-genes that were differently modulated in TAU3AAG (supplemental file S10), the vast majority of them are hypothetical conserved, as for PBS and TAU. Also, no SG presented a higher increase of expression in TAU3AAG in relation to PBS and TAU.

Other aspect that is characteristic of this gene set, very similar to that from TAU, is that the vast majority of down-regulation occurs at 24h; but one very interesting difference, that was not seen in any other gene set, is that a significant proportion of these modulated genes have functional annotation: hypothetical protein conserved (SGdmA7800, SGdmA6222, SGdmA2458, SGdmA5813, SGdmA3640, SGdmA3381, SGdm2520, SGdmA0334,

SGdmA5589, SGdmA6349, SGdmA2094, SGdmA3218, SGdmA7411, SGdmA2360, SGdmA2549, SGdmA2619, SGdmA2862, SG7527, SGdmA2676, ), hypothetical protein (SGdmA1985, SGdmA1476, SGdmA2979, SGdmA4516, SGdmA2966)), deaminase (SGdmA2769), Trk system potassium uptake (HKT1, SGdmA6951), proliferator-activated receptor interacting protein (PRIP, SGdmA4135), monoxygenase (SGdmA3981), glucosamine 6-phosphate n-acetyltransferase (SGdmA6923), CYC2-like cyclin 6 (SGdmA0664), actin-related protein 2/3 complex subunit (ARPC1, SGdmA6650), translation initiation factor EIF-2b, ADP-ribosylation factor, 8-oxoguanine DNA glycosylase (SGdmA6757), mitochondrial carrier (SGdmA3183), ABC transporter (SGdmA4131), peptydil-prolyl cis-trans isomerase (PIN1, SGdmA4019), protein kinase (SGdmA4766), 60S ribosomal protein (SGdmA7199).
All supplementary files are present in CD (ANEXOS 1).

## DISCUSSION

*Trypanosoma cruzi* is an interesting model for studying specific biological questions, mainly due to its early divergence from the eukaryotic tree. Studies cover general physiological and molecular systems, as differentiation (due to its complex cyclic life cycle) and gene expression regulation (based majorly on post transcriptional mechanisms), as well as specific structures, as glycosome, kinetoplast, acidocalcisome and flagellum. However, this early divergence represents a significant burden for functional gene annotation, as a limited fraction of *T. cruzi* proteins presents significant sequence similarity to those of a model organism. In fact, the vast majority of *T. cruzi* proteins have no known function or only a generic function attributed. Focusing on decreasing our general lack of knowledge about most of *T. cruzi* genes, we have devised a project, named TrypanosOmics (1), aiming to integrate a vast wealth of large scale data, as a functional genomics approach can give interesting clues regarding gene function. The present work represents one of many sub-projects whose main goal is to collect transcriptome data in order to classify the *T. cruzi* genes into distinct groups of co-regulation, providing important hints about gene expression regulation and function. However, it is extremely important to have an impressive number of different environmental conditions populating the transcriptome database, in order to extract useful information for this project.

Besides the main purpose of assessing the transcriptome landscape of *T. cruzi*, the present analysis also allows to indirectly assess the biological processes relevant to the specific environmental conditions. In this sense, the transcriptome response of *T. cruzi* to nutritional deprivation is an interesting model, as it is a common situation for *T. cruzi* in its life cycle and

hence evolutionary forces have shaped this response. One example of this is triggering of metacyclogenesis due to nutrient deprivation.

Although the lack of knowledge of gene function has a significant impact in a gene list analysis, creating a circular paradox for *T. cruzi* transcriptomics and functional genomics that hopefully will be solved in the near future, nevertheless it is possible to extract relevant biological information for the studied processes.

The three conditions evaluated (PBS, TAU and TAU3AAG) represent very poor nutrient media. They have a few differences, especially regarding the small source of carbon and nitrogen of TAU3AAG, but are in a general sense, similar. When we look at the transcriptome modulation profile of these conditions, they shared most patterns (figure 1), reinforcing the similarity between them. When looking specifically at the differences between conditions, the vast majority of them were represented by punctual modulation, i. e., a specific time point, generally late. Although they may represent an artifact, the fact that we have conducted a time-series approach with three replicates for each time point, covering three different conditions, increased the probability that they truly represent useful information. This is especially relevant for the future effort of data mining the transcriptome database for gene expression regulation and functional annotation.

The major transcriptome response to nutrient deprivation is down-regulation (ranging from 67.7% to 84% of DEGS) of diverse biological processes, mainly related to active metabolism (energy production, mitochondria, transcription, translation, cytoskeleton, cell cycle-associated kinases, etc). This is expected, as the lack of nutrients produces a signal for cell shutdown. Although the proportion of up-regulated genes is smaller, they have an interesting pattern as over-expressing RNA binding proteins, which have an essential role in post transcriptional regulation and could be key modulators for stress survival and differentiation.

Other interesting aspect is the over-expression of a few members of multi-genic families; although there was an impressive amount of non-modulated members, hence indicating that these families were not associated with nutrient deprivation response, it is a clue for future studies, as they have a different behavior regarding gene expression regulation. This same reasoning can be applied for large functional families (RNA binding proteins, protein kinases, protein phosphatases, helicase, calmodulin, dynein, etc) or even individual genes that will be continuously, as the transcriptome database increases its coverage, be subdivided in more specific groups.

Taken together, this work represents a first effort trying to identify the gene response to nutrient deprivation. It is important to reinforce the relevance, albeit partial, to increase our knowledge about transcriptomic dynamics in *T. cruzi*.

## METHODS

*Parasite culture and initial experimental procedures*

*T. cruzi* epimastigotes strain Dm28c were cultured at 28°C in LITB medium supplemented with 10% heat-inactivated fetal bovine serum, through repeated 7 days culture passages from an initially frozen sample. Prior to the specific procedure, *T. cruzi* epimastigotes were cultured as above, for three 3 days culture passages, at an initial cell concentration of 1x106 ml-1 parasites. In the last passage, epimastigote at the beginning of the stationary phase in the growth curve were collected by centrifugation and the specific medium was used to wash once the cell pellet. After that, 5x107 ml-1 parasites were placed in a 1.7 ml microcentrifugue tube in the appropriate medium and incubated for the specific time at 28°C.

**Medium composition**

PBS: Phosphate-buffered saline consisted of 137 mM NaCl, 2.7 mM KCl, 10mM Na2HPO4, KH2PO4 1.8 mM, pH 7.4;

TAU: Triatomine artificial urine consisted of 190 mM NaCl, 17 mM KCl, 2 mM MgCl2, 2 mM CaCl2, NaHCO3 0.6 mM, pH 6.0;

TAU3AAG: TAU medium supplemented with 10mM glucose, 10 mM L-proline, 50 mM sodium glutamate, 2 mM sodium aspartate.

*Description of the experimental design*

*Trypanosma cruzi* stationary epimastigotes were incubated in the specific medium as described above for 1h, 2h, 4h, 6h and 24h. All experiments were performed in three biological replicates.

*mRNA extraction*

After the specified time, parasite cells were pelleted and supernatant was discarded. Total RNA was extracted using the RNeasy® Mini kit (Qiagen, #74106), according to the animal cells protocol, including on-column DNase digestion. RNA concentration, 260/280 and 260/230 ratios were obtained in a Nanodrop 1000 (Nanodrop Technologies); RNA integrity

was evaluated with the RNA 6000 Nano LabChip® kit (#5065-4476), in a Bioanalyzer 2100 equipment (Agilent). Polyadenylated RNA was purified from total RNA using the PolyA+Track® mRNA Isolation System III (Promega, Z5300), following the standard recommended protocol.

*Large scale cDNA sequencing*

The mRNAs were prepared for sequencing in a SOLiD 4 system (Life Technologies), using the SOLiDTM Total RNA-Seq Kit (#4445374). Briefly, 100 ng to 500 ng of poly(A)+ RNA was fragmented using RNase III for 5 minutes at 37°C and cleaned up with RiboMinus™ Concentration Module (Invitrogen, K155005). Strand-specific adapters were hybridized to the fragmented mRNA at 16°C for 16 hours. Immediately after that, first-strand cDNA synthesis was performed with ArrayScript™ Reverse Transcriptase at 42°C for 30 minutes. cDNA was purified using MinElute® PCR Purification Kit (Qiagen, #28006) and applied to a Novex TBE-Urea 6% gel (Invitrogen, EC6865BOX) for polyacrilamide electrophoresis separation. cDNA fragments of 200 to 300 bp were cutted from the gel, submitted to a on-gel PCR using SOLiDTM RNA barcoding kit primers (Life Technologies, #4427046, #4453189) and purified with PureLink® PCR Micro Kit (Invitrogen, K310050). The cDNA was quantified with Qubit® dsDNA HS Assay Kit (Invitrogen, Q32854) on a Qubit® 2.0 fluorometer. Equal masses of each sample, containing specific barcodes, were pooled together and the mixture used as DNA template for emulsion PCR on SOLiD® EZ Bead™ E80 system (Life Technologies, #4453095). After bead enrichment and 3' end modification with terminal transferase, template beads were deposited onto glass slides and sequenced on a SOLiDTM 4 system using multiplex fragment sequencing protocol.

*Sequenced read processing*

*Trypanosoma cruzi* Dm28c strain genome (MBSY00000000) data was retrieved from GenBank. All CDS were extracted and organized into groups of genes containing nucleotide sequences with high similarity (supra-genes, SG), in order to eliminate redundancy in the transcriptome profile when allowing for multiple mapping positions of a single read. Briefly, all CDS nucleotide sequences were compared against each other using blastn software, without filtering and with an e-value threshold of 1x10-10; the resulting blast output was processed with the MCL algorithm (2), using an inflation value of 6. The description of the 7,805 supra-genes generated, including the gene ID of its closest *T. cruzi* CL Brener homolog is available on supplemental file 1 (S1).

All reads were mapped against the *Trypanosoma cruzi* using SHRiMP2 (3) with default parameters, including --strata --max-alignments 1000. After genome mapping, the resulting SAM files were processed by custom perl scripts to compute supra-gene read count. Briefly, all mapping positions of a specific read, with score higher than 300, genome location within an annotated CDS and in the correct strand, were identified. Only reads whose mapping positions were from the same supra-gene were considered; the number of reads assigned to a specific supra-gene was summed up. Read counts were processed by the edgeR package (5) using the TMM method (6) and differentially expressed supra-genes (DEGS) were identified using a GLM approach.

*Transcript modulation adjustment*

A representation of the supra-gene modulation across all time points, using all data, was created using the function lowess of the R software (7), with smoother span f=0.2. The resulting vector, containing a value for each time point, was used for pattern comparisons between the treatments, by means of Pearson's correlation.

*Clustering of DEGS*

Self-organizing maps (SOM) were created for DEGS in each condition, with a square grid of 5x5, using the software Expander (8).

*Gene ontology analysis*

One representative for each supra-gene was selected, as the largest CDS of each supra-gene, which had no intervening frameshift or stop codons, and the corresponding protein sequence was submitted for gene ontology term assignment in the Blast2GO software (9), with default parameters. The blast search was performed against GenBank RefSeq protein database version 77, with 1x10-5 e-value threshold, word size of 5, and at most 80 results returned from the search. Enrichment analysis by Fisher exact test was performed with the BLAST2GO software as well.

*KEGG pathway mapping*

The same representatives used for GO term assignment were submitted to the KEGG Automatic Annotation server, using the bi-directional best hit algorithm for the genes representative set, including the available kinetoplastida genomes. The resulting KEGGID attribution for each supra-gene is on supplementary file S2.

**ACKNOWLEDGMENTS**

We would like to thank Paulo Claude Arauco for helping preparing and sequencing the cDNA libraries; CNPq, Fundação Araucária and Fiocruz for financial support.

**REFERENCES**

1. Christian Macagnan Probst, Fabricio Klerynton Marchini, Henrique Preti, Michel Batista, Lyris Godoy, Daniela Parada Pavoni, et al. TrypanosOmics: a integrated initiative for *Trypanosoma cruzi* functional genomics. BioXarchive.

2. Enright AJ, Van Dongen S, Ouzounis CA. An efficient algorithm for large- scale detection of protein families. Nucleic Acids Res. 2002 Apr 1;30(7):1575–84.

3. David M, Dzamba M, Lister D, Ilie L, Brudno M. SHRiMP2: Sensitive yet Practical Short Read Mapping. Bioinformatics. 2011 Apr 1;27(7):1011–2.

4. SHRiMP2: sensitive yet practical SHort Read Mapping. - PubMed - NCBI [Internet]. [cited 2016 Aug 3]. Available from: http://www.ncbi.nlm.nih.gov/pubmed/?term=David+M%2C+Dzamba+M%2C+Lister+D%2C+Ilie+L%2C+Brudno+M

5. Robinson MD, McCarthy DJ, Smyth GK. edgeR: a Bioconductor package for differential expression analysis of digital gene expression data. Bioinformatics. 2010 Jan 1;26(1):139–40.

6. Robinson MD, Oshlack A. A scaling normalization method for differential expression analysis of RNA-seq data. Genome Biol. 2010;11(3):R25.

7. R Development Core Team. R: A Language and Environment for Statistical Computing [Internet]. Vienna, Austria: R Foundation for Statistical Computing; 2016. Available from: http://www.R-project.org/

8. Sharan R, Maron-Katz A, Shamir R. CLICK and EXPANDER: a system for clustering and visualizing gene expression data. Bioinforma Oxf Engl. 2003 Sep 22;19(14):1787–99.

9. Götz S, García-Gómez JM, Terol J, Williams TD, Nagaraj SH, Nueda MJ, et al. High-throughput functional annotation and data mining with the Blast2GO suite. Nucleic Acids Res. 2008 Jun;36(10):3420–35.

## FIGURES

Figure 1. Scatter plot of the euclidean distance of the gene expression profile for each SG (density heat map, where areas of the scatter plot with a higher incidence of SG are in red).

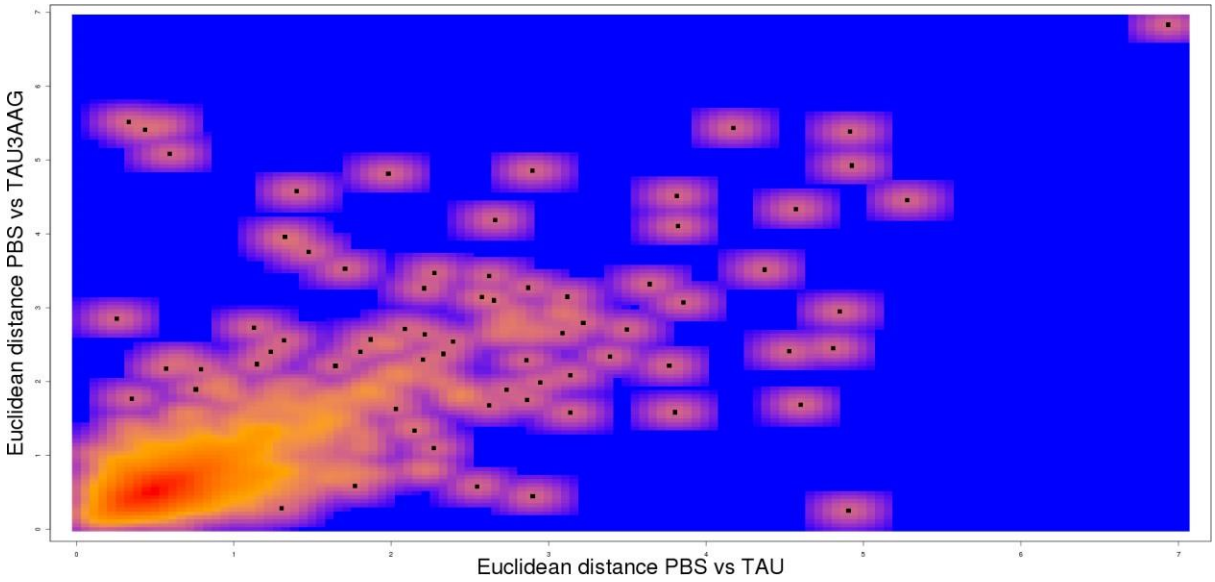

Table 1: Supra-Genes with functional annotation in analysis of modulation in PBS, considering decrease or increase of expression gene.

| ***ANALYSIS OF MODULATION IN PBS*** | |
|---|---|
| **Decrease of expression** | |
| Oxireduction | SGdmA1067, SGdmA1189, SGdmA2907, SGdmA3029, SGdmA3292 and SGdmA3899 |
| Energy metabolism | SGdmA0722, SGdmA1790, SGdmA2769, SGdmA2953, SGdmA3104, SGdmA3659, SGdmA3964, SGdmA4634, SGdmA5065, SGdmA5156, SGdmA5181, SGdmA5220, SGdmA5236, SGdmA5298, SGdmA5333, SGdmA5359, SGdmA5638, SGdmA6413, SGdmA7314, SGdmA7327, SGdmA7437, SGdmA7620 and SGdmA6931 |
| Mitochondrial function | SGdmA1450, SGdmA2900, SGdmA3003, SGdmA3424, SGdmA3747, SGdmA5581, SGdmA5912, SGdmA6566, SGdmA6874 and SGdmA7367 |
| Cytoskeleton | SGdmA2860, SGdmA3161, SGdmA3282, SGdmA5646, SGdmA5906, SGdmA6451, SGdmA6582, SGdmA6659 and SGdmA7319 |
| Dynein | SGdmA3161, SGdmA3282, SGdmA5646, SGdmA6451 and SGdmA6659 |
| Calmodulin | SGdmA1838, SGdmA4703 and SGdm5447 |
| Cytochrome | SGdmA2900, SGdmA5581 and SGdmA7367 |
| Cyclophilin | SGdmA0801 and SGdmA5787 |
| RNA polymerase | SGdmA0847, SGdmA4146, SGdmA5515 and SGdm5448 |
| Histone deacetylase | SGdmA3642 and SGdmA7734 |
| Mitochondrial carrier | SGdmA1450, SGdmA3003, SGdmA5912 and SGdmA6566 |
| RNA binding | SGdmA3405, SGdmA4150 and SGdmA5338 |
| Sm-like protein | SGdmA1796, SGdmA5064 and SGdmA5675 |
| **Increase of expression** | |
| RNA binding proteins | SGdmA1149, SGdmA1958, SGdmA1762, SGdmA1880, SGdmA2324, SGdmA3052, SGdmA3719, SGdmA4033, SGdmA5093 and SGdmA6426 |
| Trans-sialidase | SGdmA0256 and SGdmA1477 |
| gp63 | SGdmA0121 and SGdmA2825 |
| MASP | SGdmA0153, SGdmA0653 and SGdmA1478 |

Table 2: Supra-Genes with functional annotation in analysis of modulation in TAU, considering decrease or increase of expression gene.

| *Analysis of modulation in TAU* | |
|---|---|
| **Decrease of expression** | |
| Ribosome | SGdmA0322, SGdmA3495, SGdmA4699, SGdmA7309 and SGdmA7768 |
| Vacuole | SGdmA0570, SGdmA1130, SGdmA3067, SGdmA4121, SGdmA4405 and SGdmA7677 |
| Oxireduction | SGdmA0630, SGdmA0690, SGdmA1189, SGdmA2907, SGdmA3029, SGdmA3124, SGdmA3292, SGdmA4174 and SGdmA4634 |
| Energy metabolism | SGdmA0475, SGdmA1784, SGdmA2174, SGdmA2658, SGdmA2721, SGdmA2889, SGdmA2953, SGdmA3104, SGdmA3173, SGdmA3436, SGdmA3659, SGdmA3814, SGdmA3964, SGdmA4128, SGdmA4667, SGdmA5071, SGdmA5181, SGdmA5220, SGdmA5236, SGdmA5298, SGdmA5359, SGdmA5638, SGdmA638, SGdmA6413, SGdmA6915, SGdmA6923, SGdmA6931 and SGdmA7620 |
| Mitochondrial function | SGdmA1433, SGdmA1450, SGdmA2328, SGdmA2900, SGdmA3424, SGdmA3747, SGdmA5066, SGdmA5501, SGdmA5581, SGdmA5636, SGdmA5912, SGdmA6566, SGdmA6874, SGdmA7077, SGdmA7644 and SGdmA7768 |
| Cytoskeleton | SGdmA0022, SGdmA2860, SGdmA3101, SGdmA5906, SGdmA6050 and SGdmA6735 |
| DNA repair | SGdmA5758 and SGdmA7326 |
| Dynein | SGdmA3161, SGdmA3282, SGdmA5646, SGdmA6451 and SGdmA6630 |
| Cytochrome | SGdmA2900, SGdmA5066 and SGdmA7077 |
| Cyclophilin | SGdmA0451, SGdmA0801, SGdmA2946, SGdmA4776, SGdmA5581, SGdmA5787 and SGdmA7033 |
| RNA polymerase | SGdmA0847, SGdmA4993, SGdmA5448, SGdmA6373 and SGdmA6635 |
| Mitochondrial carrier | SGdmA1433, SGdmA1450, SGdmA5912, SGdmA6566 and SGdmA7644 |
| RNA binding | SGdmA1878, SGdmA2328, SGdmA3405, SGdmA3448, SGdmA4150, SGdmA5338, SGdmA5501 and SGdmA7768 |
| Chaperonin | SGdmA1038, SGdmA1630, SGdmA1781 and SGdmA2545 |
| Sm-like proteins | SGdmA1796, SGdmA2972, SGdmA5064, SGdmA5675 and SGdmA7289 |
| **Increase of expression** | |
| RNA binding proteins | SGdmA1149, SGdmA1958, SGdmA1880, SGdmA2324, SGdmA3052, SGdmA3719, SGdmA4033 and SGdmA6426 |
| Trans-sialidase | SGdmA6271 |
| gp63 S | GdmA0121 |

| | |
|---|---|
| Mucin TcMucII | SGdmA0251, SGdmA0252 and SGdmA0262 |
| MASP | SGdmA0153, SGdmA0258, SGdmA0653, SGdmA1478 and SGdmA1490 |

Table 3: Supra-Genes with functional annotation in analysis of modulation in TAU3AAG, considering decrease or increase of expression gene.

| | *TAU3AAG* |
|---|---|
| **Decrease of expression** | |
| Ribosome | SGdmA3495, SGdmA5333, SGdmA5548, SGdmA6413, SGdmA6637, SGdmA7199, SGdmA7277, SGdmA7309, and SGdmA7768 |
| Vacuole | SGdmA0570, SGdmA1130, SGdmA3067, SGdmA4121 and SGdmA4405 |
| Oxireduction | SGdmA0630, SGdmA1067, SGdmA1189, SGdmA1995, SGdmA2907, SGdmA3029, SGdmA3292, SGdmA3981, SGdmA4174, SGdmA6088 and SGdmA7243 |
| Energy metabolism | SGdmA1536, SGdmA2889, SGdmA2953, SGdmA3104, SGdmA3436, SGdmA3659, SGdmA3964, SGdmA4667, SGdmA4811, SGdmA5181, SGdmA5236, SGdmA5298, SGdmA5331, SGdmA5359, SGdmA5638, SGdmA6348, SGdmA6757, SGdmA6915, SGdmA6923, SGdmA6931 and SGdmA7314 |
| Mitochondrial function | SGdmA1240, SGdmA1450, SGdmA2075, SGdmA2621, SGdmA3183, SGdmA3747, SGdmA4713, SGdmA5912, SGdmA6335, SGdmA6441 and SGdmA6874 |
| Cytoskeleton | SGdmA0022, SGdmA2746, SGdmA2860, SGdmA3101, SGdmA5906, SGdmA6582, SGdmA6605, SGdmA6650 and SGdmA6735 |
| DNA repair | SGdmA5758 and SGdmA7326 |
| Anaphase complex | SGdmA4753 and SGdmA6443 |
| Calmodulin | SGdmA4703 and SGdmA5447 |
| Cyclophilin | SGdmA0451, SGdmA0801, SGdmA2946, SGdmA2884, SGdmA4776, SGdmA5787 and SGdmA7033 |
| Cyclin | SGdmA0664 and SGdmA7511 |
| RNA polymerase | SGdmA0253, SGdmA0847, SGdmA4146, SGdmA5448, SGdmA5515 and SGdmA6373 |
| Mitochondrial carrier | SGdmA1450, SGdmA2621, SGdmA3183, SGdmA4713, SGdmA5912, SGdmA6335 and SGdmA6441 |

| | |
|---|---|
| RNA binding | SGdmA1878, SGdmA2328, SGdmA3405, SGdmA4150 and SGdmA5338 |
| Chaperonin | SGdmA0622, SGdmA1038, SGdmA1630, SGdmA1781, SGdmA3067, SGdmA3210 and SGdmA6707 |
| Sm-like proteins | SGdmA1796, SGdmA2972, SGdmA5064, SGdmA5675 and SGdmA6416 |
| ADP-ribosylation | SGdmA5069, SGdmA6454 and SGdmA6955 |
| Amastin | SGdmA0183 |
| **Increase of expression** | |
| RNA binding proteins | SGdmA1149, SGdmA1269, SGdmA1880, SGdmA1958, SGdmA2324, SGdmA3719, SGdmA4033, SGdmA5501 and SGdmA6426 |
| Trans-sialidase | SGdmA1477, SGdmA3129 and SGdmA6271 |
| gp63 | SGdmA0121 and SGdmA0286 |
| Mucin TcMucII | SGdmA0065, SGdmA0137, SGdmA0194, SGdmA0252, SGdmA0262, *SGdmA0263 and* SGdmA0314 |
| MASP | SGdmA0153, SGdmA0258 and SGdmA0653 |

Table 4: DEGs with functional annotation in analysis of modulation in PBS, considering decrease or increase of expression gene.

| | ***PBS*** |
|---|---|
| **Decrease of expression** | |
| Hypothetical protein conserved | SGdmA6558, SGdmA4854, SGdmA2580, SGdmA5601, SGdmA1529, SGdmA7662, SGDmA3326, SGdmA1069, SGdmA4856, SGdmA7460, SGdmA4707, SGdmA7330, SGdmA4971, SGdmA4987, SGdmA4949, SGdmA0924, SGdmA0353, SGdmA6711 and SGdmA0350 |
| Hypothetical protein | SGdmA4116 and SGdmA3977 |
| General genes | ARP2/3 complex subunit (SGdmA5906), histone H1 (SGdmA1365), POMP37 (SGdmA1240), cytochrome B5 (SGdm5066), prefoldin subunit (SGdmA1110), ADG1-like (SGdmA3232), endonuclease III (SGdmA1877), monothiol glutaredoxin (SGdmA1189), pterin-4-alpha-carbinolamine dehydratase (SGdmA4168), DNA repair and recombination protein RAD54 (SGdmA7326) and DNA/RNA non-specific endonuclease (SGdmA0860) |
| Specific at 1 hour | hypothetical protein conserved (SGdmA0932, SGdmA0934, SGdmA0519), hypothetical protein (SGdmA0518, SGdmA0606), cation transporter (SGdmA0327) and calpain−like cysteine peptidase (SGdmA0435, SGdmA0436) |
| Specific at 2 hour | hypothetical protein conserved (SGdmA1887, SGdmA6057, SGdmA0517, SGdmA0878, SG7343) and polypeptide deformylase-like protein (SGdmA6371) |
| aSpecifict 4 hour | hypothetical protein conserved (SGdmA6692, SGdmA6722, SGdmA0736, SGdmA7039, SGdmA2899, SGdmA0600, SGdmA1659) and hypothetical protein (SGdmA0825) |
| Specific at 6 hour | hypothetical protein conserved (SGdmA3432, SGdmA0802, SGdmA04500, SGdmA5635, SGdmA1701, SGdmA3939, SGdmA3750, SGdmA0921), hypothetical protein (SGdmA5186), map-kinase 4 (SGdmA0921), dynein light chain 2b, cytoplasmic (SGdmA3161), vacuolar transporter chaperone (SGdmA3067) and ARF-like 2 binding protein (SGdmA6582) |
| Specific at 24 hour | hypothetical protein conserved ( SGdmA3644, SGdmA3503 and SGdmA3989) |

Table 5: DEGs with functional annotation in analysis of modulation in TAU, considering

| *FUNCTIONAL ANALYSIS OF MODULATED SUPRA-GENES SPECIFIC TO TAU* | |
|---|---|
| **Decrease of expression** | |
| Hypothetical protein conserved at 24 hours | SGdmA3654, SGdmA4074, SGdm0845, SGdmA1290, SGdmA2459, SGdmA1771, SGdmA4619, SGdmA3788, SGdmA1647, SGdmA7420, SGdmA3022, SGdmA2886, SGdmA3832, SGdmA4132, SGdmA5940SGdmA4402, SGdmA1604, SGdmA6670, SGdmA6362 and SGdmA0275 |
| Hypothetical protein at 24 hours | SGdmA2718, ubiquinone biosynthesis protein (SGdmA2907), mitochondrial carrier protein (SGdmA7644), dephospho-CoA kinase (SGdmA2953), DNA-directed RNA polymerase I (SGdmA0847), histone deacetylase 1 (SGdmA3642), triglyceride lipase (SGdmA0919), RNA triphosphatase (SGdmA4395) and origin recognition complex subunit 1 (ORC1, SGdmA4138) |
| Hypothetical protein conserved at 6 hours | SGdmA5370, SGdmA6919, SGdmA2817 and SGdmA1134 |

decrease or increase of expression gene.

Table 6: Supra-Genes with functional annotation in analysis of modulation in TAU3AAG, considering decrease or increase of expression gene.

| ***FUNCTIONAL ANALYSIS OF MODULATED SUPRA-GENES SPECIFIC TO TAU3AAG*** | |
|---|---|
| **Decrease of expression** | |
| Hypothetical protein conserved at 24 hours | SGdmA7800, SGdmA6222, SGdmA2458, SGdmA5813, SGdmA3640, SGdmA3381, SGdm2520, SGdmA0334, SGdmA5589, SGdmA6349, SGdmA2094, SGdmA3218, SGdmA7411, SGdmA2360, SGdmA2549, SGdmA2619, SGdmA2862, SG7527 and SGdmA2676 |
| Hypothetical protein at 24 hours | SGdmA1985, SGdmA1476, SGdmA2979, SGdmA4516 and SGdmA2966) |
| Specific genes at 24 hours | deaminase (SGdmA2769), Trk system potassium uptake (HKT1, SGdmA6951), proliferator-activated receptor interacting protein (PRIP, SGdmA4135), monoxygenase (SGdmA3981), glucosamine 6-phosphate n-acetyltransferase (SGdmA6923), CYC2-like cyclin 6 (SGdmA0664), actin-related protein 2/3 complex subunit (ARPC1, SGdmA6650), translation initiation factor EIF-2b, ADP-ribosylation factor, 8-oxoguanine DNA glycosylase (SGdmA6757), mitochondrial carrier (SGdmA3183), ABC transporter (SGdmA4131), peptydil-prolyl cis-trans isomerase (PIN1, SGdmA4019), protein kinase (SGdmA4766) and 60S ribosomal protein (SGdmA7199) |

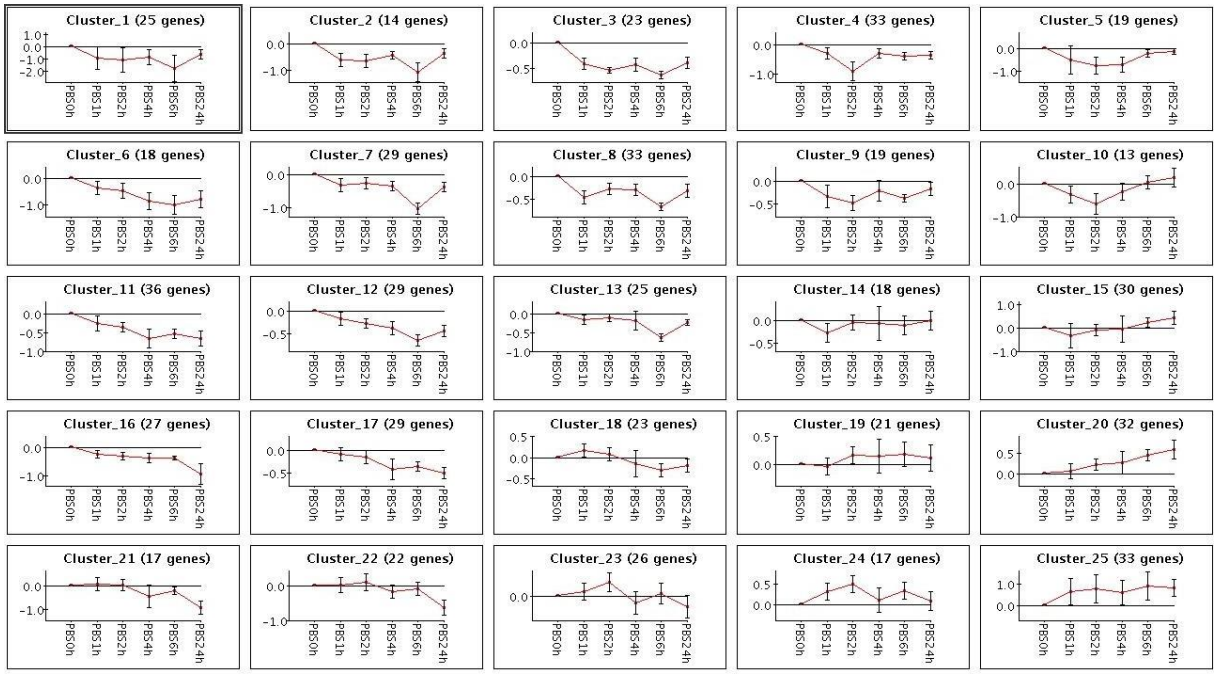


Figure 2. SOM clustering of DEGS in PBS condition.

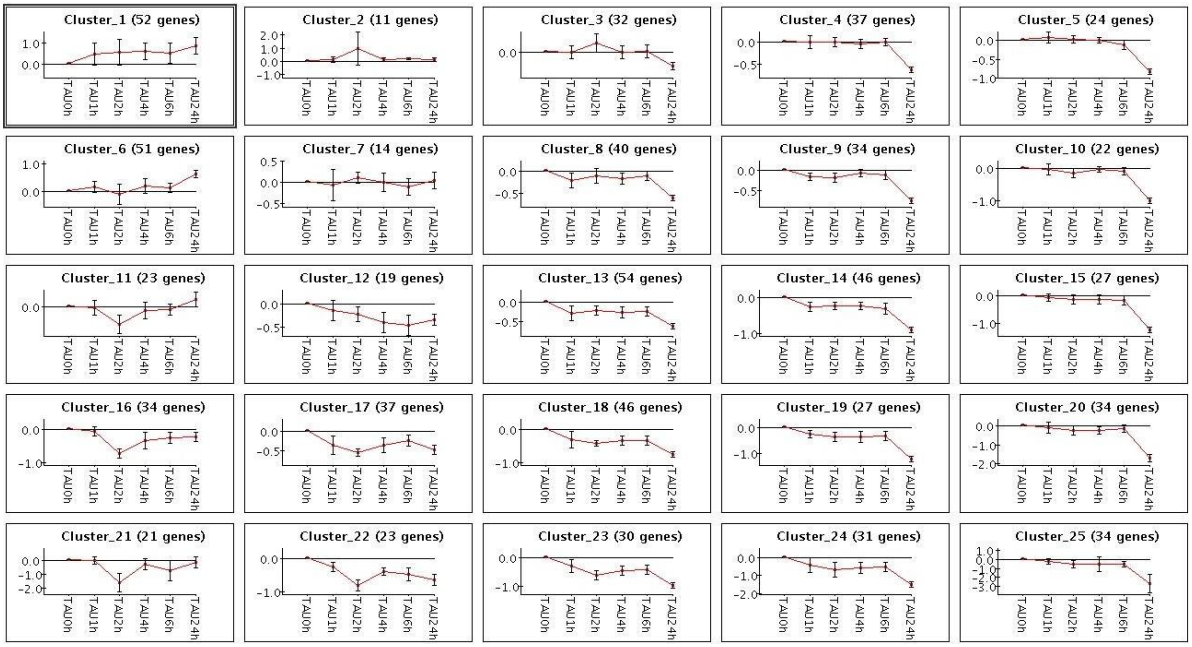


Figure 3. SOM clustering of DEGS in TAU condition.

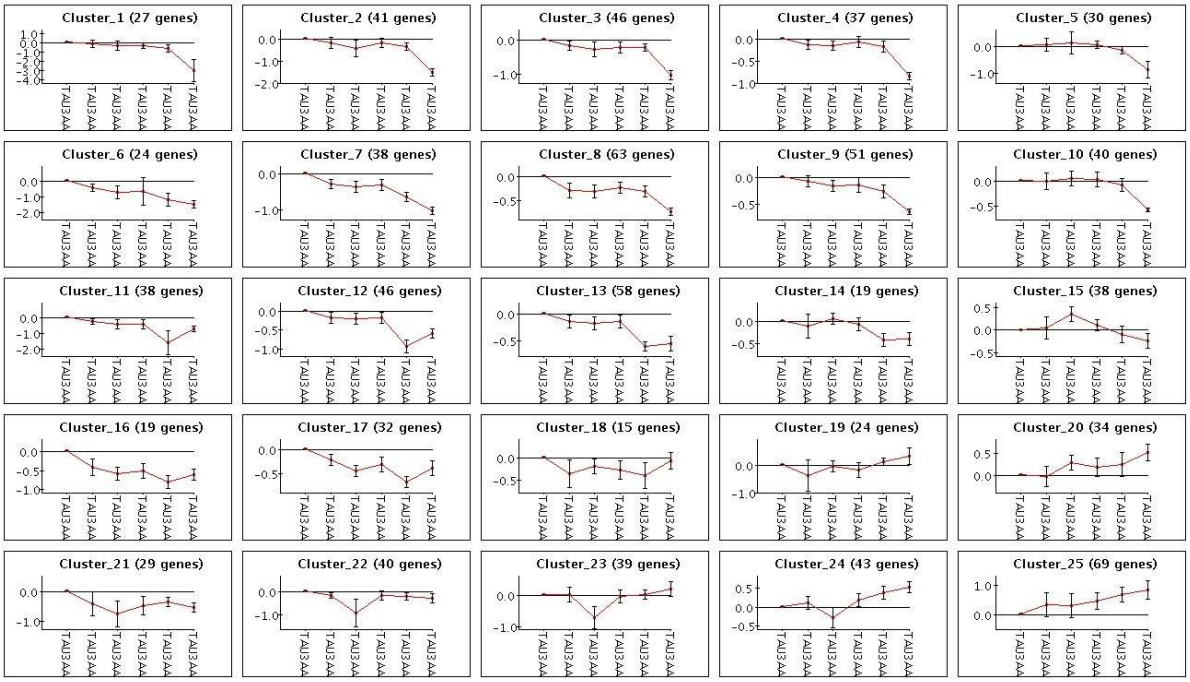


Figure 4. SOM clustering of DEGS in TAU3AAG condition.

## SUPPORTING INFORMATION

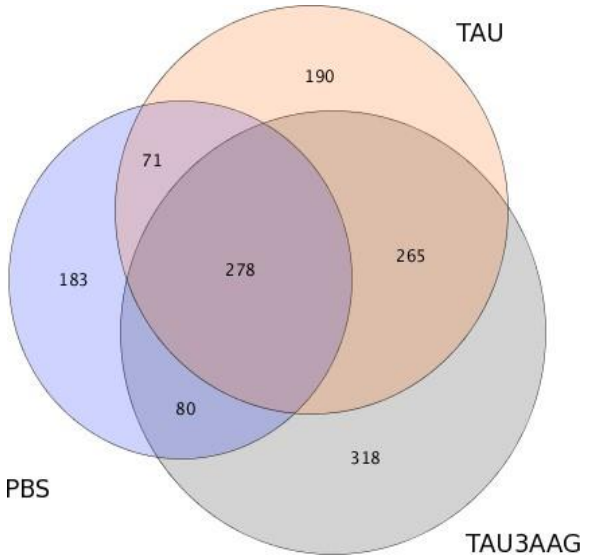


Figure S1. Euler diagram of DESG considering 5% FDR and 1.5 fold change thresholds

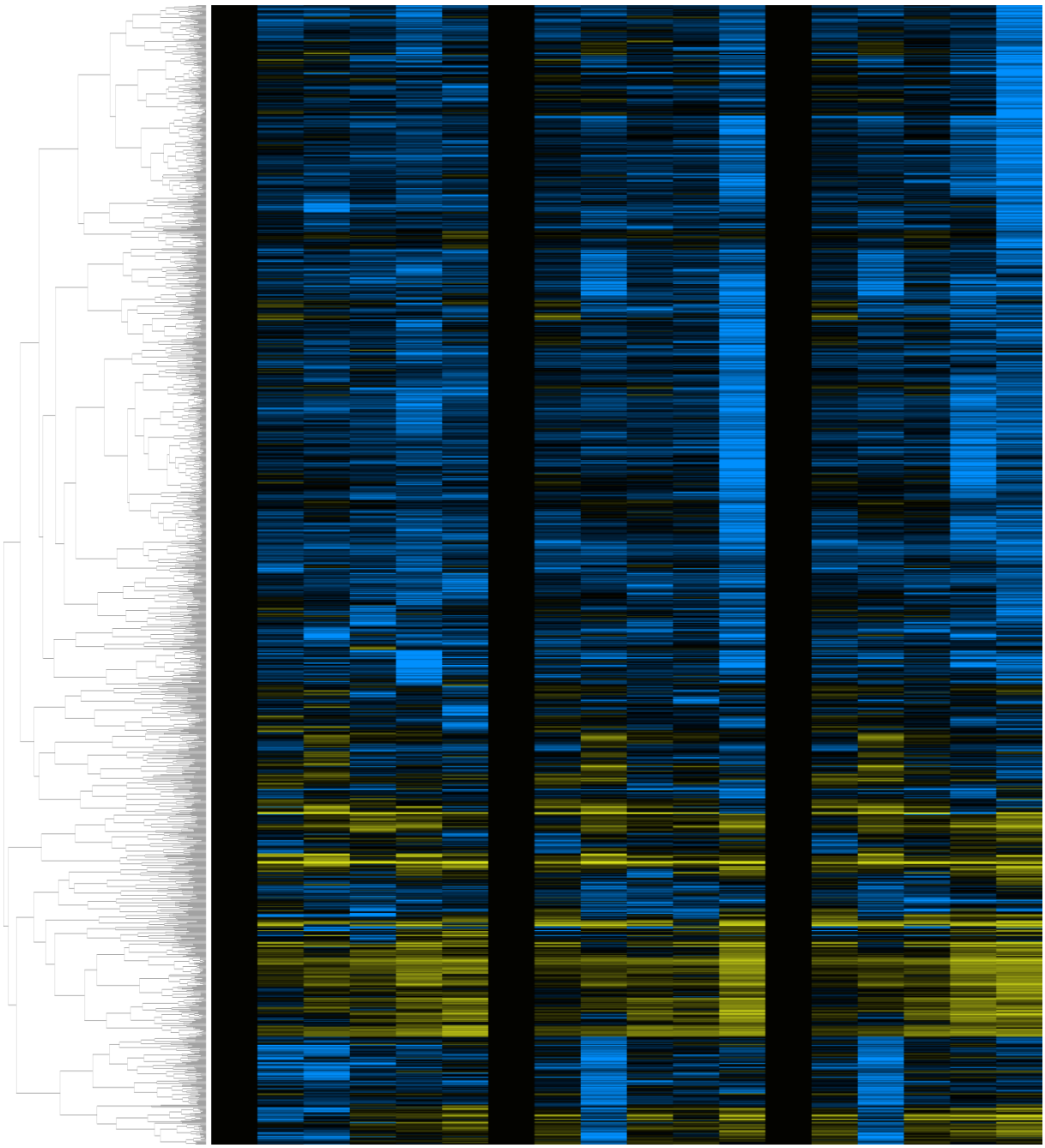

Figure S2. Heatmap of the complete set of DESG, representing PBS, TAU and TAU3AAG modulation across the time points of 0h (stationary epimastigote), 1h, 2h, 4h, 6h and 24h of treatment. Grades of blue and yellow represent decrease or increase, respectively, of log2-ratio time point against stationary epimastigote

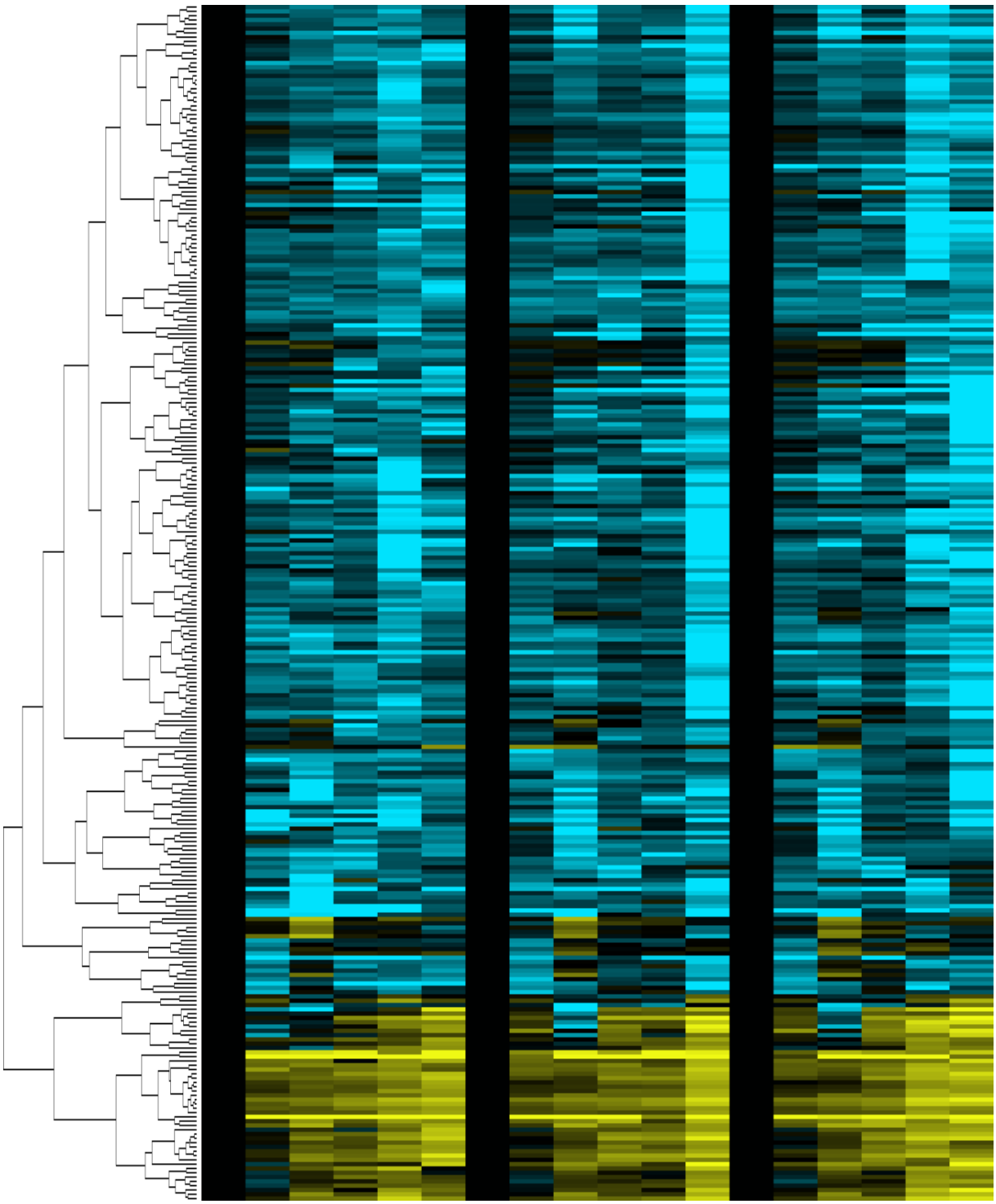

Figure S3. Heatmap of the complete set of DESG, representing PBS, TAU and TAU3AAG modulation across the time points of 0h (stationary epimastigote), 1h, 2h, 4h, 6h and 24h of treatment. Grades of blue and yellow represent decrease or increase, respectively, of log2-ratio time point against stationary epimastigote.

# 6 CONCLUSÃO

A análise de curva de crescimento em microrganismos permite avaliar as mudanças que as células sofrem durante a transição entre as diferentes fases da curva. Este trabalho demonstrou que a forma epimastigota da cepa Dm28c de *T. cruzi* possui uma curva de crescimento padrão, com a definição de quatro distintas fases quando cultivada in vitro: fase lag, exponencial, estacionária inicial e estacionária. Poucas modificações morfológicas no parasita são observadas nos primeiros dias de cultivo. Porém, com o avanço da fase estacionária observamos alterações celulares e de motilidade em grande parte dos parasitas. A presença de parasitas com pouco ou nenhuma mobilidade ao longo da fase estacionária nos intrigou para avaliar se esses parasitas estavam mortos. Análise de viabilidade celular indicou que uma pequena porcentagem das células estavam morrendo nesta fase, corroborando a ideia de que os parasitas atingem um estado de quiescência.

Dados de ciclo celular ao longo da curva nos mostraram que a maior parte dos parasitas estava em fase G1. Porém, na fase estacionária, uma grande proporção de células se encontrava nas fases S e G2/M, indicando que os parasitas podem estar parados nessas fases já que há uma grande redução da proliferação.

A fase estacionária é um aspecto crítico da biologia de células de diferentes microrganismos, porém em tripanossomatídeos existem poucos estudos sobre essa fase. Tem sido sugerido que a fase estacionária de epimastigotas é um estágio pré-adaptativo para a célula sofrer o processo de metaciclogênese, pois é observado que em cultivo algumas células transformam-se em tripomastigotas metacíclicos. Além disso, a redução da concentração de glicose e outros nutrientes mostrado por diversos autores corrobora com a ideia de que nesta fase ocorra uma reprogramação gênica para que a célula se mantenha viva e pronta para se diferenciar. Outras questões básicas a respeito deste estado de repouso permanecem sem resposta. Dessa maneira um importante ponto deste trabalho foi a busca pelo entendimento sobre de que forma as células quiescentes são reguladas e reprogramadas geneticamente. Nesse trabalho estudamos as transições das fases da curva de crescimento, enfatizando a fase estacionária, por análises de transcritômica e proteômica, além do estudo de transcritômica do parasita em fase estacionária inicial sob estresse em diferentes condições de meio empobrecido.

As análises de RNA-seq da curva de crescimento promoveram um amplo cenário para discussão. Em trabalhos de larga escala, o entendimento global dos dados pode ser obtido por

análises de agrupamento dos genes modulados, seguido de análises de ontologia gênica (GO, do inglês *Gene Ontology*). Essas ferramentas são importantes na compreensão dos processos envolvidos em padrões de modulação da expressão gênica, o que nos permitiu identificar mecanismos celulares e moleculares ao longo da curva de crescimento.

Além disso, nós realizamos análises pontuais de algumas vias e genes que nos forneceram informações relevantes que foram discutidas no Capítulo 1, principalmente em relação a via de resposta a depleção da glicose. Devido ao grande número de proteínas hipotéticas encontradas no *T. cruzi* e também devido a grande distância evolutiva em relação a organismos modelo, a compreensão da modulação desses genes somente a partir de GO não seriam alcançados.

Para as análises de proteômica da curva de crescimento utilizamos duas réplicas biológicas. Para cada réplica, amostras de oito dias consecutivos foram preparadas para serem lidas no espectrômetro duas vezes cada uma, totalizando 32 corridas. Trinta corridas foram concluídas (com perda de apenas 2 corridas do estimado). Os resultados analisados até o momento se mostraram promissores com a identificação de um grande número de grupos de proteínas. Além disso, 92 proteínas diferencialmente expressas foram encontradas e dentro dessas aproximadamente 30% mostraram correlação do seu padrão de expressão proteica aos dados de transcritômica. Os dez principais termos de ontologia gênica encontrados estão relacionados com citosol, complexo proteicos, processos metabólicos de aminoácidos, atividade oxidoredutase, mitocôndria, processos catabólicos, tradução, geração de precursores metabólicos e energia, ribossomo e cofatores de processos metabólicos. Ainda serão realizadas análises mais robustas o que poderá nos fornecer dados mais específicos. No Capítulo 1 foi observado um grande número de genes com expressão aumentada na fração de RNA polissomal, os quais parecem estar associados a grânulos ribonucleoproteicos no citoplasma. Com a finalização das análises de proteômica, esperamos conseguir avaliar quais conjuntos de mRNAs poderiam estar associados a esses grânulos e quais estão realmente ligados a polissomos.

As análises de transcritômica de parasitas submetidos a estresse nutricional pode apresentar uma forma eficiente de avaliar o parasita em condições semelhantes a do seu habitat no inseto vetor e que são determinantes para o processo de diferenciação em tripomastigota metacíclicos. Epimastigotas de fase estacionária inicial nas diferentes condições de estresse nutricional analisadas (PBS, TAU e TAU3AAG) apresentaram um padrão de modulação semelhante. Foi possível observar que a grande parte dos genes com expressão diminuída estão

relacionados principalmente a processos de metabolismo, o que é condizente com o estado de indução a quiescência. Em uma menor proporção estão os genes com expressão aumentada, sendo principalmente codificadores de proteínas de ligação a RNA.

Este estudo está contribuindo para expandir e buscar avanços no conhecimento sobre a atividade metabólica, abundância relativa de mRNAs e proteínas em fases exponencial e estacionária do T. cruzi, um organismo de importância médica e biologicamente peculiar. Esforços de análises em larga escala podem fornecer uma compreensão da biologia básica desse parasita, levando a um maior acúmulo de dados e conhecimento que podem também contribuir para o entendimento da doença de Chagas.

# REFERÊNCIAS


AEBERSOLD, R.; HOOD, L. E.; WATTS, J. D. Equipping scientists for the new biology. **Nature biotechnology**, v. 18, n. 4, p. 359, 2000.

AGABIAN, N. Trans splicing of nuclear pre-mRNAs. **Cell**, v. 61, n. 6, p. 1157–1160, 1990.

ALOIA, R. C.; RAISON, J. K. Membrane function in mammalian hibernation. **Biochimica et biophysica acta**, v. 988, n. 1, p. 123–46, 1989.

ALVAREZ, V. E. et al. Autophagy Is Involved in Nutritional Stress Response and Differentiation in Trypanosoma cruzi. **Journal of Biological Chemistry**, v. 283, n. 6, p. 3454–3464, 2008.

ALVES, M. J. M.; COLLI, W. Trypanosoma cruzi: adhesion to the host cell and intracellular survival. **IUBMB life**, v. 59, n. May, p. 274–279, 2007.

ANDRADE, L. O.; ANDREWS, N. W. Opinion: The Trypanosoma cruzi–host-cell interplay: location, invasion, retention. **Nature Reviews Microbiology**, v. 3, n. 10, p. 819–823, 2005.

ANDREWS, N. W. Living dangerously: how Trypanosoma cruzi uses lysosomes to get inside host cells, and then escapes into the cytoplasm. **Biological research**, v. 26, n. 1–2, p. 65–7, 1993.

ARCHER, S. K. et al. The cell cycle regulated transcriptome of Trypanosoma brucei. **PLoS ONE**, v. 6, n. 3, 2011.

ASLETT, M. et al. TriTrypDB: A functional genomic resource for the Trypanosomatidae. **Nucleic Acids Research**, v. 38, n. SUPPL.1, p. 457–462, 2009.

ATWOOD, J. A. et al. The Trypanosoma cruzi proteome. **Science (New York, N.Y.)**, v. 309, n. 5733, p. 473–6, 2005.

ÁVILA, A. R. et al. Cloning and characterization of the metacyclogenin gene, which is specifically expressed during Trypanosoma cruzi metacyclogenesis. **Molecular and Biochemical Parasitology**, v. 117, p. 169–177, 2001.

ÁVILA, A. R. et al. Stage-specific gene expression during Trypanosoma cruzi metacyclogenesis. **Genetics and Molecular Research**, v. 2, n. 1, p. 159–168, 2003.

BALOGH, G. et al. Key role of lipids in heat stress management. **FEBS Letters**, v. 587, n. 13, p. 1970–1980, 2013.

BARDERI, P. et al. The NADP+-linked glutamate dehydrogenase from Trypanosoma cruzi : sequence, genomic organization and expression. **Biochem. J**, v. 330, p. 951–958, 1998.

BAYER-SANTOS, E. et al. Expression and cellular trafficking of GP82 and GP90 glycoproteins during Trypanosoma cruzi metacyclogenesis. **Parasites & vectors**, v. 6, p. 127, 2013.

BENJAMINI, Y.; HOCHBERG, Y. Benjamini Y, Hochberg Y. Controlling the false discovery rate: a practical and powerful approach to multiple testing. **Journal of the Royal Statistical Society B**, v. 57, n. 1, p. 289–300, 1995.

BERN, C. et al. Evaluation and treatment of chagas disease in the United States: a systematic review. **JAMA**, v. 298, n. 18, p. 2171–81, 2007.

BERN, C. Chagas' Disease. **New England Journal of Medicine**, v. 373, n. 5, p. 456–466, 2015.

BERRIMAN, M. et al. The genome of the African trypanosome Trypanosoma brucei. **Science (New York, N.Y.)**, v. 309, n. 5733, p. 416–22, 2005.

BONALDO, M. C. et al. Cell-substrate adhesion during Trypanosoma cruzi differentiation. **The Journal of cell biology**, v. 106, n. 4, p. 1349–58, 1988.

BRENER, Z. Biology of Trypanosoma cruzi. **Annual review of microbiology**, v. 27, p. 347–382, 1973.

BRINGAUD, F.; RIVIÈRE, L.; COUSTOU, V. Energy metabolism of trypanosomatids: Adaptation to available carbon sources. **Molecular and Biochemical Parasitology**, v. 149, p. 1–9, 2006.

BRIONES, M. R. S. et al. **Trans-Sialidase and sialic acid acceptors from insect to mammalian stages of Trypanosoma cruzi.Experimental Parasitology**, 1994.

BUDA, C. et al. Structural order of membranes and composition of phospholipids in fish brain cells during thermal acclimatization. **Proceedings of the National Academy of Sciences of the United States of America**, v. 91, n. 17, p. 8234–8238, 1994.

BURCHMORE, R. J.; BARRETT, M. P. Life in vacuoles--nutrient acquisition by Leishmania amastigotes. **International journal for parasitology**, v. 31, n. 12, p. 1311–1320, 2001.

BURLEIGH, B. A; ANDREWS, N. W. The mechanisms of Trypanosoma cruzi invasion of mammalian cells. **Annual review of microbiology**, v. 49, p. 175–200, 1995.

BURSELL, E. The Role of Proline in Energy Metabolism. In: **Energy Metabolism in Insects**. Boston, MA: Springer US, p. 135–154, 1981.

CALER, E. V et al. Dual Role of Signaling Pathways Leading to Ca2+ and Cyclic AMP Elevation in Host Cell Invasion byTrypanosoma cruzi. **Infection and Immunity**, v. 68, n. 12, p. 6602–6610, 2000.

CAMARGO, E. P. Growth and differentiation in trypanosoma cruzi. I. Origin of metacyclic trypanosomes in liquid media. **Revista do Instituto de Medicina Tropical de São Paulo**, v. 6, p. 93–100, 1964a.

CAMARGO, E. P. **Growth and differentiation in Trypanosoma cruzi**, Rev. Inst. Med. Trop. São Paulo, 1964b.

CAMPBELL, D. A.; THOMAS, S.; STURM, N. R. Transcription in kinetoplastid protozoa: Why be normal? **Microbes and Infection**, v. 5, n. 13, p. 1231–1240, 2003.

CAMPBELL, D. A.; WESTENBERGER, S. J.; STURM, N. R. The determinants of Chagas disease: connecting parasite and host genetics. **Current molecular medicine**, v. 4, n. 6, p. 549–62, 2004.

CAMPOS, P. C. et al. Sequences involved in mRNA processing in Trypanosoma cruzi. **International journal for parasitology**, v. 38, n. 12, p. 1383–9, 2008.

CAMPOS, R. A. et al. Gene expression and molecular modeling of the HSP104 chaperone of Trypanosoma cruzi. **Genetics and molecular research : GMR**, v. 11, n. 3, p. 2122–2129, 2012.

CANNATA, J. J.; CAZZULO, J. J. The aerobic fermentation of glucose by Trypanosoma cruzi. **Comparative biochemistry and physiology. B, Comparative biochemistry**, v. 79, n. 3, p. 297–308, 1984.

CAPEWELL, P. et al. Regulation of Trypanosoma brucei Total and Polysomal mRNA during Development within Its Mammalian Host. **PLoS ONE**, v. 8, n. 6, p. e67069, 2013.

CAROLINA, M. et al. Transcription rate modulation through the Trypanosoma cruzi life cycle occurs in parallel with changes in nuclear organisation. v. 112, p. 79–90, 2001.

CASSOLA, A.; GAUDENZI, J. G. DE; FRASCH, A. C. Recruitment of mRNAs to cytoplasmic ribonucleoprotein granules in trypanosomes. v. 65, p. 655–670, 2007.

CAZZULO, J. J. et al. End products and enzyme levels of aerobic glucose fermentation in trypanosomatids. **Molecular and biochemical parasitology**, v. 16, n. 3, p. 329–43, 1985.

CAZZULO, J. J. Aerobic fermentation of glucose by trypanosomatids. **The FASEB journal : official publication of the Federation of American Societies for Experimental Biology**, v. 6, p. 3153–3161, 1992.

CAZZULO, J. J. Intermediate metabolism in Trypanosoma cruzi. **Journal of bioenergetics and biomembranes**, v. 26, n. 2, p. 157–165, 1994.

CELESTE, B. J.; GUIMARÃES, M. C. Growth curves of Leishmania braziliensis braziliensis promastigotes and surface antigen expression before and after adaptation to Schneider's Drosophila medium as assessed by anti-Leishmania human sera. **Revista do Instituto de Medicina Tropical de Sao Paulo**, v. 30, n. 2, p. 63–67, 1988.

CEVALLOS, A. M. et al. The stabilization of housekeeping transcripts in Trypanosoma cruzi epimastigotes evidences a global regulation of RNA decay during stationary phase. **FEMS microbiology letters**, v. 246, n. 2, p. 259–264, 2005.

CHAGAS, C. Nova tripanozomiaze humana: Estudos sobre a morfolojia e o ciclo evolutivo

do Schizotrypanum cruzi n. gen., n. sp., ajente etiolojico de nova entidade morbida do homem. **Memórias do Instituto Oswaldo Cruz**, v. 1, n. 2, p. 159–218, 1909.

CLAYTON, C. The regulation of trypanosome gene expression by RNA-binding proteins. **PLoS pathogens**, v. 9, n. 11, p. e1003680, 2013.

CLAYTON, C.; SHAPIRA, M. Post-transcriptional regulation of gene expression in trypanosomes and leishmanias. **Molecular and Biochemical Parasitology**, v. 156, n. 2, p. 93–101, 2007.

CONCEIC, L. E. C. A reference growth curve for nutritional experiments in zebrafish ( Danio rerio ) and changes in whole body proteome during development. p. 1199–1215, 2010.

CONESA, A. et al. Blast2GO: A universal tool for annotation, visualization and analysis in functional genomics research. **Bioinformatics**, v. 21, n. 18, p. 3674–3676, 2005.

CONRAD, M. et al. Nutrient sensing and signaling in the yeast Saccharomyces cerevisiae. **FEMS Microbiology Reviews**, v. 38, n. 2, p. 254–299, 2014.

CONTRERAS, V. T. et al. In vitro differentiation of Trypanosoma cruzi under chemically defined conditions. **Molecular and biochemical parasitology**, v. 16, p. 315–327, 1985.

CONTRERAS, V. T.; MOREL, C. M.; GOLDENBERG, S. Stage specific gene expression precedes morphological changes during Trypanosoma cruzi metacyclogenesis. **Molecular and biochemical parasitology**, v. 14, p. 83–96, 1985.

CONTRERAS, V. T. et al. Biological aspects of the Dm 28c clone of Trypanosoma cruzi after metacyclogenesis in chemically defined media. **Memórias do Instituto Oswaldo Cruz**, v. 83, n. 1, p. 123–33, 1988.

CONTRERAS A., V. T.; DE LIMA R., A. R.; NAVARRO A., M. C. Para La Diferenciación in Vitro Trypanosoma Cruzi Morphogenesis : Relevant Factors for in Vitro Differentiation. **Acta Biol. Venez.**, v. 26, n. 2, p. 49–60, 2006.

CORNELISSEN, A. W. et al. Transcription and RNA polymerases in Trypanosoma brucei. **Acta Leidensia**, v. 58, n. 2, p. 75–96, 1989.

CORNELISSEN, A. W. et al. Transcription analysis in Trypanosoma brucei. **Biochemical Society transactions**, v. 18, n. 5, p. 710–4, 1990.

COURA, J. R.; DIAS, J. C. P. Epidemiology, control and surveillance of Chagas disease: 100 years after its discovery. **Memorias do Instituto Oswaldo Cruz**, v. 104 Suppl, n. i, p. 31–40, 2009.

COX, J.; MANN, M. MaxQuant enables high peptide identification rates, individualized p.p.b.-range mass accuracies and proteome-wide protein quantification. **Nature biotechnology**, v. 26, n. 12, p. 1367–72, dez. 2008.

COX, J. et al. Andromeda: a peptide search engine integrated into the MaxQuant environment. **Journal of proteome research**, v. 10, n. 4, p. 1794–805, abr. 2011.

DALLAGIOVANNA, B. et al. Trypanosoma cruzi: a gene family encoding chitin-binding-like proteins is posttranscriptionally regulated during metacyclogenesis. **Experimental parasitology**, v. 99, n. 1, p. 7–16, 2001.

DAS, A. et al. The essential polysome-associated RNA-binding protein RBP42 targets mRNAs involved in Trypanosoma brucei energy metabolism. **RNA**, p. 1968–1983, 2012.

DAVID, M. et al. SHRiMP2: Sensitive yet Practical Short Read Mapping. **Bioinformatics**, v. 27, n. 7, p. 1011–1012, 2011.

DE ANDRADE, A F. et al. Changes in cell-surface carbohydrates of Trypanosoma cruzi during metacyclogenesis under chemically defined conditions. **Journal of general microbiology**, v. 137, p. 2845–2849, 1991.

DE CARVALHO, E. F. et al. HSP 70 gene expression in Trypanosoma cruzi is regulated at different levels. **J Cell Physiol**, v. 143, n. 3, p. 439–444, 1990.

DE GAUDENZI, J.; FRASCH, A. C.; CLAYTON, C. RNA-Binding Domain Proteins in Kinetoplastids: a Comparative Analysis. **Eukaryotic Cell**, v. 4, n. 12, p. 2106–2114, 1, 2005.

DE GAUDENZI, J. G. et al. Gene expression regulation in trypanosomatids. **Essays in biochemistry**, v. 51, p. 31–46, 2011.

DE GODOY, L. M. F. et al. Comprehensive mass-spectrometry-based proteome quantification of haploid versus diploid yeast. **Nature**, v. 455, n. 7217, p. 1251–4, 2008.

DE LANGE, T. et al. Comparison of the genes coding for the common 5' terminal sequence of messenger RNAs in three trypanosome species. **Nucleic acids research**, v. 12, n. 11, p. 4431–43, 1984.

DE LIMA, A. R. et al. Cultivation of Trypanosoma cruzi epimastigotes in low glucose axenic media shifts its competence to differentiate at metacyclic trypomastigotes. **Experimental Parasitology**, v. 119, p. 336–342, 2008.

DE SOUZA, W. Cell biology of Trypanosoma cruzi. **International review of cytology**, v. 86, p. 197–283, 1984.

DIAS, J. C. [Epidemiological surveillance of Chagas disease]. **Cadernos de saúde pública**, v. 16 Suppl 2, p. 43–59, 2000.

DOS SANTOS, P. F. et al. Molecular characterization of the hexose transporter gene in benznidazole resistant and susceptible populations of Trypanosoma cruzi. **Parasites & Vectors**, v. 5, n. 1, p. 161, 2012.

DROLL, D. et al. Post-Transcriptional Regulation of the Trypanosome Heat Shock Response by a Zinc Finger Protein. **PLoS Pathogens**, v. 9, n. 4, 2013.

EL-SAYED, N. M. et al. The genome sequence of Trypanosoma cruzi, etiologic agent of Chagas disease. **Science (New York, N.Y.)**, v. 309, n. 5733, p. 409–15, 2005.

ELIAS, M. C. Q. B. et al. Transcription rate modulation through the Trypanosoma cruzi life cycle occurs in parallel with changes in nuclear organisation. **Molecular and Biochemical Parasitology**, v. 112, n. 1, p. 79–90, 2001.

ENDERS, B.; BRAUNS, F.; ZWISLER, O. Biochemical and technical considerations regarding the mass production of certain parasitic protozoa. **Bulletin of the World Health Organization**, v. 55, n. 2–3, p. 393–402, 1977.

ENGMAN, D. M. et al. Trypanosoma cruzi: Accumulation of polycistronic hsp70 RNAs during severe heat shock. **Experimental Parasitology**, v. 80, n. 3, p. 575–577, 1995.

ESTEVES, M. G. et al. Changes in fatty acid composition associated with differentiation of Trypanosoma cruzi. **FEMS microbiology letters**, v. 50, n. 1–2, p. 31–4, 1989.

FADDA, A. et al. Transcriptome-wide analysis of trypanosome mRNA decay reveals complex degradation kinetics and suggests a role for co-transcriptional degradation in determining mRNA levels. **Molecular Microbiology**, v. 94, p. 307–326, 2014.

FERNANDES, M. et al. Gene characterization and predicted protein structure of the mitochondrial chaperonin HSP10 of Trypanosoma cruzi. **Gene**, v. 349, p. 135–142, 2005.

FIGUEIREDO, R. C.; ROSA, D. S.; SOARES, M. J. Differentiation of Trypanosoma cruzi epimastigotes: metacyclogenesis and adhesion to substrate are triggered by nutritional stress. **The Journal of parasitology**, v. 86, n. 6, p. 1213–1218, 2000.

FLORIN-CHRISTENSEN, M. et al. Temperature acclimation of Trypanosoma cruzi epimastigote and metacyclic trypomastigote lipids. **Molecular and Biochemical Parasitology**, v. 88, n. 1–2, p. 25–33, 1997.

FOLGUEIRA, C.; REQUENA, J. M. A postgenomic view of the heat shock proteins in kinetoplastids. **FEMS Microbiology Reviews**, v. 31, n. 4, p. 359–377, 2007.

FUTSCHIK, M. E.; CARLISLE, B. Noise-robust soft clustering of gene expression time-course data. **Journal of bioinformatics and computational biology**, v. 3, n. 4, p. 965–88, 2005.

GASCH, A. P.; WERNER-WASHBURNE, M. The genomics of yeast responses to environmental stress and starvation. **Functional and Integrative Genomics**, v. 2, p. 181–192, 2002.

GIAMBIAGI-DEMARVAL, M.; SOUTO-PADRÓN, T.; RONDINELLI, E. Characterization and cellular distribution of heat-shock proteins HSP70 and HSP60 in Trypanosoma cruzi. **Experimental parasitology**, v. 83, n. 3, p. 335–45, 1996.

GOLDENBERG, S. et al. Characterization of messenger RNA from epimastigotes and metacyclic trypomastigotes of Trypanosoma cruzi. **FEBS Letters**, v. 180, n. 2, p. 265–270, 1985.

GONZALES-PERDOMO, M.; ROMERO, P.; GOLDENBERG, S. Cyclic AMP and adenylate cyclase activators stimulate Trypanosoma cruzi differentiation. **Experimental**

**parasitology**, v. 66, p. 205–212, 1988.

GOTELLI, N. J.; COLWELL, R. K. Quantifying biodiversity: procedures and pitfalls in the measurement and comparison of species richness. **Ecology Letters**, v. 4, n. 4, p. 379–391, 2001.

GOURGUECHON, S.; SAVICH, J. M.; WANG, C. C. The Multiple Roles of cyclin E1 in Controlling Cell Cycle Progression and Cellular Morphology of Trypanosoma brucei. **Journal of Molecular Biology**, v. 368, n. 4, p. 939–950, 2007.

GREIF, G. et al. Transcriptome analysis of the bloodstream stage from the parasite Trypanosoma vivax. **BMC genomics**, v. 14, p. 149, 2013.

GÜNZL, A. et al. RNA polymerase I transcribes procyclin genes and variant surface glycoprotein gene expression sites in Trypanosoma brucei. **Eukaryotic cell**, v. 2, n. 3, p. 542–51, 2003.

HAILE, S.; PAPADOPOULOU, B. Developmental regulation of gene expression in trypanosomatid parasitic protozoa. **Current Opinion in Microbiology**, v. 10, p. 569–577, 2007.

HAMMARTON, T. C.; MONNERAT, S.; MOTTRAM, J. C. **Cytokinesis in trypanosomatidsCurrent Opinion in Microbiology**, 2007.

HÄUSLER, T.; CLAYTON, C. Post-transcriptional control of hsp70 mRNA in Trypanosoma brucei. **Molecular and Biochemical Parasitology**, v. 76, n. 1–2, p. 57–71, 1996.

HEDBACKER, K.; CARLSON, M. SNF1/AMPK pathways in yeast. **Frontiers in bioscience : a journal and virtual library**, v. 13, p. 2408–20, 2008.

HENDRIKS, E. F.; MATTHEWS, K. R. Disruption of the developmental programme of Trypanosoma brucei by genetic ablation of TbZFP1, a differentiation-enriched CCCH protein. **Molecular Microbiology**, v. 57, n. 3, p. 706–716, 2005.

HENRIQUEZ, D. A. et al. Mechanisms of protein degradation in Trypanosoma cruzi. **Biological research**, v. 26, n. 1–2, p. 151–7, 1993.

HERNÁNDEZ, R. et al. Stationary phase in Trypanosoma cruzi epimastigotes as a preadaptive stage for metacyclogenesis. **Parasitology Research**, v. 111, p. 509–514, 2012.

HOLETZ, F. B. et al. Evidence of P-body-like structures in Trypanosoma cruzi. **Biochemical and Biophysical Research Communications**, v. 356, p. 1062–1067, 2007.

IGOILLO-ESTEVE, M.; CAZZULO, J. J. The glucose-6-phosphate dehydrogenase from Trypanosoma cruzi: its role in the defense of the parasite against oxidative stress. **Molecular and biochemical parasitology**, v. 149, n. 2, p. 170–81, 2006.

IVENS, A. C. et al. The genome of the kinetoplastid parasite, Leishmania major. **Science (New York, N.Y.)**, v. 309, n. 5733, p. 436–42, 2005.

JIANG, R.; CARLSON, M. The Snf1 protein kinase and its activating subunit, Snf4, interact with distinct domains of the Sip1/Sip2/Gal83 component in the kinase complex. **Molecular and cellular biology**, v. 17, n. 4, p. 2099–2106, 1997.

JOHANSSON, J. et al. An RNA thermosensor controls expression of virulence genes in Listeria monocytogenes. **Cell**, v. 110, n. 5, p. 551–561, 2002.

KOLEV, N. G. et al. The transcriptome of the human pathogen Trypanosoma brucei at single-nucleotide resolution. **PLoS Pathogens**, v. 6, n. 9, p. 1–15, 2010.

KOLEV, N. G. et al. Developmental Progression to Infectivity in Trypanosoma brucei Triggered by an RNA-Binding Protein. **Science**, v. 338, n. 6112, p. 1352–1353, 2012.

KOLLIEN, A. H.; SCHAUB, G. A. The development of Trypanosoma cruzi in triatominae. **Parasitology Today**, v. 16, n. 9, p. 381–387, 2000.

KOLLIEN, A. H.; SCHMIDT, J.; SCHAUB, G. A. Modes of association of Trypanosoma cruzi with the intestinal tract of the vector Triatoma infestans. **Acta Tropica**, v. 70, p. 127–141, 1998.

KRAMER, S.; KIMBLIN, N. C.; CARRINGTON, M. Genome-wide in silico screen for CCCH-type zinc finger proteins of Trypanosoma brucei, Trypanosoma cruzi and Leishmania major. **BMC Genomics**, v. 11, n. 1, p. 283, 2010.

KRAMER, S. Developmental regulation of gene expression in the absence of transcriptional control : The case of kinetoplastids. **Molecular & Biochemical Parasitology**, v. 181, n. 2, p. 61–72, 2012.

KRASSNER, S. M. et al. Action of exogenous potassium and calcium ions on in vitro metacyclogenesis in Trypanosoma cruzi. **The Journal of protozoology**, v. 38, n. 6, p. 602–8, 1991.

LAMMEL, E. M. et al. Trypanosoma cruzi: involvement of intracellular calcium in multiplication and differentiation. **Experimental parasitology**, v. 83, n. 2, p. 240–9, 1996.

LEBOWITZ, J. H. et al. Coupling of poly(A) site selection and trans-splicing in Leishmania. **Genes & development**, v. 7, n. 6, p. 996–1007, 1993.

LI, Y. et al. Transcriptome Remodeling in Trypanosoma cruzi and Human Cells during Intracellular Infection. **PLoS pathogens**, v. 12, n. 4, p. e1005511, 2016.

LI, Z. Regulation of the cell division cycle in Trypanosoma brucei. **Eukaryotic Cell**, v. 11, n. 10, p. 1180–1190, 2012.

LIANG, X. H. et al. trans and cis splicing in trypanosomatids: Mechanism, factors, and regulation. **Eukaryotic Cell**, v. 2, n. 5, p. 830–840, 2003.

LING, A. S.; TROTTER, J. R.; HENDRIKS, E. F. A Zinc Finger Protein, TbZC3H20, Stabilizes Two Developmentally Regulated mRNAs in Trypanosomes. **Journal of Biological Chemistry**, v. 286, n. 23, p. 20152–20162, 2011.

LUNDBY, A. et al. Proteomic analysis of lysine acetylation sites in rat tissues reveals organ specificity and subcellular patterns. **Cell reports**, v. 2, n. 2, p. 419–31, 2012.

LUO, H.; BELLOFATTO, V. Characterization of two protein activities that interact at the promoter of the trypanosomatid spliced leader RNA. **The Journal of biological chemistry**, v. 272, n. 52, p. 33344–52, 1997.

MAIR, G. et al. A new twist in trypanosome RNA metabolism: cis-splicing of pre-mRNA. **RNA (New York, N.Y.)**, v. 6, p. 163–169, 2000.

MANI, J. et al. Alba-Domain Proteins of Trypanosoma brucei Are Cytoplasmic RNA-Binding Proteins That Interact with the Translation Machinery. **PLoS ONE**, v. 6, n. 7, p. e22463, 2011.

MANNING-CELA, R.; GONZÁLEZ, A.; SWINDLE, J. Alternative splicing of LYT1 transcripts in Trypanosoma cruzi. **Infection and immunity**, v. 70, n. 8, p. 4726–8, 2002.

MANOEL-CAETANO, F. DA S.; SILVA, A. E. Implications of genetic variability of Trypanosoma cruzi for the pathogenesis of Chagas disease. **Cadernos de saúde pública**, v. 23, n. 10, p. 2263–74, 2007.

MARIC, D.; EPTING, C. L.; ENGMAN, D. M. Composition and sensory function of the trypanosome flagellar membrane. **Current opinion in microbiology**, v. 13, n. 4, p. 466–72, 2010.

MARIC, D. et al. Molecular determinants of ciliary membrane localization of Trypanosoma cruzi flagellar calcium-binding protein. **Journal of Biological Chemistry**, v. 286, n. 38, p. 33109–33117, 2011.

MARTÍNEZ-CALVILLO, S. et al. Gene expression in trypanosomatid parasites. **Journal of biomedicine & biotechnology**, v. 2010, p. 525241, 2010.

MATTHEWS, K. R.; TSCHUDI, C.; ULLU, E. A common pyrimidine-rich motif governs trans-splicing and polyadenylation of tubulin polycistronic pre-mRNA in trypanosomes. **Genes & development**, v. 8, n. 4, p. 491–501, 1994.

MAUGERI, D. A.; CAZZULO, J. J. The pentose phosphate pathway in Trypanosoma cruzi. **FEMS Microbiology Letters**, v. 234, p. 117–123, 2004.

MAUGERI, D. A.; CANNATA, J. J. B.; CAZZULO, J.-J. Glucose metabolism in Trypanosoma cruzi. **Essays in biochemistry**, v. 51, p. 15–30, 2011.

MICHELS, P. A. M. et al. Metabolic functions of glycosomes in trypanosomatids. **Biochimica et biophysica acta**, v. 1763, n. 12, p. 1463–77, 2006.

MILLER, M. B.; BASSLER, B. L. Quorum Sensing in Bacteria. **Annual Review of Microbiology**, v. 55, n. 1, p. 165–199, 2001.

MINISTÉRIO DA SAÚDE. Doença de Chagas aguda no Brasil: série histórica de 2000 a 2013. **Boletim Epidemiológico**, v. 46, n. 21, p. 1–9, 2015.

MITTLER, R.; FINKA, A.; GOLOUBINOFF, P. How do plants feel the heat? **Trends in Biochemical Sciences**, v. 37, n. 3, p. 118–125, 2012.

MONTEIRO, V. **Análise Genômica Funcional do Trypanosoma cruzi submetido a diferentes tipos de estresse**. [s.l.] Instituto Oswaldo Cruz, Curitiba, 2008.

MONY, B. M.; MATTHEWS, K. R. Assembling the components of the quorum sensing pathway in African trypanosomes. **Molecular microbiology**, v. 96, n. 2, p. 220–32, 2015.

MOROZOVA, O.; HIRST, M.; MARRA, M. A. Applications of New Sequencing Technologies for Transcriptome Analysis. **Annu. Rev. Genomics Hum. Genet**, v. 10, p. 135–51, jan. 2009.

NAGY, E. et al. Hyperfluidization-coupled membrane microdomain reorganization is linked to activation of the heat shock response in a murine melanoma cell line. **Proceedings of the National Academy of Sciences of the United States of America**, v. 104, n. 19, p. 7945–50, 2007.

NÁZER, E.; VERDÚN, R. E.; SÁNCHEZ, D. O. Severe heat shock induces nucleolar accumulation of mRNAs in Trypanosoma cruzi. **PloS one**, v. 7, n. 8, p. e43715, 2012.

NEALSON, K. H.; HASTINGS, J. W. Bacterial bioluminescence: its control and ecological significance. **Microbiological reviews**, v. 43, n. 4, p. 496–518, 1979.

NEPOMUCENO-MEJÍA, T. et al. The Trypanosoma cruzi nucleolus: a morphometrical analysis of cultured epimastigotes in the exponential and stationary phases. **FEMS microbiology letters**, v. 313, n. 1, p. 41–6, 2010.

NOGUEIRA, N.; BIANCO, C.; COHN, Z. Studies on the selective lysis and purification of Trypanosoma cruzi. **The Journal of experimental medicine**, v. 142, n. 1, p. 224–9, 1975.

O'FARRELL, P. H. High resolution two-dimensional electrophoresis of proteins. **The Journal of biological chemistry**, v. 250, n. 10, p. 4007–21, 1975.

OBERHOLZER, M. et al. Independent analysis of the flagellum surface and matrix proteomes provides insight into flagellum signaling in mammalian-infectious Trypanosoma brucei. **Molecular & cellular proteomics : MCP**, v. 10, n. 10, p. M111.010538, out. 2011.

OLIVEIRA, M. DE F. et al. Tratamento etiológico da doença de Chagas no Brasil. **Revista de Patologia Tropical**, v. 37, n. 3, p. 209–228, 2008.

OLSEN, J. V et al. Parts per million mass accuracy on an Orbitrap mass spectrometer via lock mass injection into a C-trap. **Molecular & cellular proteomics : MCP**, v. 4, n. 12, p. 2010–21, dez. 2005.

PALENCHAR, J. B.; BELLOFATTO, V. Gene transcription in trypanosomes. v. 146, p. 135–141, 2006.

PARODI-TALICE, A. et al. Proteomic analysis of metacyclic trypomastigotes undergoing Trypanosoma cruzi metacyclogenesis. **Journal of mass spectrometry : JMS**, v. 42, n. 11, p.

1422–32, 2007.

PECKOVÁ, H.; LOM, J. Growth, morphology and division of flagellates of the genus Trypanoplasma (Protozoa, Kinetoplastida) in vitro. **Parasitology Research**, v. 76, p. 553–558, 1990.

PEREIRA, M. G. et al. Trypanosoma cruzi epimastigotes are able to store and mobilize high amounts of cholesterol in reservosome lipid inclusions. **PLoS ONE**, v. 6, n. 7, p. e22359, 2011.

PÉREZ-MORALES, D.; OSTOA-SALOMA, P.; ESPINOZA, B. Trypanosoma cruzi SHSP16: Characterization of an alpha-crystallin small heat shock protein. **Experimental parasitology**, v. 123, n. 2, p. 182–9, 2009.

PÉREZ-MORALES, D. et al. Proteomic analysis of Trypanosoma cruzi epimastigotes subjected to heat shock. **Journal of Biomedicine and Biotechnology**, v. 2012, 2012.

PERRY, K. L.; WATKINS, K. P.; AGABIAN, N. Trypanosome mRNAs have unusual "cap 4" structures acquired by addition of a spliced leader. **Proceedings of the National Academy of Sciences of the United States of America**, v. 84, n. 23, p. 8190–4, 1987.

PORTMAN, N.; GULL, K. The paraflagellar rod of kinetoplastid parasites: From structure to components and function. **International Journal for Parasitology**, v. 40, n. 2, p. 135–148, 2010.

POTENZA, M. et al. Functional characterization of TcCYC2 cyclin from Trypanosoma cruzi. **Experimental Parasitology**, v. 132, n. 4, p. 537–545, 2012.

RAPPSILBER, J.; ISHIHAMA, Y.; MANN, M. Stop and Go Extraction Tips for Matrix-Assisted Laser Desorption/Ionization, Nanoelectrospray, and LC/MS Sample Pretreatment in Proteomics. **Analytical Chemistry**, v. 75, n. 3, p. 663–670, 2003.

RASSI, A.; RASSI, A.; MARIN-NETO, J. A. Chagas disease. **The Lancet**, v. 375, n. 9723, p. 1388–1402, 2010.

RASSI, A.; RASSI, A.; MARCONDES DE REZENDE, J. American trypanosomiasis (Chagas disease). **Infectious disease clinics of North America**, v. 26, n. 2, p. 275–91, 2012.

RASTROJO, A. et al. The transcriptome of Leishmania major in the axenic promastigote stage: transcript annotation and relative expression levels by RNA-seq. **BMC genomics**, v. 14, p. 223, 2013.

ROBINSON, M. D.; MCCARTHY, D. J.; SMYTH, G. K. edgeR: A Bioconductor package for differential expression analysis of digital gene expression data. **Bioinformatics**, v. 26, n. 1, p. 139–140, 2009.

RODRIGUES, D. C. et al. Trypanosoma cruzi: modulation of HSP70 mRNA stability by untranslated regions during heat shock. **Experimental parasitology**, v. 126, n. 2, p. 245–53, 2010.

ROLIN, S. et al. Mild acid stress as a differentiation trigger in Trypanosoma brucei. **Molecular and Biochemical Parasitology**, v. 93, p. 251–262, 1998.

SAAR, Y. et al. Characterization of developmentally-regulated activities in axenic amastigotes of Leishmania donovani. **Molecular and Biochemical Parasitology**, v. 95, n. 1, p. 9–20, 1998.

SANTOS, C. et al. Trypanosoma cruzi transcriptome during axenic epimastigote growth curve. **Parasitology**, p. In preparation., 2016.

SCHELTEMA, R. A. et al. The Q Exactive HF , a Benchtop Mass Spectrometer with a Pre-filter , High Performance Quadrupole and an Ultra- High Field Orbitrap Analyzer. p. 1–29, 2014.

SCHUMANN BURKARD, G. et al. Nucleolar proteins regulate stage-specific gene expression and ribosomal RNA maturation in Trypanosoma brucei. **Molecular Microbiology**, v. 88, n. 4, p. 827–840, 2013.

SCHWEDE, A.; KRAMER, S.; CARRINGTON, M. How do trypanosomes change gene expression in response to the environment? **Protoplasma**, v. 249, n. 2, p. 223–238, 2012.

SHAPIRO, R. S.; COWEN, L. E. Thermal control of microbial development and virulence: Molecular mechanisms of microbial temperature sensing. **mBio**, v. 3, n. 5, p. 1–6, 2012.

SHAW, A. K.; KALEM, M. C.; ZIMMER, S. L. Mitochondrial Gene Expression Is Responsive to Starvation Stress and Developmental Transition in Trypanosoma cruzi. v. 1, n. 2, 2016.

SHIGAPOVA, N. et al. Membrane fluidization triggers membrane remodeling which affects the thermotolerance in Escherichia coli. **Biochemical and Biophysical Research Communications**, v. 328, n. 4, p. 1216–1223, 2005.

SIEGEL, T. N. et al. Four histone variants mark the boundaries of polycistronic transcription units in Trypanosoma brucei. **Genes & development**, v. 23, n. 9, p. 1063–76, 2009.

SILBER, A. M. et al. Amino acid metabolic routes in Trypanosoma cruzi: possible therapeutic targets against Chagas' disease. **Current drug targets. Infectious disorders**, v. 5, n. 1, p. 53–64, 2005.

SILBER, A. M. et al. Biochemical characterization of the glutamate transport in Trypanosoma cruzi. **International Journal for Parasitology**, v. 36, n. 2, p. 157–163, 2006.

SILBER, A. M. et al. Glucose uptake in the mammalian stages of Trypanosoma cruzi. **Molecular and Biochemical Parasitology**, v. 168, p. 102–108, 2009.

SINENSKY, M. Homeoviscous adaptation--a homeostatic process that regulates the viscosity of membrane lipids in Escherichia coli. **Proceedings of the National Academy of Sciences of the United States of America**, v. 71, n. 2, p. 522–5, 1974.

SNAPP, E. L.; LANDFEAR, S. M. Cytoskeletal association is important for differential

targeting of glucose transporter isoforms in Leishmania. **The Journal of cell biology**, v. 139, n. 7, p. 1775–83, 1997.

SOARES, M. J. et al. A stereological study of the differentiation process in Trypanosoma cruzi. **Parasitology research**, v. 75, n. 7, p. 522–7, 1989.

SONENBERG, N.; HINNEBUSCH, A. G. Regulation of translation initiation in eukaryotes: mechanisms and biological targets. **Cell**, v. 136, n. 4, p. 731–45, 2009.

TANOWITZ, H. B. et al. Chagas' Disease. v. 5, n. 4, p. 400–419, 1992.

TAYLOR, G. K. et al. Web and database software for identification of intact proteins using "top down" mass spectrometry. **Analytical chemistry**, v. 75, n. 16, p. 4081–6, 2003.

TEIXEIRA, S. M. Control of gene expression in Trypanosomatidae. **Brazilian journal of medical and biological research**, v. 31, n. 12, p. 1503–16, 1998.

TETAUD, E. et al. Characterization of glucose transport and cloning of a hexose transporter gene in Trypanosoma cruzi. **Proceedings of the National Academy of Sciences of the United States of America**, v. 91, n. 17, p. 8278–82, 1994.

TIBAYRENC, M. Genetic subdivisions within Trypanosoma cruzi (Discrete Typing Units) and their relevance for molecular epidemiology and experimental evolution. **Kinetoplastid biology and disease**, v. 2, n. 1, p. 12, 2003.

TIBBETTS, R. S. et al. The DnaJ family of protein chaperones in Trypanosoma cruzi. **Molecular and Biochemical Parasitology**, v. 91, n. 2, p. 319–326, 1998.

TOMLINSON, S. et al. The induction of Trypanosoma cruzi trypomastigote to amastigote transformation by low pH. **Parasitology**, v. 110, n. 5, p. 547, 1995.

TONELLI, R. R. et al. Protein synthesis attenuation by phosphorylation of eIF2α is required for the differentiation of Trypanosoma cruzi into infective forms. **PloS one**, v. 6, n. 11, p. e27904, 2011.

TORTORA, G.; FUNKE, B.; CASE, C. **Microbiologia**. 10ed. ed. Porto Alegre: Artmed, 2012.

TYANOVA, S. et al. The Perseus computational platform for comprehensive analysis of (prote)omics data. **Nature Methods**, n. June, 2016.

TYLER, K. M. et al. Flagellar membrane localization via association with lipid rafts. **Journal of cell science**, v. 122, n. 6, p. 859–866, 2009.

TYLER, K. M.; ENGMAN, D. M. Flagellar elongation induced by glucose limitation is preadaptive for Trypanosoma cruzi differentiation. **Cell Motility and the Cytoskeleton**, v. 46, n. 4, p. 269–278, 2000.

TYLER, K. M.; ENGMAN, D. M. The life cycle of Trypanosoma cruzi revisited. **International Journal for Parasitology**, v. 31, p. 472–481, 2001.

URBINA, J. A.; OSORNO, C. E.; ROJAS, A. Inhibition of phosphoenolpyruvate carboxykinase from Trypanosoma (Schizotrypanum) cruzi epimastigotes by 3-mercaptopicolinic acid: in vitro and in vivo studies. **Archives of biochemistry and biophysics**, v. 282, n. 1, p. 91–9, 1990.

URBINA, J. A. Intermediary Metabolism of Trypanosoma cruzi. **Parasitology today**, v. I, n. 3, p. 107–110, 1994.

VAN RIPER, S. K. et al. Mass spectrometry-based proteomics: basic principles and emerging technologies and directions. **Advances in experimental medicine and biology**, v. 990, p. 1–35, 2013.

VANHAMME, L.; PAYS, E. Control of gene expression in trypanosomes. **Microbiological reviews**, v. 59, n. 2, p. 223–240, 1995.

VIVES, S.; SALICRÚ, M. Accuracy in the estimation of quantitative minimal area from the diversity/area curve. **Mathematical biosciences**, v. 195, n. 1, p. 65–75, 2005.

WERNER-WASHBURNE, M. et al. Stationary phase in the yeast Saccharomyces cerevisiae. **Microbiology and Molecular Biology Reviews**, v. 57, n. 2, p. 383–401, 1993.

WHO. Chagas disease (American trypanosomiasis). 2016.

WU, C. et al. A protease for "middle-down" proteomics. **Nature methods**, v. 9, n. 8, p. 822–4, 2012.

WURST, M. et al. Expression of the RNA recognition motif protein RBP10 promotes a bloodstream-form transcript pattern in Trypanosoma brucei. **Molecular Microbiology**, v. 83, n. February, p. 1048–1063, 2012.

YATES, G. T.; SMOTZER, T. On the lag phase and initial decline of microbial growth curves. **Journal of Theoretical Biology**, v. 244, n. 3, p. 511–517, 2007.

YORIMITSU, T.; KLIONSKY, D. J. Autophagy: molecular machinery for self-eating. **Cell death and differentiation**, v. 12 Suppl 2, p. 1542–52, 2005.

ZELEDON, R. Comparative physiological studies on four species of hemoflagellates in culture. II. Effect of carbohydrates and related substances and some amino compounds on the respiration. **The Journal of parasitology**, v. 46, p. 541–51, 1960.

ZELEDÓN, R. Some morphological and molecular aspects of the life cycle of Trypansoma cruzi in the insect vector. **Memórias do Instituto Oswaldo Cruz**, v. 94, p. 217–218, 1999.

ZHANG, J.; OLSSON, L.; NIELSEN, J. The beta-subunits of the Snf1 kinase in Saccharomyces cerevisiae, Gal83 and Sip2, but not Sip1, are redundant in glucose derepression and regulation of sterol biosynthesis. **Molecular Microbiology**, v. 77, n. 2, p. 371–383, 2010.

ZILBERSTEIN, D.; SHAPIRA, M. The role of pH and temperature in the development of Leishmania parasites. **Annual review of microbiology**, v. 48, p. 449–70, 1994.

ZINGALES, B. et al. Epidemiology, biochemistry and evolution of Trypanosoma cruzi lineages based on ribosomal RNA sequences. **Memórias do Instituto Oswaldo Cruz**, v. 94 Suppl 1, p. 159–64, 1999.

ZINGALES, B. et al. A new consensus for Trypanosoma cruzi intraspecific nomenclature : second revision meeting recommends TcI to TcVI. v. 104, n. November, p. 1051–1054, 2009.

ZINGALES, B. Trypanosoma cruzi: um parasita, dois parasitas ou vários parasitas da doença de chagas? **Revista da Biologia**, v. 6b, p. 44–48, 2011.

ZWIERZYNSKI, T. A; BUCK, G. A. RNA-protein complexes mediate in vitro capping of the spliced-leader primary transcript and U-RNAs in Trypanosoma cruzi. **Proceedings of the National Academy of Sciences of the United States of America**, v. 88, n. 13, p. 5626–30, 1991.

# ANEXO 1 - CD